# PhD Thesis

## Morphology control of microspheres based on polymer blends containing block copolymers

**HOSSEIN TAHERZADEH**

**Adviser: Professor Kenji Ogino**

**2015-3-16**

# Chapter1

# Introduction

## 1-1) Polymer Blends

If two chemically-different polymers are mixed together, it often is found that they undergo almost complete phase separation and form two separate phases. Historically, it was thought that polymer-polymer miscibility would take place only relatively rarely, but these days it is recognized that different polymer-polymer combinations can show a variety of different types of behavior ranging from complete phase separation to partial miscibility and even complete miscibility in some cases. In the following Table, there are some examples of particular polymer pairs that are found to be either miscible or immiscible.

**Table 1-1**: Miscibility of Polymer Blends

| Polymer 1 | Polymer 2 | Miscible |
|---|---|---|
| Polystyrene | Poly(2,6-dimethyl-1,4-phenylene oxide) | ✔ |
| Polystyrene | Poly(Vinyl methyl ether) | ✔ |
| Poly(methyl methacrylate) | Poly(vinylidene fluoride) | ✔ |
| Poly(vinyl chloride) | Poly(butylenes terephthalate) | ✔ |
| Poly(ethylene oxide) | Poly(acrylic acid) | ✔ |
| Polystyrene | Polybutadiene | * |
| Polystyrene | Poly(methyl methacrylate) | * |
| Polystyrene | Poly(dimethyl siloxane) | * |
| Nylon 6 | Poly(ethylene terephthalate) | * |

***Source**:* Adapted from Sperling, L.H., *Introduction to Physical Polymer Science*, 4th edn., Wiley Interscience, Hoboken, NJ, 2006.

## 1-1.1) Compatibilization of Polymer Blends

The blending of different polymers can lead to materials with novel or improved properties. The difficulty in creating polymer blends is that most polymers are immiscible and macrophase separation occurs. Therefore, compatibilizers are necessary to stabilize polymer blends, and a number of techniques have been developed to achieve this objective [1]. There are a number of ways in which compatibilization can be achieved.

The process of ***in situ polymerization*** can be used to produce covalent bonding between the constituent polymers resulting in graft or block copolymers that stabilizes the interface between the two phases [2].

Another method is to add a ***ternary polymeric component*** to the blend of immiscible polymers. This normally is a polymer that has good interfacial adhesion with both phases and so concentrates in the interfacial regions leading to a good dispersion and facilitating efficient stress transfer across the interface between the two phases [3].

One of the neatest methods of compatibilization is simply to add a ***block copolymer*** in which each of the blocks has the same or similar composition to that of the component polymers of the blend. This system will have its lowest free energy when the block copolymer is concentrated at the interface between the phases. This concept is used widely in incompatible blend systems and leads to good control of the morphology combined with an improvement in interfacial adhesion and hence mechanical properties [4].

## 1-1.2) Thermodynamics of Polymer Blends

### 1-1.2.1) Flory-Huggins Equation

The basic thermodynamic relationship governing the mixing of dissimilar polymers established by Gibbs [5] is:

$$\Delta G_m = \Delta H_m - T\Delta S_m \quad (1)$$

$\Delta G_m$ : the free energy of mixing, $\Delta H_m$ : the enthalpy of mixing and $\Delta S_m$ : the entropy of mixing with $T$ being the temperature. For the two polymers to be miscible, $\Delta G_m$ must be negative. This is a necessary criterion, but is not sufficient as the equation below must also be met:

$$\left(\frac{\partial^2 \Delta G_m}{\partial \varphi_i^2}\right)_{T,p} > 0 \tag{2}$$

The basic theory for assessing the miscibility of polymer blends was developed by Flory [6, 7] and Huggins [8, 9] and is thus referred to as the Flory-Huggins theory. The equation resulting from their analysis is termed by the Flory-Huggins Equation as noted:

$$\Delta G_m = kTV\left[\frac{\varphi_1}{V_1}\ln\varphi_1 + \frac{\varphi_2}{V_2}\ln\varphi_2\right] + \varphi_1\varphi_2\chi_{12}kTV / \upsilon_r \tag{3}$$

In which: $V$ = total volume, $Vi$ = molecular volume of component $i$, $\varphi i$ = volume fraction of component $i$, $k$ = Boltzman's constant, $\chi_{12}$ = Flory-Huggins interaction parameter and $\upsilon_r$ = interacting segment volume (such as a repeat unit volume) and is also referred to as the reference volume. This equation was primarily employed for solvent-polymer mixtures but is applicable to higher molecular weight polymer mixtures. The Flory-Huggins Equation successfully applied to demonstrate the basic reason for decreased miscibility of solvent-polymer mixtures compared to solvent-solvent mixtures as the combinatorial entropy of mixing is decreased. With polymer-polymer mixtures, the combinatorial entropy of mixing approaches insignificant values in the limit of high molecular weight polymer mixtures. Thus to achieve miscibility, a negative heat of mixing must be obtained (*i.e.*, $\chi_{12} < 0$).

In the case of low molar mass materials, an increase at temperature leads to an increase in the $T\Delta S_m$ term thus making $\Delta G_m$ more negative and leading to better miscibility as the temperature is increased. It is possible to employ the Flory-Huggins theory, developed initially for polymer-solvent mixtures, to model also the thermodynamic behavior of polymer blends. In this case, the two types of polymer chains are considered to be made up of segments that sit on lattice of identical cells as shown in Figure 1-1. Polymer 1 occupies a continuous sequence of $\boldsymbol{x_1}$ segment and polymer 2 occupies a continuous sequence of $\boldsymbol{x_2}$ segment.

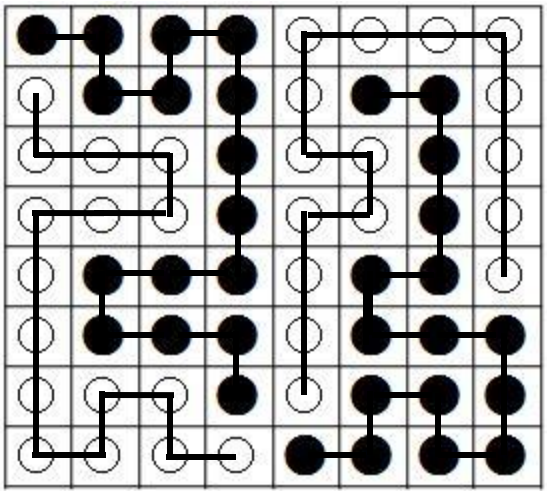

**Figure 1-1**: Flory-Huggins lattice model for a polymer blend. The black segments represent one type of polymer and white ones the other type

The volume fractions of the two polymers are given by:

$$\Phi_1 = N_1\boldsymbol{x_1} / (N_1\boldsymbol{x_1} + N_2\boldsymbol{x_2}) \quad (4)$$

$$\Phi_2 = N_2\boldsymbol{x_2} / (N_1\boldsymbol{x_1} + N_2\boldsymbol{x_2}) \quad (5)$$

Where: $N_1$ and $N_2$ are the number of molecules of each type of polymer. In blends, the interactions that have to be considered are either between segments of the same polymer or between segments of the different polymers. It is possible to use the following equation for two polymers:

$$\Delta G_m^{\text{contact}} = \boldsymbol{R}\, T\boldsymbol{x_1} n_1 \Phi_2 \boldsymbol{X} \quad (6)$$

Where: $n_1$ represent the number of moles of polymer 1, and $\boldsymbol{X}$ is the Flory-Huggins polymer-polymer interaction parameter. The combination entropy equation for polymer-polymer solution mixtures is:

$$\Delta S_m^{\text{comb}} = -\boldsymbol{R}\,[n_1 \ln\Phi_1 + n_2 \ln\Phi_2] \quad (7)$$

Hence, $\Delta G_m = \Delta G_m^{\text{contact}} - T\Delta S_m^{\text{comb}}$ (8)

and $\Delta G_m = \boldsymbol{R}\, T\,[n_1 \ln\Phi_1 + n_2 \ln\Phi_2 + \boldsymbol{x_1} n_1 \Phi_2 \boldsymbol{X}]$ (9)

In this equation, the combination entropy term becomes less important because both $n_1$ and $n_2$ are relatively small, and the thermodynamics of mixing is dominated by the enthalpy term, $\boldsymbol{RTx_1 n_1 \Phi_2 X}$. The interaction parameter $\boldsymbol{X}$ has temperature dependence:

$$\boldsymbol{X} = a + b/T \quad (10)$$

This temperature dependence of $\boldsymbol{X}$ can lead to the enthalpy term and hence $\Delta G_m$ in the mentioned equation becomes less negative as the temperature raise resulting in decreasing miscibility for the polymer blend. Although the Flory-Huggins approach is useful in analyzing the characteristics of polymer blends, it is only able to show trends and is not capable of predicting the behavior accurately as it ignores a number of factors such as any volume changes that may take place upon mixing.

## 1-1.2.2) Solubility Parameter Concept

The solubility parameter concept allows for a predictive capability of assessing the potential of miscibility of liquids. The concept traces back to Hildebrand [10], where the solubility of a material was noted to be influenced by the solvent internal pressure. This concept was further developed by Scatchard [11]. Scatchard defined the cohesive energy density (CED) as the energy of vaporization ($\Delta E_v$) per unit volume (V). Hildebrand and Scott [12] then defined the solubility parameter ($\delta p$) as the square root function of the cohesive energy density:

$$\delta_p = (CED)^{1/2} = \left(\frac{\Delta E_v}{V}\right)^{1/2} \quad (11)$$

The basic concept involves matching the solubility parameter to achieve miscibility. For solvent-solvent mixtures, the solubility parameter difference can be rather large for miscibility to be achieved. With solvent-polymer mixtures, the solubility parameter difference is much lower to achieve miscibility but still significant. This approach works quite well for non-polar solvent mixtures with some divergence for highly polar or hydrogen bonding liquids as well as other specifically interacting molecules. With polymer-polymer mixtures, the solubility parameters need to be virtually identical to achieve miscibility in the absence of strong polar or hydrogen bonding interactions. With polymers, the energy of vaporization cannot be determined. The polymer solubility parameter is typically determined by swelling a crosslinked sample in a series

of solvents and assigning the solubility parameter value, where the highest swelling (best solvent) occurs. In order to address polar and hydrogen bonding polymers, three dimensional solubility parameters were proposed by Hansen [13], who has found utility for solvent-polymer mixtures but limited applicability for polymer-polymer mixtures. An useful approach for predicting the solubility parameter for polymers involves a group contribution method. The most utilized approach was given by Small [14] with additional approaches noted by van Krevelan [15], Hoy [16] and Coleman [17]. While the solubility parameter approach has some qualitative utility, the inability to address specific interactions is a major limitation. The relationship of Flory-Huggins interaction parameter with the solubility parameter is:

$$\frac{\chi_{12}}{\upsilon_r} = (\delta_{p1} - \delta_{p2})^2 / RT \qquad (12)$$

Therefore, negative values (indicative of specific interactions) cannot be obtained.

## 1-1.2.3) Equation of State (EOS)

An equation of state (EOS) is typically a mathematical relationship between several variables most commonly employed with pressure, volume and temperatures of gases. The equation of state approach can also be applied to liquid and polymer systems. Prigogine developed an equation of state for liquid mixtures [18]. Flory developed an EOS for solvent-polymer mixtures following the formalism developed by Prigogine but accounting for chain segments to accommodate polymers [19-21]. These approaches employ reduced pressure, reduced volume, reduced temperature and a partition function to describe the system. The Flory EOS approach allows for compressibility effects whereas the Flory-Huggins lattice model is an incompressible model. This difference can lead to the conditions that allow the EOS approach to predict lower critical solution temperature (LCST) behavior. The lattice model can only predict this if the Flory-Huggins interaction parameter (***X)*** is dependent on temperature. McMaster [22] applied the Flory EOS approach to polymer-polymer mixtures and investigated the effect of key variables on the predicted phase behavior. It was found that LCST behavior was predicted for polymer-polymer blends and probably the expected case. The temperature dependence of the thermal expansion coefficient, the thermal pressure coefficient and the interaction coefficient (related to the Flory-Huggins interaction parameter) showed the effect of these variables on the temperature-composition phase diagrams.

## 1-1.3) Phase Behavior

Phase behavior of polymer blend is accompanied with phase diagram. They can be used in a similar way with polymer blends. A schematic phase diagram of polymer blend is shown in Figure 1-2. The diagram shows three regions with different degree of miscibility: A single-phase region between the two binodals, metastable regions between the binodals and spinodals, and two-phase regions of immiscibility that are bordered by spinodals. The diagram also shows two critical solution temperatures; the LCST at high temperature and the UCST at lower temperature. The miscible (one-phase) and metastable regions are separated by the binodals and the metastable and two-phase regions are separated by the spinodals. Phase separation will take place when a single-phase system undergoes either a change in composition or, more commonly, a change in temperature that forces it to cross the binodals or spinodals. The two-phase regions within the spinodal correspond to areas where phase separation occurs by a process akin to crystallization, by there is ***nucleation and growth*** of the phase-separated domains. In contrast, in the metastable regions between the binodals and spinodals, if the energy barrier can be overcome, phase separation will occur by a spontaneous process known as ***spinodal decomposition***.

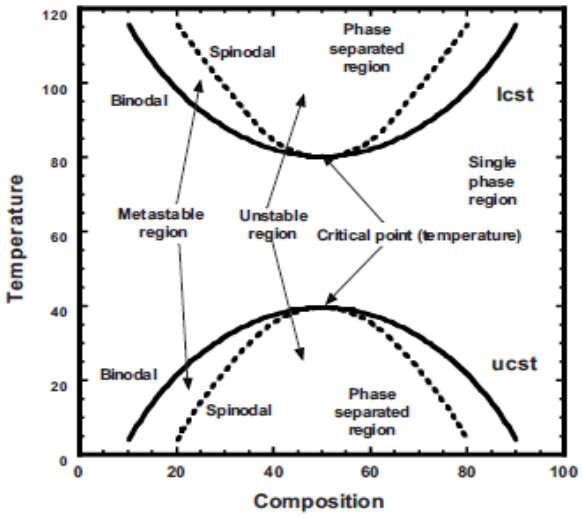


**Figure 1-2**: Phase diagram for binary polymer blend (temperature *versus* composition) with illustration of lower critical solution temperature (LCST) and upper critical solution temperature (UCST) behavior. (Adapted from Robenson, L.M., *Polymer Blends: A Comprehensive Review*, Hanser, Cincinnati, OH, 2007)

In general solvent-solvent and polymer-solvent mixture usually show an UCST and become more miscible as the temperature is increased, where polymer-polymer mixtures, normally become less miscible with increasing temperature, exhibit a LCST. Figure 1-3 is a schematic phase diagram for a polymer blend showing LCST behavior. For a given temperature above the LCST, the points of intersection with the phase boundary lines denote the limits of miscibility of

the two polymers, $\Phi_a$ and $\Phi_b$ at this temperature. For a given blend composition $\Phi$, the volume fractions of the phase rich in component 1, $\Phi^{1\text{ rich}}$ and that rich in component 2, $\Phi^{2\text{ rich}}$ in the two-phase region can be determined by undertaking the tie-line calculation illustrated in Figure 1-3 such that:

$$\Phi^{1\text{ rich}} / \Phi^{2\text{ rich}} = (\Phi_b - \Phi) / (\Phi - \Phi_a) \quad (13)$$

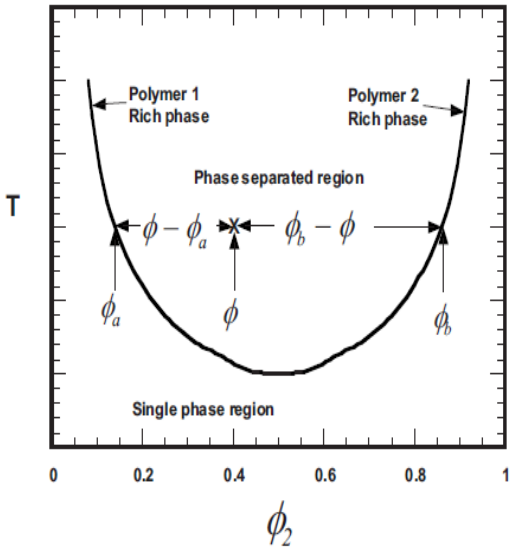


**Figure 1-3**: Tie-line calculation to determine the phase composition in a polymer blend. (Adapted from Robenson, L.M., *Polymer Blends: A Comprehensive Review*, Hanser, Cincinnati, OH, 2007)

## 1-2) Polymer Particles: Definition, Application and Classification

Polymer particles (PPs) have attracted the interest of many research groups and have been utilized in an increasing number of fields during the last decades. Generally, two main strategies are employed for their preparation; the dispersion of preformed polymers and the polymerization of monomers. Various techniques can be used to produce polymer particles, some of the former item include: solvent evaporation, salting-out, nano-micro precipitation, dialysis and some of the latter item is concerned: Emulsion (conventional, soap-free) emulsion, dispersion and suspension polymerization (heterogeneous process). The choice of method depends on a number of factors such as, particle size, particle- size distribution, area of application, etc.

The field of PPs is quickly expanding and playing a pivotal role in a wide spectrum of areas ranging from electronics to photonics, conducting materials to sensors, medicine to bio technology, pollution control to environmental technology, and so forth [23-31]. The properties of PPs have to be optimized depending on the particular application. In order to achieve the properties of interest, the mode of preparation plays a vital role. Thus, it is highly advantageous

to have preparation techniques at hand to obtain PPs with the desired properties for a particular application. The particle size and the particle size distribution of PPs are of great importance because they determine their key properties such as viscosity, surface area, and packing density.

PPs are frequently defined as solid, colloidal particles in the range 10 nm–100 µm [32, 33]. The term PPs is a collective term given for any type of polymer particle, but specifically for nano-microspheres (N-MSs) and nano-microcapsules (N-MCs). N-MSs are matrix particles, i.e., particles whose entire mass is solid and molecules may be adsorbed at the sphere surface or encapsulated within the particle. In general, they are spherical, but "N-MSs" with a nonspherical shape are also described in the literature [34]. N-MCs are vesicular systems, acting as a kind of reservoir, in which the entrapped substances are confined to a cavity consisting of a liquid core (either oil or water) surrounded by a solid material shell [35]. A schematic representation of N-MSs & N-MCs is shown in Figure 1-4.


**Figure 1-4**: Illustration of classification of N-MSs (a), N-MCs containing oil (b) and water (c) [35].

## 1-2.1) Overview of the Preparation Techniques for Polymer Particles

As mentioned already, PPs can be conveniently prepared either from preformed polymers or by direct polymerization of monomers using classical polymerization. The choice of preparation method is made on the basis of a number of factors such as the type of polymeric system, area of application, size requirement, etc. These are just a few of many factors that have to be considered before choosing a particular technique for the PPs preparation.

### 1-2.1.1) Dispersion of Preformed Polymers

Several methods developed and successfully utilized to prepare PPs by dispersing preformed polymers are discussed summery in the following sections.

#### 1-2.1.1.1) Solvent Evaporation

Solvent evaporation was the first method developed to prepare PPs from a preformed polymer [36]. In this method, polymer solutions are prepared in volatile solvents and emulsions

are formulated. The emulsion is converted into a nano-micro particle suspension on evaporation of the solvent for the polymer, which is allowed to diffuse through the continuous phase of the emulsion [37, 38]. Usually, two main strategies are being used for the formation of emulsions; the preparation of single-emulsions, oil-in-water (o/w) or double-emulsions, (water-in-oil)-in-water, (w/o)/w. Generally, a polymer dissolved in an organic solvent forms the oil phase, whereas the aqueous phase containing the stabilizer forms the water phase. Figure 1-5 summarizes the preparation method using the double-emulsion-solvent evaporation method.

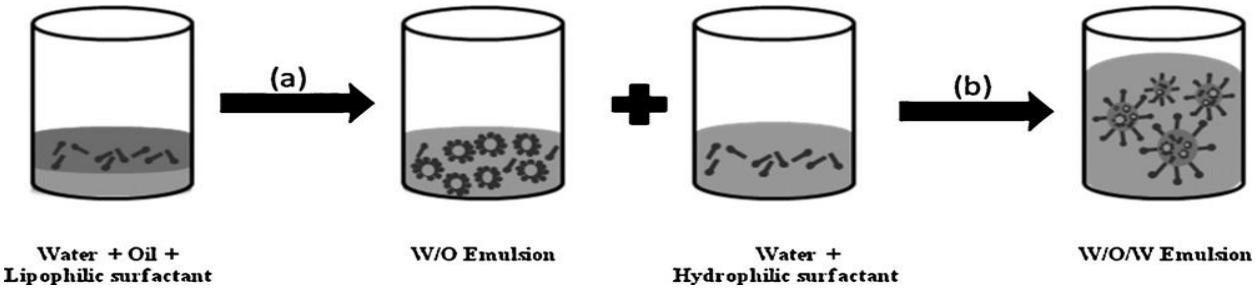


**Figure 1-5**: Preparation of w/o/w double emulsion: (a) high-shear emulsification and (b) low-shear emulsification

It's time consuming and possible coalescence of the nano-micro droplets during the evaporation process may affect the final particle size and morphology.

### 1-2.1.1.2) Salting-out

The method discussed in the previous section requires the use of organic solvents, which are hazardous to the environment as well as tothe physiological systems. To overcome this hurdle, a modified version of emulsion process that involves a salting-out process, which avoids surfactants and chlorinated solvents were disclosed [39]. The emulsion is formulated with a polymer solvent which is normally totally miscible with water, such as; acetone, and emulsification of the polymer solution in the aqueous phase is achieved, by dissolving high concentration of salt or sucrose chosen for a strong salting-out effect in the aqueous phase. Magnesium chloride, calcium chloride and magnesium acetate are commonly used suitable electrolytes [40–42]. The miscibility properties of water with other solvents are modified as these components dissolve in the water.

#### 1-2.1.1.3) Nano-micro precipitation

The basic principle of this technique is based on the interfacial deposition of a polymer after displacement of a semi-polar solvent, miscible with water, from a lipophilic solution. Rapid diffusion of the solvent into non-solvent phase results in the decrease of interfacial tension between the two phases, which increases the surface area and leads to the formation of small droplets of organic solvent [43]. N-MP system consists of three basic components; the polymer, the polymer solvent and the non-solvent of the polymer. Acetone is the most frequently employed polymer solvent in this method [44, 45]. The non-solvent phase consisting of a non-solvent or a mixture of non-solvents is supplemented with one or more naturally surfactant. PPs are produced by slow addition of the organic phase to the aqueous phase under moderate stirring. The key variables determining the success of the method and affecting the physicochemical properties of PPs are those associated with the conditions of adding the organic phase to the aqueous phase, such as organic phase injection rate, aqueous phase agitation rate, the method of organic phase addition and the organic phase to aqueous phase ratio. Likewise, PPs characteristics are influenced by the nature and concentration of their components [46, 47]. Although, a surfactant is not required to ensure the formation of PPs by N-MP, the particle size is influenced by the surfactant nature and concentration [48]. Moreover, the addition of surfactants helps to preserve the PPs suspensions from agglomeration over long storage periods. N-MP is a simple, fast and reproducible method which is widely used for the preparation of both NMSs and NMCs. Even though low polymer surfactant concentrations are employed, challenges pertaining to low polymer concentration in the organic phase have to be addressed.

#### 1-2.1.1.4) Dialysis

Dialysis offers a simple and effective method for the preparation of small, narrow-distributed PPs [49-51]. Polymer is dissolved in an organic solvent and placed inside a dialysis tube with proper molecular weight cutoff. Dialysis is performed against a non-solvent miscible with the former miscible. The displacement of the solvent inside the membrane is followed by the progressive aggregation of polymer due to a loss of solubility and the formation of homogeneous suspensions of PPs. The mechanism of PPs formation by the dialysis method is not fully understood at present. It is thought that it may be based on a mechanism similar to that of N-MP that discussed in the previous section.

## 1-3) Seed Polymerization Techniques as Modifying for Polymer Particles Morphology

The polymer particles prepared by polymerization in heterogeneous systems have a spherical shape because of the minimization of the interfacial free energy between the particle and a medium. Various modes of emulsion and dispersion polymerization involve the formation of nuclei (primary particles), followed by gradual growth of these nuclei to produce the final polymer particles. In all of these systems, preformed polymer particles (i.e., seeds) can be added to the polymerization mixture at the onset of the polymerization instead of in situ formation of polymer nuclei. However, polymerization conditions (i.e., number of seed particles and concentrations of initiator and stabilizer) must be carefully chosen to avoid the formation of new particles. Seeded polymerization was first reported by smith in 1948 [52] to study the kinetics of emulsion polymerization. The concept of seeded polymerization has been extended by Ugelstad et al. for the preparation of monodisperse particles of up to 50 μm [53]. The method developed by this group is based on the observation that swelling of polymer particles is considerably enhanced in the presence of a small percentage of a second low molecular weight polymer (oligomer). Thus, monodisperse polystyrene latex particles obtained by emulsion polymerization are treated, first with a suitable oligomer, and then with styrene (and DVB) and an oil-soluble initiator. The mixture is allowed to stand until the oligomer and monomer are completely absorbed by the particles. Subsequent polymerization leads to the formation of the corresponding larger monodisperse particles. This method is proper for preparation of monodisperse polymer microspheres in the region of 5-20 μm, which are less readily obtained by basic heterogeneous polymerization techniques.

Since the middle of 1970s, various nonspherical polymer particles have been prepared by various seeded polymerization methods (e.g., seeded emulsion polymerization [54, 55], seeded polymerization with monomer swollen particles [56, 57], and seeded dispersion polymerization [58, 59].

### 1-3.1) Seeded Emulsion Polymerization

Seeded emulsion polymerization has received the considerable attention for the production of core-shell, hemispheres and many approaches to prepare hollow particles via this method have been reported.

About ***core-shell morphology***, Joensson et al. [60] fabricated latex particles containing equal amounts of PMMA and polystyrene (I )were prepared by polymerization of styrene in the presence of PMMA seed particles using two different initiators, potassium persulfate (II), and tert-Bu hydroperoxide (III). Styrene was added either before polymerization (batch) or continuously during the polymerization. Particles prepared using batch addition of styrene showed no signs of core-shell morphology and the surface concentration of (I) was lower than 50%, while particles with well-defined core-shell structures were obtained when styrene was added at a low feed rate. With (III) as initiator, the shell layer was compact and distinct and the surface concentration of (I) high, whereas with (II) as initiator, the shell layer was thicker and contained domains of PMMA. Composite particles prepared using a low styrene feed rate, but seed particles containing chain-transfer agent, had (I) domains distributed throughout the entire particle volume. Hence, the formation of particles with a core-shell structure was due to the suppression of radical transport to the interior of the seed particles, mainly because of the high internal viscosity of the latter. The structure and composition of the shell layer, however, depend on the chemical nature of the initiator (Figure 1-6).

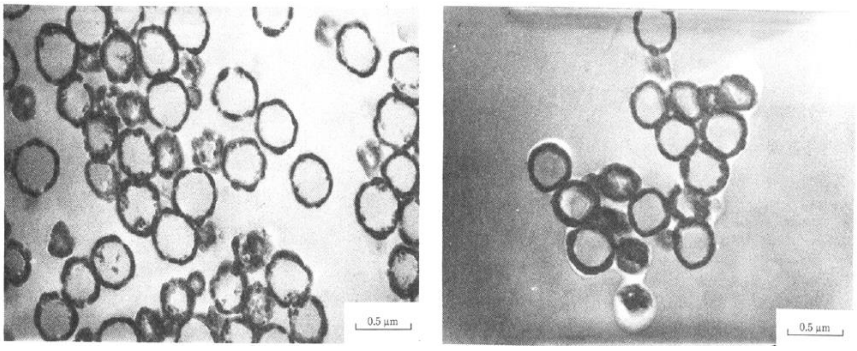


**Figure 1-6**: TEM micrographs of sectioned particles prepared by continuous addition of styrene using seed latex **S1.** Experiment **C** with KPS as initiator (left) and experiment E with t-BHP as initiator (right) [60].

About ***hemispheres morphology***, Han et al. [61] carried out seeded preswelling emulsion polymerization by using monodispersed poly(4-vinylpyridine-*co*-butyl acrylate) [P(4VP-BA)] particles as the seed, and styrene and butyl acrylate as the second-stage monomers under different polymerization conditions, to obtain hemispherical polystyrene (PS)-rich–P4VP-rich microspheres. They realized the mobility of the P(St-BA) chains influenced the diffusion of the P(St-BA) domains on the surface of the P(4VP-BA) matrix. When the mobility of the P(St-BA)

chains allowed small-size P(St-BA) domains to coalesce into one larger domain, complete phase-separated morphology (hemisphere) could be achieved (Figure 1-7).

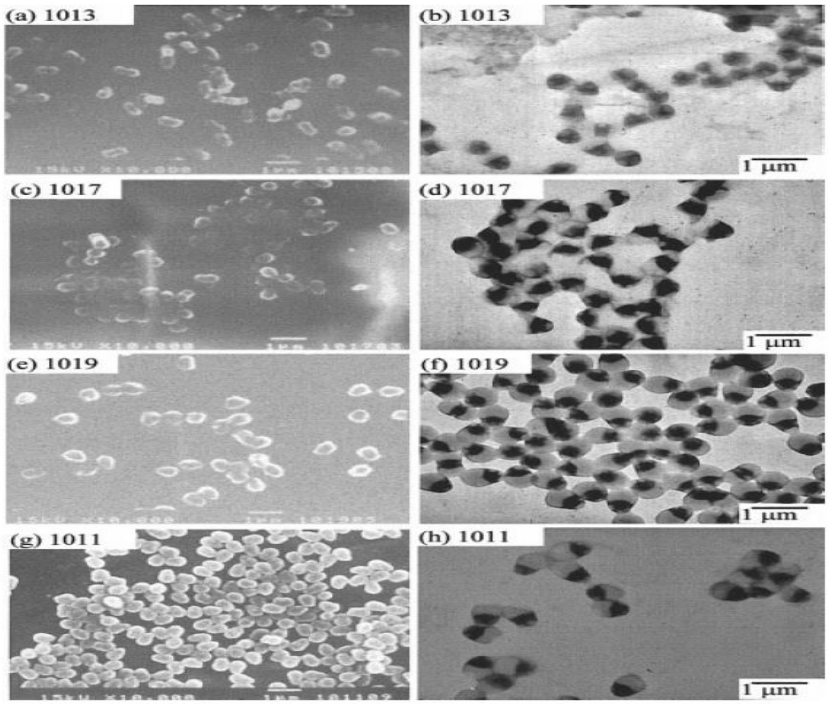


**Figure 1-7**: SEM and TEM photos of composite particles. (a, c, e, g) SEM; (b, d, f, h) TEM. (a, b) Run 1013 (no toluene); (c, d) Run 1017 (3.75 g toluene); (e, f) Run 1019 (5 g toluene); (g, h) Run 1011 (7.5 toluene) [61].

About ***hollow morphology***, Hu et al. [62] prepared hollow micronsized poly (styrene-co-divinylbenzene) particles were produced in seeded emulsions polymerization in the presence of swelling solvents. They confirmed the formation of hollow poly (styrene-co-divinylbenzene) particles depended significantly on a fast and effective phase separation between the crosslinked shell and the swollen core that occurred only in the presence of an appropriate swelling solvent (Figure 1-8).

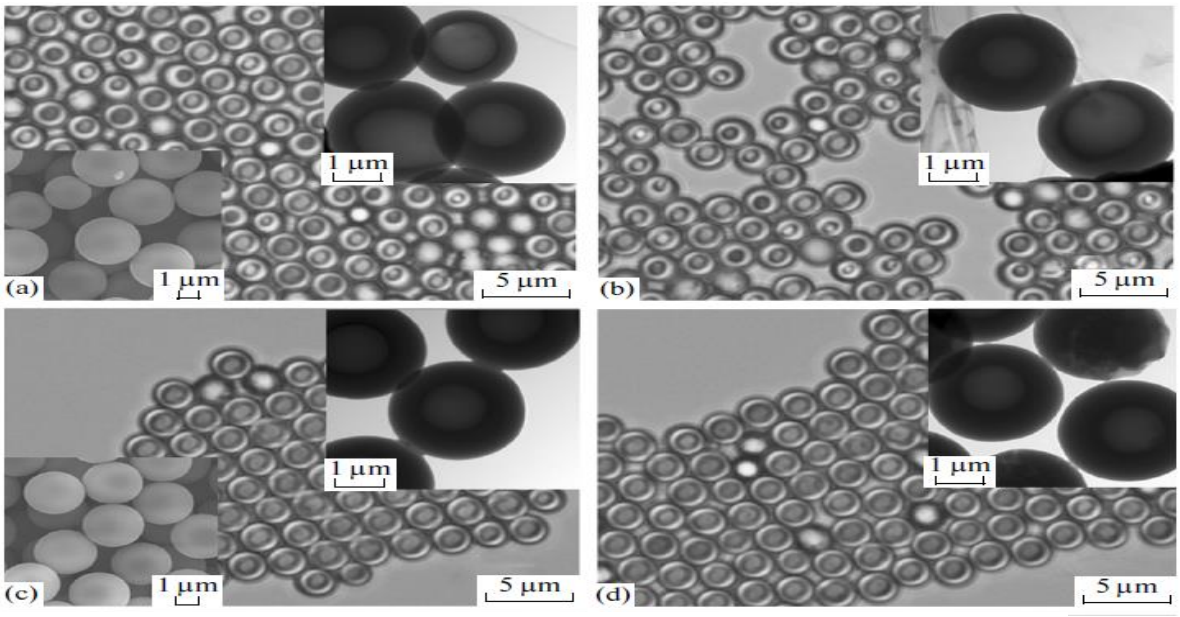


**Figure 1-8**: OM, SEM, and TEM images of polymer particles prepared in different hydrophobic solvents: (a) toluene, (b) xylene, (c) *n*-octane, (d) *n*-heptane [62].

## 1-3.2) Seeded Polymerization with Monomer Swollen Particles

Monomer-swelling with monomer-seeded polymerization is another method for preparation of non-spherical polymer particles. It has been used to construct snowman-shaped particles. Cho et al. [63] fabricated (nonspherical snowman-shaped micro-sized particles) were synthesized via monomer swelling and the polymerization of crosslinked seed particles. Monodispersed crosslinked polystyrene microspheres and methylmethacrylate were used as seed particles and the swelling monomer, respectively. Methylmethacrylate (MMA) induced crosslinked polystyrene microparticle swelling. They realized, phase separation occurred, resulting in monomer-swollen, cross-linked particles protruding from the surface of the seed particles. By changing the monomer-to-particle weight ratio from 4 to 8, the ratio of the size of the head to the body of the snowman-shaped particles was varied from 0.3 to 0.7 (Figure 1-9).

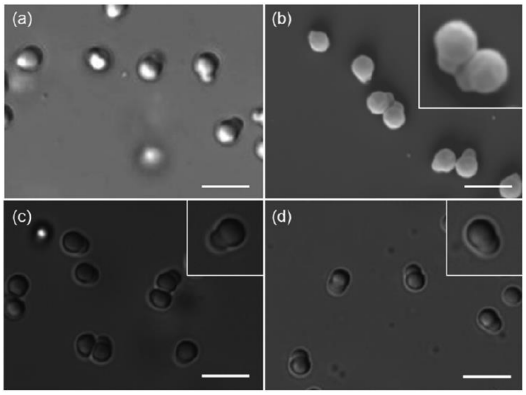


**Figure 1-9**: (a) Optical microscope image of CPS particles swollen with MMA (scale bar: 2 µm), (b) SEM image of polymerized CPS particles after swelling with MMA. Optical microscope images of polymerized monomer in swollen CPS particles after different polymerization times; (c) 6 hours and (d) 21 hours (The scale bar: 5 µm) [63].

## 1-3.3) Seeded Dispersion Polymerization

Seeded dispersion polymerization is a powerful technique for the preparation of nonspherical polymeric particles. Okubo et al. [64] reported that snowman/confetti-shaped, micron-sized, monodisperse composite particles were prepared by seeded dispersion polymerizations of n-butyl methacrylate (nBMA) with 1.28 and 2.67 µm-sized polystyrene (PS) seed particles, respectively, in an ethanol/water (80/20, w/w) medium. These nonspherical composite particles consisted of one or several poly (nBMA) protuberances on the surfaces of the spherical PS particles (Figure 1-10) and (Figure 1-11).

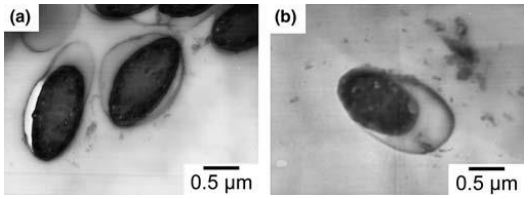


**Figure 1-10**: TEM photographs of PS/P nBMA composite particles prepared by seeded dispersion polymerizations with 1.28 µm-sized PS seed particles in the ethanol/water (80/20, w/w) medium at different AIBN concentrations (g/L): a 0.90; b 0.10 [64].

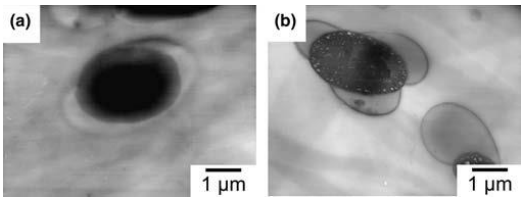


**Figure 1-11**: TEM photographs of PS/P nBMA composite particles prepared by seeded dispersion polymerizations with 2.67 µm-sized PS seed particles in the ethanol/water (80/20, w/w) medium at different AIBN concentrations (g/L): a 0.90; b 0.10 [64].

In another research they prepared micron-sized, monodisperse polymer particles having unique ‘‘disc-like’’ and ‘‘polyhedral’’ shapes were produced by seeded dispersion polymerization of various methacrylates with 1.57 µm-sized polystyrene seed particles in the presence of saturated hydrocarbon droplets in methanol/water. Such nonspherical shapes were controllable by the polymerization conditions (Figure 1-12) [65].

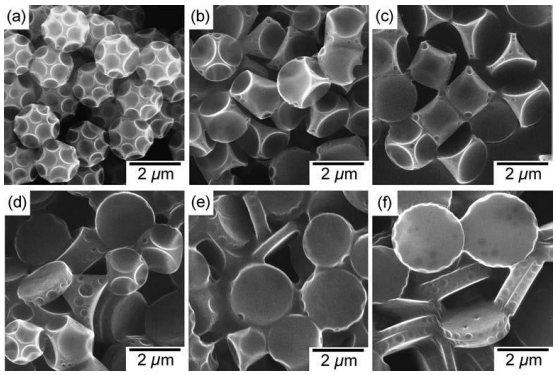


**Figure 1-12**: Scanning electron microscope photographs of PS/poly(lauryl methacrylate) (PLMA) composite particles produced by seeded dispersion polymerization in the presence of dodecane at various weight ratios of methanol/water media: a 80/20; b 82/18; c 84/16; d 86/14; e 88/12; f 90/10 [65].

## 1-4) Hole-transporting Semiconductor Polymers

The organic hole-transporting semiconductors play an important role in the field of electro-optical application. Among them, triarylamine (TAA) and its derivatives have been widely investigated because TAA has the high hole-transporting mobility and moreover it could be easily modified chemically, which allows the introduction of other functional groups to meet various requirements of different fields. Mono-butyl substituted PAA, poly(4-butyltriphenylamine) (PBTPA) showed the excellent photoconductivity compared with a conventional poly (N-vinylcarbazole) [66]. Palladium catalyzed C-N coupling reaction is also applied to prepare PAA and block copolymers consisting of PAA block from A-B type monomer [67, 68]. PAAs are also promising materials for photovoltaic [69] and photorefractive [70, 71] applications.

Meanwhile in this thesis, has been focused on polymeric microspheres for their own characteristics. Fujioka et al. [72] synthesized photo conductive PBTPA microspheres via chemical oxidative dispersion polymerization. They realized that surface morphology was dependent on the polymerization temperature so that at lower temperature (40 °C) porous particles were obtained with PVP as a dispersant. By increasing the temperature from 40 to 50 °C, porosity was disappeared. Moreover, the utilization of statistical copolymer of MMA with HEMA (30:70) afforded particles with the narrowest distribution in comparing with (50:50) and (70:30) ratios (Figure 1-13) and (Figure 1-14).

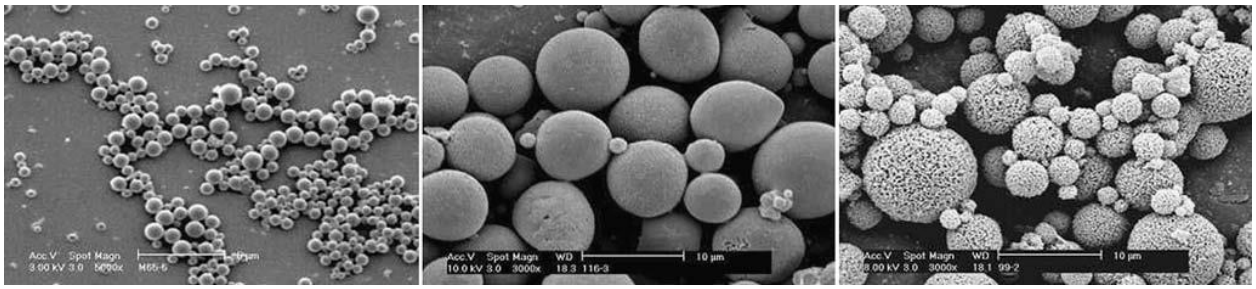

**Figure 1-13:** SEM photographs of PBTPA particles produced by chemical oxidative dispersion polymerization using PVP as a dispersant with different reaction temperature of 50 °C (a), 45 °C (b), and 40 °C (c) [72].

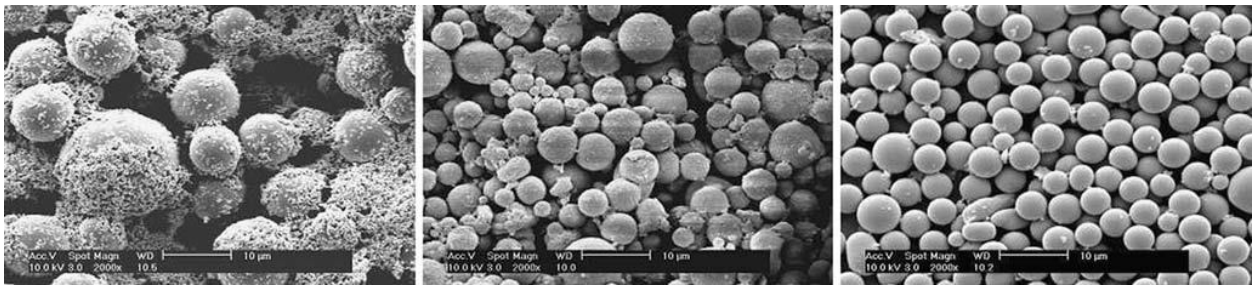

**Figure 1-14**: SEM photographs of PBTPA particles prepared by chemical oxidative dispersion polymerization using MMA–HEMA statistical copolymers as a dispersant. MMA/HEMA ratios are: 70:30 (a), 50:50 (b), and 30:70 (c) [72].

In further research, they prepared Polystyrene (PS)/poly (4-butyltriphenylamine; PBTPA) composite particles by a chemical oxidative seeded dispersion polymerization of PBTPA with PS seed particles [73]. Monodisperse composite particles were obtained when the ratio of monomer to seed, the rate of monomer feed and poly (N-vinyl pyrrolidone; PVP) concentration were appropriately selected. The size of composite particle can be controlled by changing seed particles while maintaining the monodispersity and dispersion stability. By solvent extraction with ethyl acetate it's revealed, composite particles consisted of PS core and PBTPA shell (Figure 1-15).

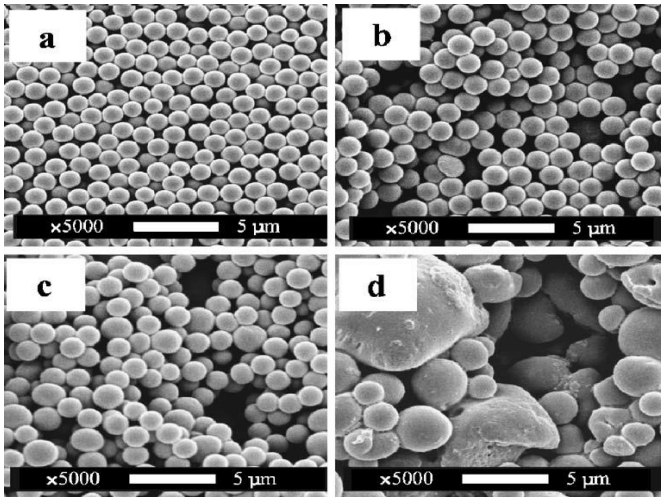


**Figure 1-15**: SEM photographs of PSt/BTPA composite particles produced by chemical oxidative seeded dispersion polymerization with different amount of BTPA (weight ratio based on PSt seed): a seed particles; b BTPA/PSt=0.5; c BTPA/ PSt=1.0; d BTPA/PSt=2 [73].

## 1-5) Porous Polymer Films

Porous polymer thin film can be prepared with a large number of different morphologies depending on the nature of polymers and on their applications. The pore may be open or closed. Their sizes (from some tens of A° to microns or more), their shapes (spheres, more or less tortuous tubes, completely disordered spaces), and the thickness of their walls may be controlled for optimization of their membrane properties [74].

Maeda et al. [75] reported that End-functional rod-coil type polymers were successfully prepared via the atom transfer radical polymerization (ATRP). Microporous films were easily fabricated by casting the polymer solution under moist air (Figure1-16).

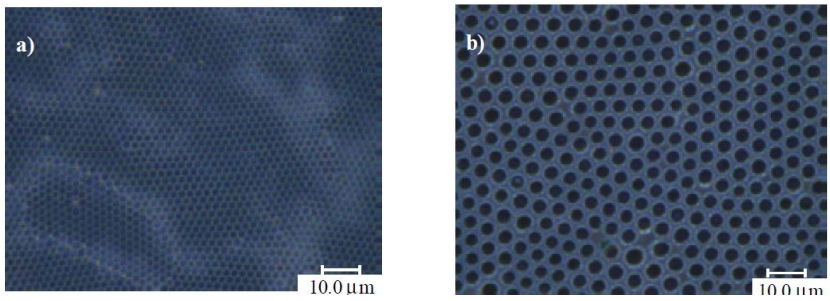


**Figure 1-16**: Optical micrograms of fabricated porous films polymer; P2b-2, a); 3 L/min, b) 10 L/min [75].

In further research, they made ordered microporous films utilizing amphiphilic block copolymers, poly(acrylic acid)-block-poly(styrene) via the controlled condensation and growth of water droplets on the cold surfaces resulting from solvent evaporation of polymer solutions. The

resulting pores became larger at higher flow rate. The copolymer characteristics including the length of hydrophilic and hydrophobic blocks, the concentration of copolymer and the type of a substrate also have effects on the pore size and its distribution (Figure 1-17) [76].

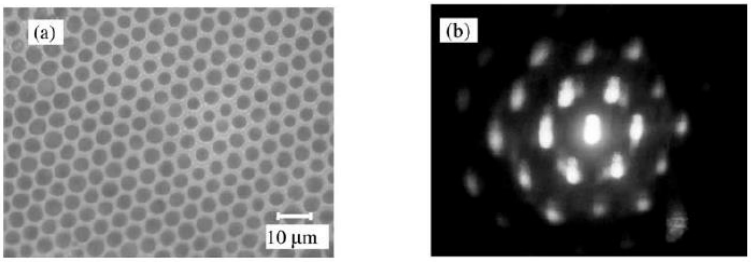


**Figure 1-17**: Microporous film fabricated using polymer 1 (concentration 0.1 wt%, flow rate 20 L/min, humidity 100 %), a): Optical micrograph, b) light scattering image with He-Ne laser [76].

Meanwhile, in another study, Li et al. [77] investigated the effects of some critical factors such as concentration of the diblock copolymer solution, solvent, temperature, particularly molar ratio of PS and PAA segment on the morphology of the obtained microporous films. The pore sizes of microporous films were decreased with the increasing concentration of diblock copolymer solution in both $CS_2$ and $CHCl_3$. Comparing with $CHCl_3$ as solvent, $CS_2$ with higher volatility benefits the formation of microporous films with smaller pores (pore size: 0.64–0.89 μm). At different temperature, microporous films with larger pore size were obtained at 25 °C than at 20 °C. The improvement of hydrophilicity from PS-*b*-P*t*BuA to PS-*b*-PAA can produce the microporous films with better regularity and larger pores. They observed no large difference in pore sizes of PS-*b*-PAA microporous films with the same amount of PAA segment, the obvious increase of pore size was shown when PAA/PS molar ratio increased while PS segment fixed.

## 1-6) Aims of This Thesis

As mentioned above, polymer particles are of great interest for a wide variety of application. In order to afford novel functionality to polymeric microspheres, it is important to control surface and inner morphology as well as the chemical structure, particle size and its distribution. In general, block copolymers show nanometer sized micro phase-separated structure, whereas simple polymer blends afford micrometer sized macro phase-separated. The addition of A-B block copolymer to the polymer blend consisting of homo polymers A and B decreases the domain size. Since phase separation in a micro sphere occurs in a limited space with large

interface, it is possible to generate specific surface and inner morphology compared with bulk samples. Therefor, it is of importance to understand the relationship between the fabrication conditions of micro spheres and resulting morphology.

The purpose of this study is the fabrication of microspheres with specific inner and surface morphologies using the polymer blend technology, including A, B homopolymers and A-B type block copolymers. As target blend systems, conventional PS/PMMA/PS-*b*-PMMA) and semiconducting poly (butyl- triphenylamine)/PMMA/ poly (butyltriphenylamine)-*b*-PMMA are considered. Firstly, all of the components of the former composite were synthesized via anionic polymerization and the latter composite, PBTPA fabricated by end-functionalized C-N coupling polymerization but PBTPA-b-PMMA block copolymer prepared using ATRP, respectively.

Here, for the first step, we should prepare well-defined (mono-disperse) polymer particles. As molecular weight and distribution of the prepared polymers influence the morphology of seeds, it's important to control both of them. For this reason, anionic polymerization and ATRP help to this issue. In our research, we utilized, the solvent evaporation method for fabrication of seed particles. In the next step, we have to optimize, the preparation conditions of polymer particles by this method. Some of these parameters are concentration of polymer solution, homogenize time, homogenize rate, speed of mechanical stirrer and so on. By considering these items, we can obtain desirable polymer particles.

Eventually, the final aim of this thesis is to control morphology of polymer particles based on polymer blends containing block copolymers.

## 1-7) Outlines of This Thesis

The title of this thesis is "morphology control of microspheres based on polymer blends containing block copolymers". Since micron-sized monodisperse polymer particles play a pivotal role in our research on final morphology for this reason at first, we should control the dispersion of them for further application by proper techniques.

In chapter 2, we will carry out living anion polymerization for synthesis of PS, PMMA and PS-b-PMMA. Then, prepare seed particles in micron size by a solvent evaporation method. We will review the obtained morphology for PS and PMMA, PS/PMMA, PS-b-PMMA and PS/PS-b-PMMA/PMMA seed particles and study about the content of block copolymer on ternary

polymer blend microspheres. In the next step, do seed polymerization of styrene and MMA utilizing above-mentioned seed particles in order to control the shape and surface morphology. By using SEM and TEM instruments, we observe the external and internal morphology.

In chapter 3, we will synthesize PBTPA and PBTPA-b-PMMA via C-N cross coupling and ATRP, respectively. By the same method (solvent evaporation method), prepare the seed particles and consider the morphology of PBTA, PBTPA/PMMA, PBTPA-b-PMMA and PBTPA/PBTPA-b-PMMA/PMMA microspheres. In addition, investigate the block content on morphology of ternary polymer blend. Meanwhile we survey the effect of polymer concentration on resulted morphology in order to select the optimum of concentration.

In chapter 4, we will fabricate microporous (honeycomb) film and microspheres hybrids from the amphiphilic block copolymer, poly (acrylic acid)-*block*-polystyrene) prepared via atom transfer radical polymerization (ATRP) followed by the acid catalyzed elimination reaction. The PS microspheres were prepared by dispersion polymerization and PS-DM by seeded dispersion polymerization, respectively. Since after drying, the surface of the film becomes hydrophobic, carboxyl groups go inside the film, hybridization did not occur via immersing the film into slurry of polymer particles, incorporation the microspheres inside the pores is possible by soaking the film in methanol. It happens because wettability increases. The embedding efficiency of microspheres modified with amino groups is much higher than conventional polystyrene microspheres. Electrostatic interaction plays an important role for the hybridization. With the increase of open pore size, multi-numbers of microspheres were embedded in a single pore.

## References


[1] Koning, C., Duin, M.V., Pagnoulle, C., *Prog. Polym. Sci.*, **23**, 707-757 (1998).

[2] Jiang, G., Wu, H., Guo, S., *Polym. Eng. Sci.*, **50**, 2273-2286 (2010).

[3] Hobbs, S.Y., Dekkers, M.E.J., Watkins, V.H., *Polymer*, **29**, 1598-1602 (1988).

[4] Chang, K., Robertson, M.L., Hillmyer, M.A., *ACS Appl. Mater. Interf.*, **1**, 2390-2399 (2009).

[5] Gibbs, J.W., *Connecticut Academy of Arts and Sciences*, New Haven, CT, 382–404 (1873).

[6] Flory, P.J., *J. Chem. Phys*., **9**, 660-661 (1941).

[7] Flory, P.J., *J. Chem. Phys.*, **10**, 51-61 (1942).

[8] Huggins, M.L., *J. Chem. Phys*., **9**, 440 (1941).

[9] Huggins, M.L., *J. Phys. Chem*., **46**, 151-158 (1942).

[10] Hildebrand, H.J., *J. Am. Chem. Soc*., **38**, 1452-1473 (1916).

[11] Scatchard, G., *Chem. Revs*., **8**, 321-333 (1931).

[12]Hildebrand, H.J., *The Solubility of Non-Electrolytes*; Reinhold: New York, NY, USA (1936).

[13] Hansen, C.M., *J. Paint. Technol.*, **39**, 104-117 (1967).

[14] Small, P.A., *J. Appl. Chem*., **3**, 71-80 (**1953).**

[15] Van Krevelan, D.W., *Properties of Polymers: Correlations with Chemical Structure*;

Elsevier:Amsterdam, The Netherlands, 135–142 (1972).

[16] Hoy, K.L., *J. Paint Technol*., **42**, 76-118 (1970).

[17] Coleman, M.M., Graf, J.F., Painter, P.C., *Specific Interactions and the Miscibility of*

*Polymer Blends*; Technomic Publishing Company Inc.: Lancaster, PA, USA (1991).

[18] Prigogine, I., *The Molecular Theory of Solutions*, North-Holland Pub., Amsterdam (1957).

[19] Flory, P.J., Orwoll, R.A., Vrij, A.J., *J. Am. Chem. Soc*., **86**, 3507-3514 (1964).

[20] Flory, P.J., Orwoll, R.A., Vrij, A.J., *J. Am. Chem. Soc*., **86**, 3515-3520 (1964).

[21] Flory, P.J., *J. Am. Chem. Soc*., **87**, 1833-1838 (1965).

[22] McMaster, L.P., *Macromolecules*, **6**, 760-773 (1973).

[23] Schmid, G., *Nanoparticles: from theory to application*, Weinheim, Wiley-VCH Pub. (2004).

[24] Geckeler, KE., Rosenberg E, editors., *Functional nanomaterials*, Valencia, Ameri. Scientif. Pub. (2006).

[25] Hosokawa, M., Nogi, K., Naito, M., Yokoyama, T., *Nanoparticle technology handbook*, Netherlands: Elsevier (2007).

[26] Geckeler, KE., Nishide, H., editors., *Advanced nanomaterials*, Weinheim, Wiley-VCH Pub. (2010).

[27] Wang, X., Summers, C.J., Wang, Z.L., *Nano Lett.*, **4**, 423-426 (2004).

[28] Jang, J.S., Oh, J.H., *Chem. Commun.*, **19**, 2200-2201 (2002).

[29] Fudouzi, H., Xia, Y., *Adv. Mater.*, **15**, 892-896 (2003).

[30] Brahim, S., Narinesingh, D., Elie, G.A., *Anal. Chim. Acta.*, **448**, 27-36 (2001).

[31] Zhang, Q., Chuang, K.T., *Adv. Environ. Res.*, **5**, 251-258 (2001).

[32] Kreuter, J., *Nanoparticles*, **66**, 219-342 (1994).

[33] Couvreur, P., *Crit. Rev. Ther. Drug. Carr. Syst.*, **5**, 1-20 (1988).

[34] Vauthier, C., *Handbook of pharmaceutical. controlled release technology*, 13-429 (2000).

[35] Couvreur, P., Dubernet, C., Puisieux, F., *Eur. J. Pharm. Biopharm.*, **41**, 2-13 (1995).

[36] Vanderhoff, JW., El Aasser, MS., Ugelstad, J., *Polymer emulsification process,* US Patent, 4, 177, 177 (1979).

[37] Allemann, E., Gurny, R., Doelker, E., *Eur. J. Pharm. Biopharm.*, **39**, 173-191 (1993).

[38] Anton, N., Benoit, JP., Saulnier, P., *J. Control Release*, **128**, 185-199 (2008).

[39] Bindschaedler, C., Gurny, R., Doelker, E., US Patent 4, 968, 350 (1990).

[40] Allemann,E., Gurny, R., Doelker, E., *Int. J. Pharm.*, **87**, 247-253 (1992).

[41] De Jaeghere, F., Allemann, E., Leroux, JC., Stevels, W., Feijen, J., Doelker, E., Gurny, R., *Pharm. Res.*, **16**, 859-866 (1999).

[42] Nguyen, CA., Allemann, E., Schwach, G., Doelker, E., Gurny, R., *Eur. J. Pharm. Sci.*, **20**, 217-222 (2003).

[43] Mishra, B., Patel, B.B., Tiwari, S., *Nanomedicine: NBM* , **6**, 9-24 (2010).

[44] Dalpiaz, A., Vighi, E., Pavan, B., Leo, E., *J. Pharm. Sci.*, **98**, 4272-4284 (2009).

[45] Fong-Yu, C., Saprina Ping-Hsien, W., Chio-Hao, S., Tsung-Liu, T., Ping- Ching, W., Dar-Bin, S., Jyh-Horng, C., Patrick Ching-Ho, H., Chen-Sheng, Y., *Biomaterials,* **29**, 2104-2112 (2008).

[46] Limayem, I., Charcosset, C., Sfar, S., Fessi, H., *Int. J. Pharm.*, **325**, 124-131 (2006).

[47] Ferranti, V., Marchais, H., Chabenat, C., Orecchioni, AM., Lafont, O., *Int. J. Pharm.*, **193**, 107-111 (1999).

[48] Moinard-Chécot, D., Chevalier, Y., Briancon, S., Beney, L., Fessi, H., *J. Colloid Interf. Sci.*, **317**, 458-468 (2008).

[49] Jeong, YI., Cho, CS., Kim, SH., Ko, KS., Kim, SI., Shim, YH., JW.*J. Appl. Polym. Sci.*, **80**, 2228-2236 (2001).

[50] Kostog, M., Kohler, S., Liebert, T., Heinze, T., *Macromol. Symp.*, **294**(2), 96-106 (2010).

[51] Jeon, HJ., Jeong, YI., Jang, MK., Park, YH., Nah, JW., *Int. J. Pharm.*, **207**, 99-108 (2000).

[52] Smith, M.W., *J. Am. Chem. Soc.*, **70**, 186 (1948).

[53] Ugelstad, J., *Sci. Tech. Colloid.*, NATO ASI, 51-99 (1983)

[54] Okubo, M., Fujiwara, T., Yamaguchi, A., *Colloid. Polym. Sci.*, **276**, 186-189 (1998).

[55] Ni, H., Ma, G., Nagai, M., Omi, S., *J. Appl. Polym. Sci.*, **80**, 2002-2017 (2001).

[56] Kegel, W.K., Breed, D., Elsesser, M., Pine, DJ., *Langmuir*, **22**, 7135–7136 (2006).

[57] Kim, J.W., Larsen, R.J., Weitz, D.A., *J. Am. Chem. Soc.*, **128**, 14374-14377 (2006).

[58] Zhou, L., Shi, S., Kuroda, S., Kubota, H., *Chem. Lett.*, **35**, 248–249 (2006).

[59] Fujibayashi, T., Okubo, M., *Langmuir*, **23**, 7958–7962 (2007).

[60] Joensson, J.E., Hassander, H., Toernell, B., *Macromolecules*, **27**, 1932-1937 (1994).

[61] Han, S.H., Ma, G.H., Du, Y.Z., Omi, S., Gu, L.X., *J. Appl. Poly. Sci.*, **90**, 3811-3821 (2003).

[62] Hu, G., Yu, D., Zhang, J., Liang, H., Cao, Z., *Colloid J.*, **73**, 557-564 (2011).

[63] Cho, Y.S., Kim, S.H., Moon, J.H., *Korean J. Chem. Eng.*, **29**, 1102-1107 (2012).

[64] Okubo, M., Fujibayashi, T., Yamada, Y., Minami, H., *Colloid Polym. Sci.*, **283**, 1041-1045 (2005).

[65] Okubo, M., Fujibayashi, T., Terada, A., *Colloid Polym. Sci.*, **283**, 793-798 (2005).

[66] Takahashi, C., Moriya, S., Fugono, N., Lee, H.C., Sato, H., *Macromol. Rap. Commun.*, **129**, 123-128 (2002).

[67] Tsuchiya, K., Shimomura, T., Ogino, K., *Polymer*, **50**, 95-101(2009).

[68] Tan, Y., Gu, Z., Tsuchiya, K., Ogino, K., *Polymer*, **53**, 1444-1452 (2012).

[69] Tsuchiya, K., Kikuchi, T., Songeun, M., Shimomura, T., Ogino, K., *Polymer*, **3**, 1051-1064 (2001).

[70] Cao, Z., Abe, Y., Nagahama, T., Tsuchiya, K., Ogino, K., *Polymer*, **54**, 269-276 (2013).

[71] Kinashi, K., Shinkai, H., Sakai, W., Tsutsumi, N., *Org. Electroni.*, **14**, 2987-2993 (2013).

[72] Fujioka, M., Kurihara, H., Kawamura, R., Sato, H., Tsuchiya, K., Ogino, K., *Colloid Polym. Sci.*, **286**, 313-318 (2008).

[73] Fujioka, M., Sato, H., Ogino, K., *Colloid Polym. Sci.*, **285**, 915-921 (2007).

[74] François, B., Pitois, O., François, J., *Adv. Mater.*, **7**, 1041 (1995).

[75] Maeda, Y., Koshiyama, Y., Shimoi, Y., Ogino, K., *Sen'i Gakkaishi*, **60**, 268 (2004).

[76] Maeda, Y., Shimoi, Y., Ogino, K., *Polym. Bulle.*, **53**, 315 (2005).

[77] Li, X.Y., Zhao, Q.L., Xu, T.T., Huang, J., Wei, L.H., Ma, Z., *Europ. Polym. J.*, **50**, 135-141 (2014).

# Chapter 2

# Morphology Control of Polymer Microspheres Containing Block Copolymers with Seed Polymerization

## 2.1) Introduction

Micron-sized, mono-disperse Polymer particles are of great interest for a wide variety of applications, for example, in the biomedical and environmental fields and in separation sciences [1-4].In past decades, several polymerization techniques have been utilized to prepare polymeric particles with different size, such as emulsion polymerization, soap-free emulsion polymerization, suspension polymerization, dispersion polymerization and seeded emulsion polymerization. Among these, seeded emulsion polymerization is a good method for the preparation of particles with unique morphologies, such as multilayered core-shell [5-12], hemispheres [13, 14], hollow structures [15, 16]. Okubo et al. reported seeded dispersion polymerization affording microspheres with specific shapes, such as snowman/confetti-like [17], hamburger-like [18], disk-like [19].

It is also expected that particles based on block copolymers and polymer blends exhibit specific morphologies resulting from phase separations. In order to fabricate nanoparticles with inner micro-phase separated structure, Yabu et al. reported self-organized precipitation method [20], in which a good solvent is evaporated from a block copolymer solution containing poor and good solvents. As for micron sized particles, the other type of solvent evaporation method have been used. In this method, a polymer solution is dispersed in an aqueous medium, and then the solvent is evaporated to solidify the polymer [22-24]. Phase-separation during the solvent evaporation afforded core-shell, inverted core-shell, microdomain, hemisphere morphologies[22], and nonspherical shape of polystyrene/poly(methyl methacrylate) composite [23, 24].

In order to afford novel functionality to polymeric microspheres, it is important to control surface and inner morphology as well as the chemical structure, particle size and its distribution. In general block copolymers show nanometer sized microphase-separated structure, whereas simple polymer blends afford micrometer sized macrophase-separated structure. The addition of A-B block copolymer to the polymer blend consisting of homopolymers A and B decrease the

domain size. Since phase separation in microspheres occurs in a limited space with large interface, it's possible to generate specific surface and inner morphology compared with bulk samples. Thus it's important to understand the relationship between the fabrication conditions of microspheres and resulting morphology. In this paper, surface and inner morphologies were investigated for the microspheres based on the blends consisting of polystyrene (PS), poly (methyl methacrylate) (PMMA) and PS-*b*-PMMA, and seed polymerizations of styrene and MMA were also conducted utilizing blend particles as the seed particles.

# 2.2) Experimental

## 2.2.1) Materials

Styrene, methyl methacrylate (MMA) (Wako Chemical, Japan), 1,1-diphenyletylene (DPE) (TCI, Japan) were purified by distillation under vacuum and stored in refrigerator before used. Tetrahydrofuran (Wako Chemical) was used as freshly distilled over sodium and benzophenone. sec-Butyl lithium (sec-BuLi) (1M in hexane) (Kanto Chemical, Japan), poly(vinyl alcohol) (PVA) (Kuraray, PVA224) as a stabilizer, 2,2'-azobis(isobutyronitrile) (AIBN) (TCI, Japan) as an initiator for radical seeded polymerization, sodium dodecyl sulfate (SDS) (TCI, Japan) as an emulsifier were used as received.

## 2.2.2) Anion Polymerization of Styrene

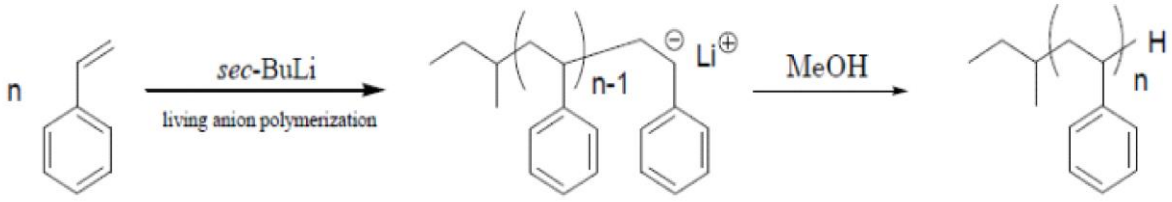


Fig. 2-1 Synthesis route of polystyrene.

After the evacuation followed with backfilling of nitrogen, 100-mL two-necked flask containing a magnetic stirrer bar was charged with dry THF (50 mL) under nitrogen atmosphere with a gas - tight syringe. After the temperature was down to -78° C with a dry ice /acetone bath, 0.96 mL (0.96 mmol) of *sec*-BuLi, and 10.1 mL of Styrene (0.096 mol) were successively injected to the

flask with gas-tight syringes. After 1 h, the reaction mixture was precipitated into methanol. The product was filtrated, washed with methanol and dried in vacuo. Yield: 9.28 g (93%).

### 2.2.3) Anion Polymerization of Methyl methacrylate

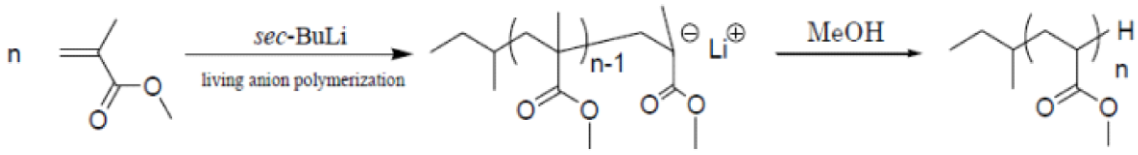


Fig. 2-2 Synthetic route of PMMA.

The procedure similar to that mentioned above was utilized. Under nitrogen atmosphere 30 mL of dry THF was added to the flask. After cooling to -78° C, 1 mL of *sec*-BuLi (1.00 mmol), and 10.6 mL of MMA (0.100 mol) were successively injected to the flask. After 1 h, the content of flask was poured into methanol. Yield: 7.36 g (73.6%).

### 2.2.4) Synthesis of Polystyrene-b-Poly (methyl methacrylate)

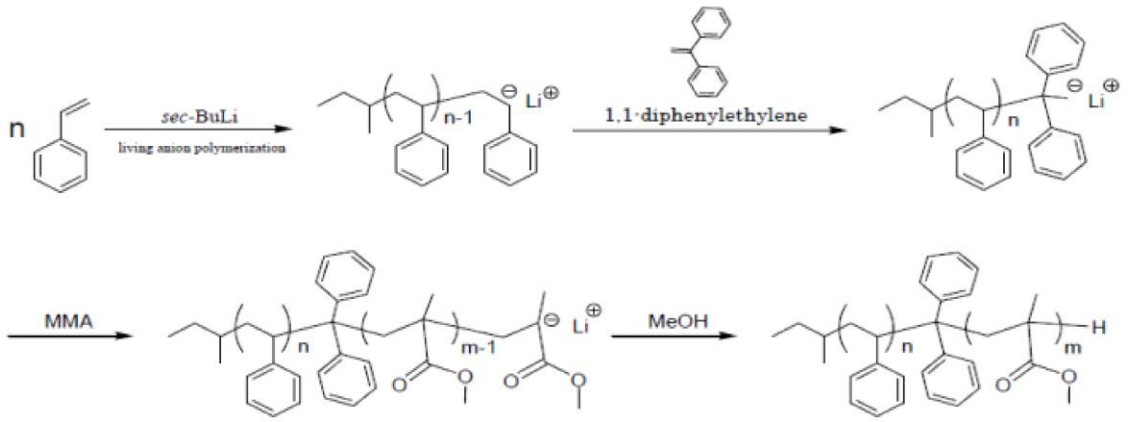


Fig. 2-3 Synthetic route of PS-*b*-PMMA.

Under nitrogen atmosphere 60 mL of dry THF was added to the flask. After cooling to -78° C, 1 mL of *sec*-BuLi (1.00 mmol), and 11.5 ml of Styrene (0.100 mol) were successively injected to the flask. After 1 h, 0.18 mL of DPE (1.00 mmol) was added dropwise. After stirring for 30 min,

10.6 mL of MMA (0.100 mol) was injected to the mixture. After 3 h, the reaction mixture was poured into methanol to precipitate the product. Yield: 18.0g (88%).

## 2.2.5) Preparation of Seed Particles

Polymers (total; 1.5 g) were dissolved in 15 mL of dichloromethane. The solution was dispersed in 150 mL of $H_2O$ containing 0.5 g of PVA with a homogenizer (X520, CAT Scientific, US) to obtain 5-15 μm sized droplets. Dispersion was transferred to 300-mL beaker equipped with a mechanical stirrer, and the stirring was continued for 24 h to evaporate the solvent. The resulting particles were washed with distilled water with a centrifugation process.

## 2.2.6) Seed Polymerization of Styrene and Methyl methacrylate

The dispersion of 0.5 g of seed particle in 40 mL of $H_2O$ containing 0.24 g of PVA and 0.1 g of SDS 0.1 g was charged into the 100-mL three-necked flask with a mechanical stirrer. At 80 rpm, the emulsion of typically 0.5 g of monomer (Styrene or MMA) and 40 mg of AIBN in 10 mL of $H_2O$ containing 0.06 g of PVA and 0.02 g of SDS 0.02 g was dropwise added to the flask. After 24 h, the temperature increased to 70° C to initiate polymerization. After polymerization for 4 h, the product was washed with water and methanol, successively.

## 2.2.7) Characterization

Resulting PS, PMMA and PS-*b*-PMMA were characterized with $^1$H-NMR (ECX 300, JEOL). Molecular weight and polydispersity (PDI) were estimated by gel permeation chromatography (GPC) equipped with JASCO 880-PU pump, a column packed with styrene-divinylbenzene gel beads [25], and a JASCO UV-970 detector. The surface feature of microspheres after evaporation of dichloromethane was characterized by scan-ning electron microscope (SEM) (JSM-6510, JEOL). Chloroform was used as an eluent, and the molecular weight was calibrated using polystyrene standards (SHODEX). The specimens for SEM observations were prepared by coating a thin gold film on the sample with an ion sputter coater (IB-3, Eiko Engineering, Japan). The morphologies inside the polymer particles were observed with transmission electron microscope (TEM) (JEM-2100, JEOL, Japan). The TEM specimens were prepared by cutting ultrathin films (ca. 70 nm in thickness) from particles embedded in epoxy resin (Epok 812) with an ultramicrotome (EM UC7, Leica, Germany) and setting them on the copper meshes. The PS

domain was stained by exposing the specimens to the vapor of an aqueous $RuO_4$ solution (0.5%) for 90 min in a sealed bottle at room temperature.

## 2.3) Results and Discussion

### 2.3.1) Synthesis of Various Polymers by Anionic Polymerization

#### 2.3.1.1) Synthesis of PS

The addition of sec-BuLi / n-hexane to the colorless THF solution changed to pale yellow. Adding the St leaded to red color was appeared. When the reaction is stopped by adding methanol, the color of the solution varied from red color to pale yellowish white. The PS obtained by Re-precipitation purification was a white solid. The yield of white solid was obtained by vacuum drying 9.28 g, yield 93%. Obtained from the results of GPC measurement of the synthesized PS, I referred to a number average molecular weight (Mn), molecular weight distribution of (PDI) in the Table 2-1. In addition, from the results of 1H-NMR, the peak derived from phenyl groups are observed in the vicinity of 6 ~ 7 ppm, we confirmed the PS is generated.

**Table 2-1**: PS Synthesis

| Sample No. | Target $M_n$ | Feed ratio /mol% | | $M_n$ | PDI |
|---|---|---|---|---|---|
| | | $[Li]_0$ | $[St]_0$ | | |
| **PS-1** | 10000 | 1 | 100 | 11000 | 1.23 |
| **PS-2** | 10000 | 1 | 100 | 12000 | 1.25 |
| **PS-3** | 10000 | 1 | 100 | 10000 | 1.15 |

#### 2.3.1.2) Synthesis of PMMA

The addition of sec-BuLi / n-hexane to the colorless THF solution changed to pale yellow. Adding the MMA didn't change the color of solution. MeOH was utilized to terminate the reaction while solution color was unchanged. The PMMA was obtained by re-precipitation purification that was a white solid. The yield of white solid was obtained by vacuum drying 7.36 g, the yield was 67%. Obtained from the results of GPC measurement of the synthesized PMMA, I referred to a number average molecular weight (Mn), molecular weight distribution of (PDI) in

the Table 2-2, The results of 1H-NMR, α- peak derived from methyl groups are observed in the vicinity of 0 ~ 1 ppm , we confirmed that the PMMA is generated.

**Table 2-2**: PMMA Synthesis

| Sample No. | Target $M_n$ | Feed ratio /mol% | | $M_n$ | PDI |
|---|---|---|---|---|---|
| | | $[Li]_0$ | $[MMA]_0$ | | |
| **PMMA-1** | 10000 | 1 | 100 | 13000 | 1.45 |
| **PMMA-2** | 10000 | 1 | 100 | 12000 | 1.25 |
| **PMMA-3** | 10000 | 1 | 100 | 12000 | 1.32 |

## 2.3.1.3) Synthesis of PS-b-PMMA

The addition of sec-BuLi / n-hexane to the colorless THF solution changed the color to pale yellow. Adding the Styrene leaded to red color was appeared. The color of the solution didn't change by injecting 1, 1-diphenylethylene, but injection of MMA changed red color to pale yellowish white so that obtained color remained even after methanol was added as a reaction terminator. The dry white solid product was obtained by Re-precipitated of row product and then drying under vacuum. The yield of a white solid 8.84 g, yield was 88%. Obtained from the results of GPC measurement of the synthesized PS-b-PMMA, I referred to a number average molecular weight (Mn), molecular weight distribution of (PDI) in the Table 2-3. Then, I show the results of 1H-NMR in following diagram. The PS unit phenyl group derived from peak 6 ~ 7 ppm from the peak derived from α- methyl group derived from PMMA unit was observed in 0 ~ 1 ppm. Each peak was integrated, was determined the composition ratio of PS and PMMA in block copolymer, and PS: PMMA = 1: 1.

**Table 2-3**: PS-b-PMMA synthesis

| Sample No. | Target $M_n$ | Feed ratio /mol% | | | | $M_n$ | PDI |
|---|---|---|---|---|---|---|---|
| | | $[Li]_0$ | $[St]_0$ | $[DPE]_0$ | $[MMA]_0$ | | |
| **Block-1** | 20680 | 1 | 100 | 1 | 100 | 23000 | 1.40 |
| **Block-2** | 20680 | 1 | 100 | 1 | 100 | 28000 | 1.28 |
| **Block-3** | 20680 | 1 | 100 | 1 | 100 | 25000 | 1.24 |

## 2.3.2) Preparation of Seed Particles

Table 2-4 shows number average molecular weight, $M_n$ of PS, PMMA and PS-*b*-PMMA, obtained from anion polymerization. All the seed particles were fabricated using these three polymers. PVA concentration was adjusted to 0.6 wt% so that regular, spherical particles with a diameter of 3-10 μm are obtained.

**Table 2-4**: Molecular weight of PS, PMMA and PS-b-PMMA

| Polymer | $M_n^{PS}$(g mol$^{-1}$) [a] | $M_n^{PMMA}$(g mol$^{-1}$) [a] | PDI [b] | $f_{PS}$ [c] |
|---|---|---|---|---|
| **PS** | 10,000 | ---------- | 1.15 | ----- |
| **PMMA** | -------- | 12,000 | 1.25 | ----- |
| **PS-b-PMMA** | 13,000 | 12,000 | 1.24 | 0.5 |

a. Determined by GPC., b. polydispersity index determinded by GPC, c. volume fraction of PS

### 2.3.2.1) Preparation of Seed Particles Using PS

For attainment to mono-disperse as possible in micrometer particle size, stirring method and stirring time also dispersion stabilizer (surfactant) concentration using PS are investigated.

#### *2.3.2.1.1) Consideration of Stirring Method and Stirring Time*

Size of seed particles is determined by size of oil droplets when suspended in water-oil mixture by solvent evaporation method. Thus, it's important to control size of oil droplets. Then we focused on stirring time of dispersion.

1) Dispersed by ultrasonic for 10 min, 2) Dispersed by ultrasonic for 10 min and decantation, 3) Dispersed by homogenizer for 30 min and decantation, 4) Dispersed by homogenizer for 60 min and decantation

Figure 2-1shows the mentioned methods. The time for dispersion by ultrasonic dispersion machine should be short. By increasing the time, size of particles changed from micrometer to nanometer that is not desirable. Since in this study are intended to obtain particles of micrometer size, time dispersion by ultrasonic wave was adjusted to 10 minutes.

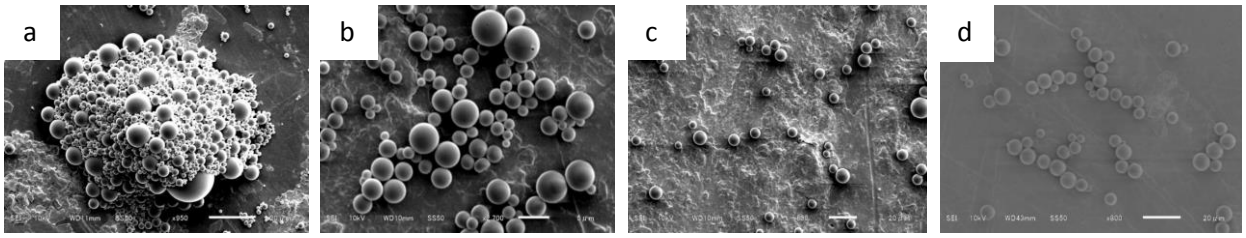


**Figure 2-1**: SEM images of (a, b) ultrasonic, (c, d) homogenization

### *2.3.2.1.2) Consideration of Concentration of Stabilizer*

Figure 2-2 exhibits various concentrations of PVA. As, we know concentration of stabilizer in the emulsion influences size of oil droplet during the process. Therefore, we adjusted it in which size of seed particles to be about 3 ~ 10 µm. Observations indicated that by increasing the concentration, particle size diameter decreased. In addition, high content of PVA lead to formation of secondary nucleation.

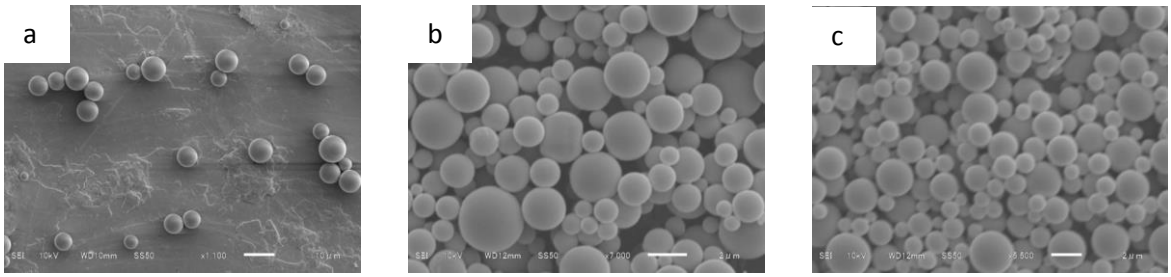


**Figure 2-2**: SEM images of polymer particles prepared with (a) 0.6, (b) 1.5, (c) 3 %wt PVA

## 2.3.2.2) Preparation of Various Types of Seed Particles

### *2.3.2.2.1) Polymer Particles Produced of Singular (PS, PMMA) Homopolymer*

Figure 2-3 shows SEM images of PS and PMMA homo-polymer seed particles. As seen in shapes, spherical seed particles obtained with size 3 ~ 10 µm. Since both of particles made from a single polymer, there is no phase separation inside the particles so that in it's considered to be a single internal structure.

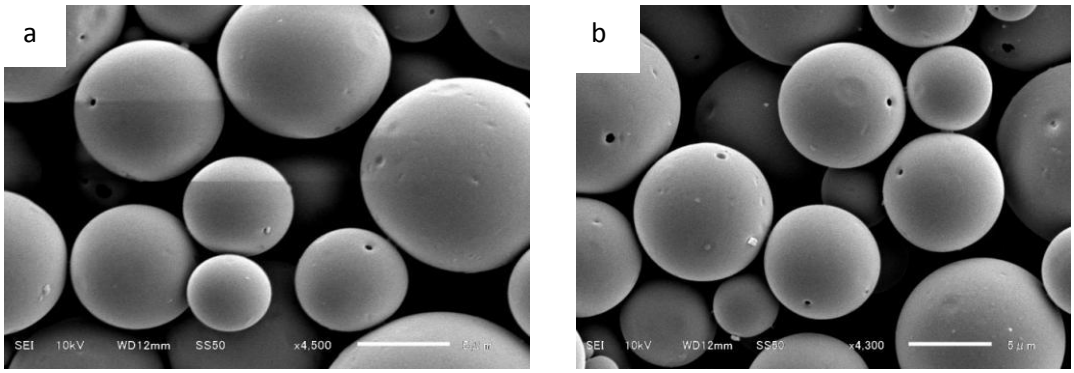


**Figure 2-3**: SEM photographs of homopolymer seed particles. (a) PS; (b) PMMA

### *2.3.2.2.2) Polymer Particles Produced of Binary (PS/PMMA) Polymer Blend*

Figure 2-4 shows SEM images of PS/PMMA (PS/PMMA=1:1) polymer blend seed particles. As seen in shapes, spherical seed particles obtained with size 3 ~ 10 µm. Surface structure were substantially the same as when using a homopolymer. As Ma et al. reported typical core-shell phase-separated structure obtained when PVA was used as a stabilizer in which, PS particles belong to core and PMMA particles form shell of structure [22].

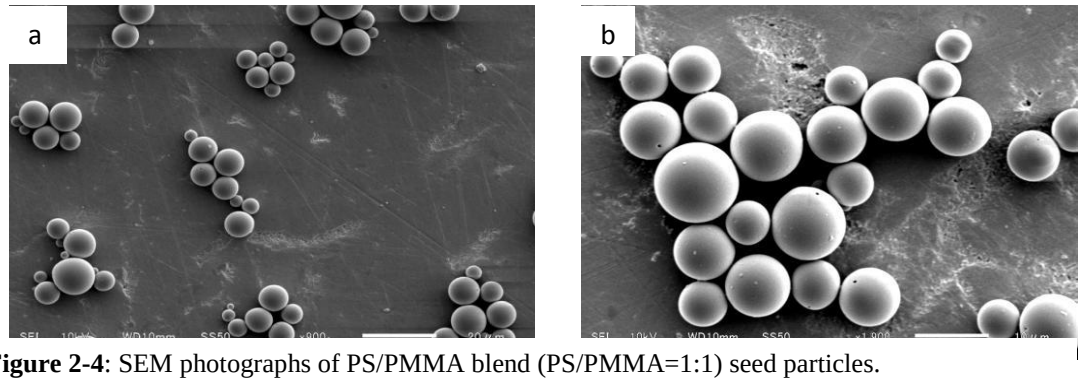


**Figure 2-4**: SEM photographs of PS/PMMA blend (PS/PMMA=1:1) seed particles.

### *2.3.2.2.3) Polymer Particles Produced of (PS-b-PMMA) Block Copolymer*

Figure 2-5 shows SEM images of PS-b-PMMA seed particles. The surface and size of these particles is similar to homo polymer and polymer blend that already mentioned. Unlike polymer blend with macrophase-separated morphology (core-shell), onion-like microphase-separated structure obtained in which PMMA particles form outermost layer [21].

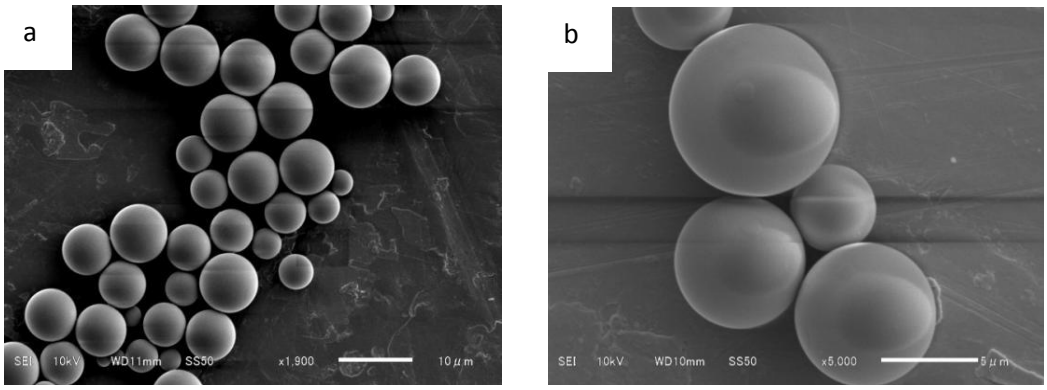


**Figure 2-5**: SEM photographs of PS-b-PMMA seed particles.

***2.3.2.2.4) Polymer Particles Produced of Ternary (PS/PS-b-PMMA/PMMA) Polymer Blend***

Figure 2-6 shows SEM images of PS/PS-b-PMMA/PMMA seed particles. As seen in the images particles with a boundary were obtained. The addition of %10 of PS-b-PMMA afforded particles having line-shaped recess near the center of seed (a). By increasing of the content of PS-b-PMMA to 20 %, particles with one smooth side and another rough side were obtained (b). In the case of 30 and 40 %, the portion of rough surface seemed to increase compared with 20 % particles (c, d).

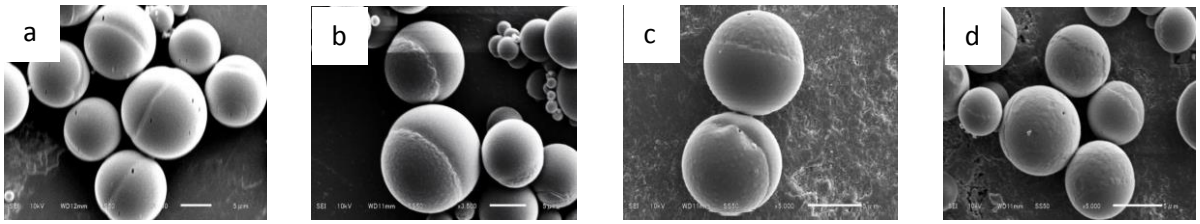


**Figure 2-6**: SEM photographs of PS/PS-b-PMMA/PMMA seed particles. φ PS/φPS-b-PMMA/ φPMMA: (a) 0.45/0.1/0.45; (b) 0.4/0.2/0.4; (c) 0.35/0.3/0.35; (d) 0.3/0.4/0.3.

Figure 2-7 shows TEM images of PS/PS-b-PMMA/PMMA seed particles having %10 of block copolymer. As PS is preferentially stained, black sites represent PS rich domain. According to typical three types of images Figure 2-7 (a-c), plausible morphology inside the particle is schematically represented in Figure 2-7 (d). It is found that the observed morphology is complex and intermediate between Janus and core-shell types.

Taking the low content and the comparable segment molecular masses of the block copolymer into consideration, macroscopic phase separation is expected. In general, it is

supposed that A-B type block or graft copolymer acts as a compatibilizer for the homopolymers (A and B) blend. Block or graft copolymer decreases the free energy of interface between the polymer blend to facilitate the mixing of two phases. In this report, it is reasonable that PS-*b*-PMMA exists both in PS-rich and PMMA-rich phases, which decreases the difference of the surface energies at the interface between both oil and water phases (PS-rich phase and PMMA-rich phase). As a result, a part of PS-rich phase can locate at the interface with water to exhibit the intermediate morphology. In this morphology, PMMA unit of PS-*b*-PMMA in PS-rich domain is considered to be located at the interface between polymer and water phases to decrease the interfacial energy. Therefore, surface roughness observed in Figure 2-7(b-d) was probably derived from the aggregation of PS-*b*-PMMA near the surface of PS-rich domain.

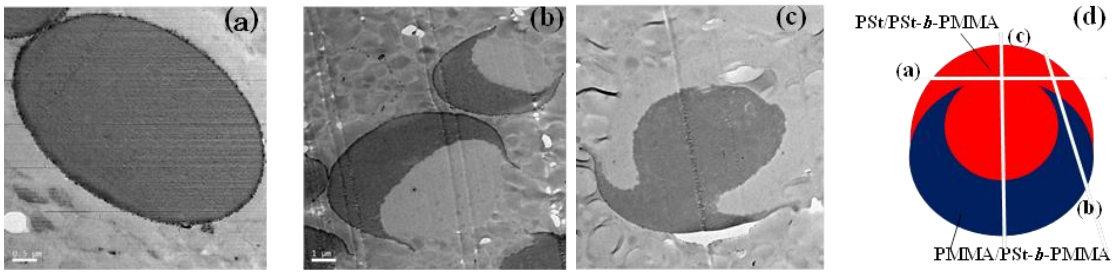


**Figure 2-7**: TEM photographs of ultrathin cross sections of RuO4-stained PS/PS-b-PMMA/PMMA seed particles prepared by solvent evaporation method. φ PS/φPS-b-PMMA/φPMMA: 0.45/0.1/0.45.

## 2.3.3) Seed Polymerization

In a previous session, microspheres with various morphologies were obtained. Seed polymerizations of styrene and MMA were carried out in order to elucidate the effect of polymerization conditions on the final morphology.

### 2.3.3.1) Seed Polymerization of MMA by PS and PMMA Homopolymer Seeds

Figure 2-8 shows SEM images of polymer particles prepared by seed polymerization of MMA using (a) PS and (b) PMMA homopolymer seed particles. Spherical seed particles with size of 3 ~ 10 μm were used. As is observed, there is no change in the microspheres surface using either PS or PMMA seed particles by MMA monomer. Since the MMA monomer is hydrophilic, skin layer of PMMA is formed on the surface of seed particles.

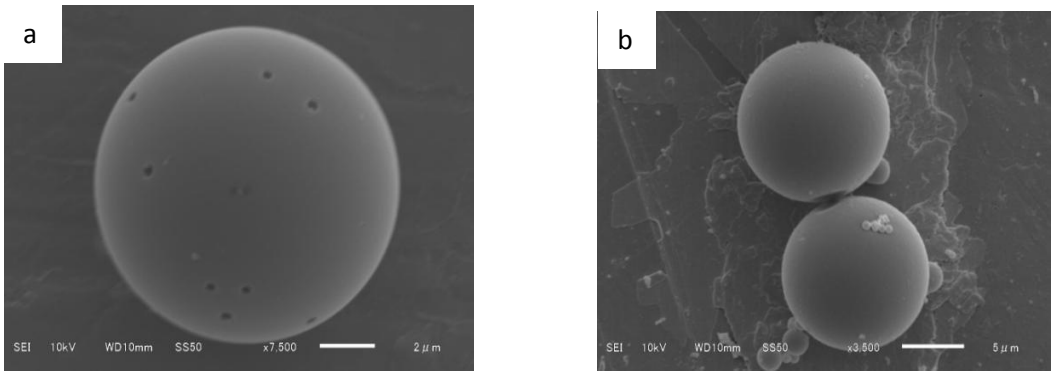


**Figure 2-8**: SEM photographs of polymer particles prepared by seed polymerization of MMA using (a) PS and (b) PMMA seed particles.

## 2.3.3.2) Seed Polymerization of MMA and Styrene by Binary (PS/PMMA) Polymer Blend Seeds

We have carried out seed polymerization using the monomer MMA and styrene, respectively. Seed particles used in this case is spherical particles of 3 ~ 10 μm.

### *2.3.3.2.1) Using MMA Monomer*

Figure 2-9 shows SEM images of polymer particles prepared by seed polymerization of MMA using PS/PMMA polymer blend seed particles. When the amount of MMA was 10 or 100 wt% (a, b), respectively, no significant change was observed, and spherical particles with smooth surfaces were obtained. On the other hand, seed polymerization of 200 wt% of MMA afforded non-spherical particles with a bulge. From the optical microscope observation, swollen particles with MMA monomer show spherical shapes. Therefore it is considered that polymerization induced the irregular shape in the case of 200 wt% of MMA. As described in a previous session, seed particles have a core-shell morphology, hydrophilic PMMA shell, and hydrophobic PS core. MMA monomer absorbed into seed particles is considered to be located in the shell part, and to be polymerized to form PMMA skin layer when the amount of MMA is not so high. With the increase of MMA monomer, the location of absorbed MMA extends over PS core as well as PMMA shell. Polymerization of MMA in PS phase induces the phase separation, resulting in the bulge.

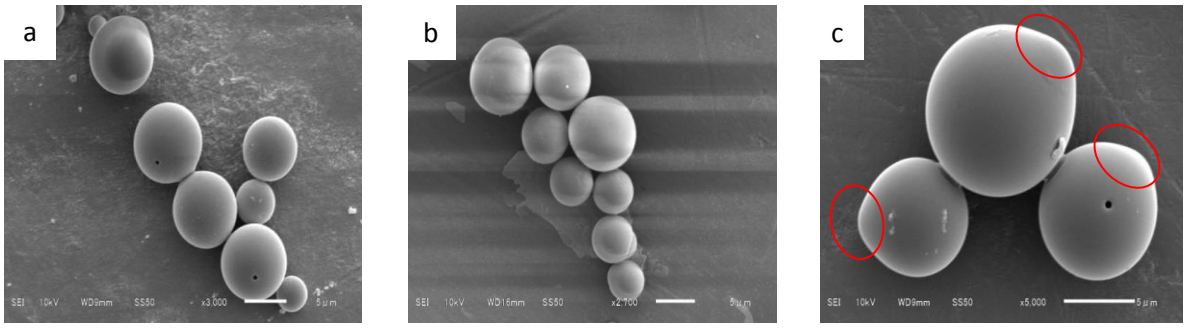


**Figure 2-9**: SEM photographs of polymer particles prepared by seed polymerization of MMA using PS/PMMA polymer blend seed particles. (a) MMA %10; (b) MMA %100; (c) MMA %200 wt.

### *2.3.3.2.2) Using Styrene Monomer*

Figure 2-10 shows SEM images of polymer particles after seed polymerization of styrene using PS/PMMA polymer blend seed particles. When 10 and 20 wt% of styrene was used, snowman-like particles were obtained Figure 2-10 (a, b). In the case of styrene, absorption of monomer also preferentially occurs at the PMMA shell, and stronger affinity between monomer and PS core makes it possible to swell PS core, resulting in protrusion of PS/styrene mixture from the surface consisting of PMMA and styrene monomer. Indeed Figure 2-11 indicated that snowman-like droplets were formed before polymerization both for 10 and 100 wt% of styrene. When 10 and 20 wt% of styrene was used, the viscosity in the protruded mixture is much higher than that for 100 wt % of styrene. Higher viscosity leads to fixation of the morphologies before polymerization. On the other hand, the decrease of viscosity in 100 wt% mixture changes the shape from the swollen stage during polymerization Figure 2-10 (c).

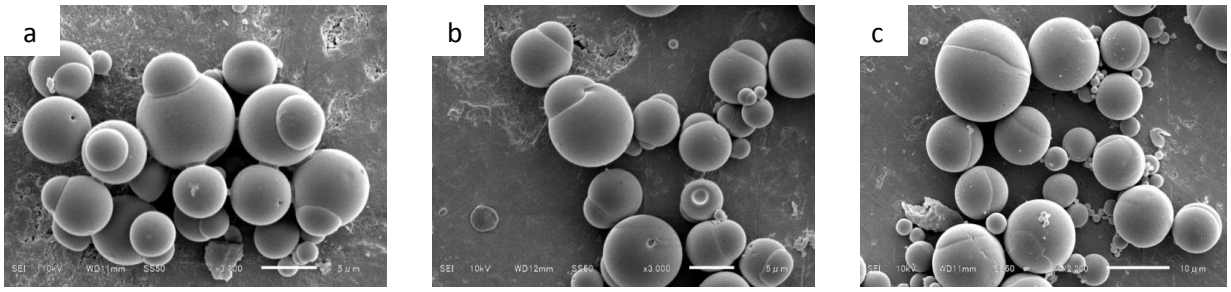


**Figure 2-10**: SEM photographs of polymer particles prepared by seed polymerization of styrene using PS/PMMA polymer blend seed paricles. (a) styrene %10 wt; (b) styrene %20 wt; styrene %100 wt.

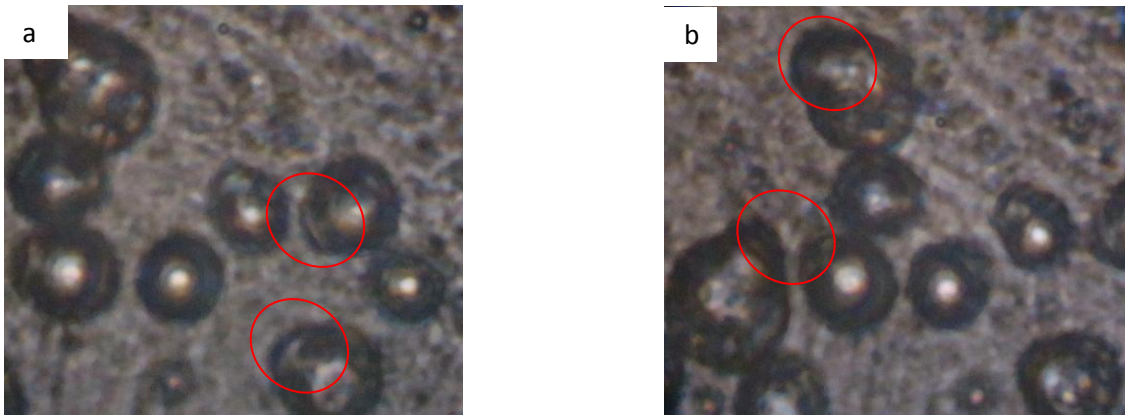


**Figure 2-11**: Optical microscope images of PS/PMMA seed particles after swelling with styrene (a); styrene %10 wt, (b) styrene %100 wt.

## 2.3.3.3) Seed Polymerization of MMA and Styrene by (PS-b-PMMA) Block Copolymer Seeds

We have carried out seed polymerization of PS-b-PMMA using the monomer MMA and styrene, respectively. Seed particles used in this case is spherical particles of 3 ~ 10 μm.

### *2.3.3.3.1) Using MMA Monomer*

Figure 2-12 shows SEM images of polymer particles after seed polymerization of MMA. Although the surface of seed particle is smooth (see Figure 2-12 (b)), small protrusions with 100 nm size emerged after polymerization. At the stage of monomer absorption, surface is considered to consist of the mixture of MMA and the block copolymer. During polymerization, phase separation of resulting PMMA occurs near the surface to form the protrusions. With the increase of MMA amount, the surface tended to be covered with resulting PMMA more smoothly, and the surface roughness became discreet.

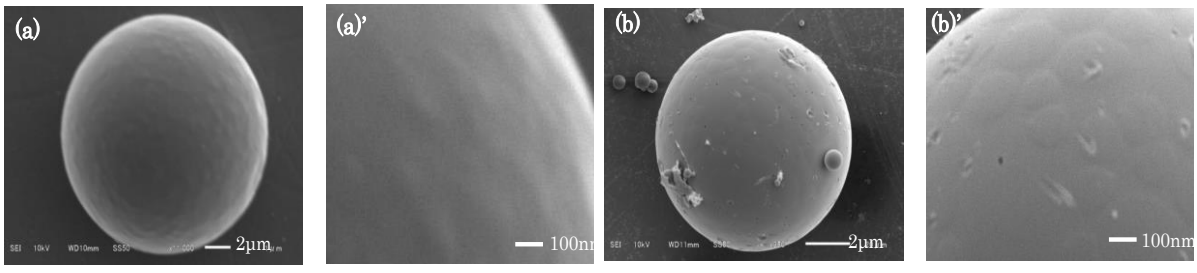


**Figure 2-12**: SEM photographs of polymer particles prepared by seed polymerization of MMA using PS-b-PMMA block copolymer seed particles. (a) (a)'; MMA %10 wt; (b) (b)';MMA %20 wt.

### *2.3.3.3.2) Using Styrene Monomer*

Figure 2-13 shows SEM images of polymer particles prepared by seed polymerization of styrene using PS-b-PMMA block copolymer seed particles. No significant morphology change was observed when styrene was used as a monomer as shown in Figure 2-13. Because of hydrophobicity of styrene, the absorbed monomer diffused toward the core direction compared with MMA. Polymerization of styrene and phase separation at the inside seems to have small effect on the surface morphology.

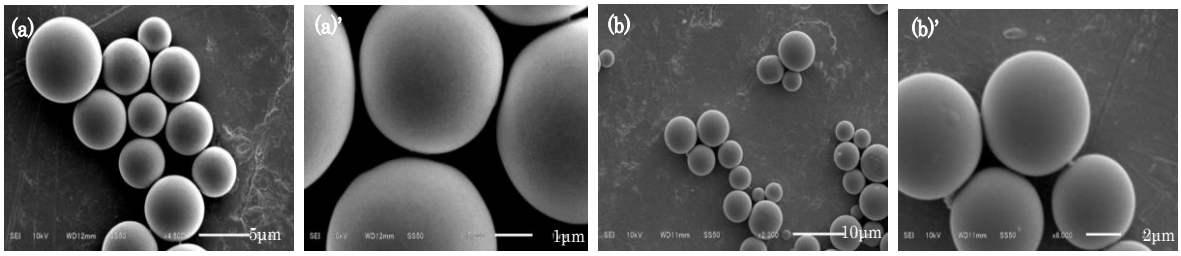


**Figure 2-13**: SEM photographs of polymer particles prepared by seed polymerization of styrene using PS-b-PMMA block copolymer seed particles. (a) %10 wt; (b) %20 wt; (c) %30 wt; (d) %40 wt; (e) %50 wt of styrene.

## 2.3.3.4) Seed Polymerization of MMA and Styrene by Ternary (PS/PS-b-PMMA/PMMA) Polymer Blend Seeds

### *2.3.3.4.1) Using MMA Monomer*

Fig 2-14 shows SEM images of polymer particles prepared by seed polymerization of 10 wt % of MMA using ternary (PS/PS-b-PMMA/PMMA) polymer blend seed particles. As discussed above, ternary blends consisting of PS, PS-*b*-PMMA, and PMMA show the unique bi-compartment morphologies. Seed particles with 20 or 30 wt % of the block copolymer have rough surface of one side due to the aggregation of PS-*b*-PMMA near the surface of PS-rich domain. As shown in Figure 2-14, the surface became smoother after polymerization. This is probably due to the averaging effect by the formation of skin layer of hydrophilic PMMA which is caused by the homogeneous distribution of MMA monomer on both surfaces.

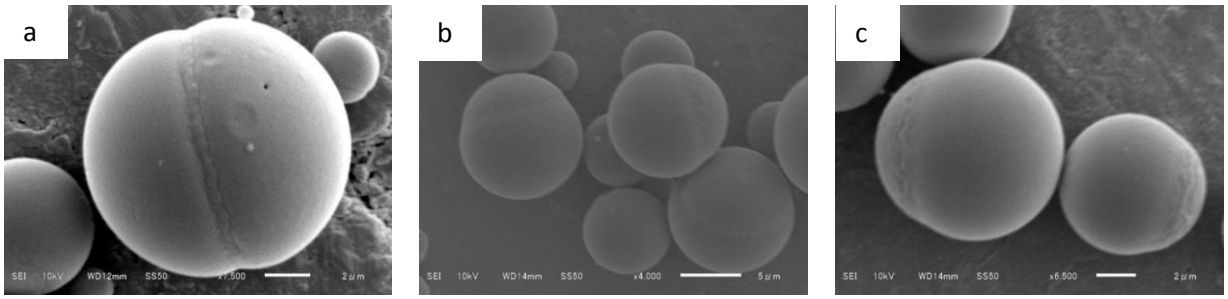


**Figure 2-14**: SEM photographs of polymer particles prepared by seed polymerization of 10 wt % MMA using ternary (PS/PS-b-PMMA/PMMA) polymer blend seed particles. φPS/φPS-b-PMMA/φ PMMA: (a) 0.45/0.1/0.45; (b) 0.4/0.2/0.4; (c) 0.35/0.3/0.35.

### *2.3.3.4.2) Using Styrene Monomer*

Figure 2-15 shows SEM images of polymer particles prepared by seed polymerization of styrene using ternary (PS/PS-b-PMMA/PMMA) polymer blend seed particles. The surface of PMMA-rich phase became rougher with the increase of the block copolymer content Figure 2-15 (b, c). More styrene monomer is probably absorbed in PMMA-rich phase for the particles with the high content of PS -*b*-PMMA, and polymerization induced phase separation inside the particle formed the protrusions.

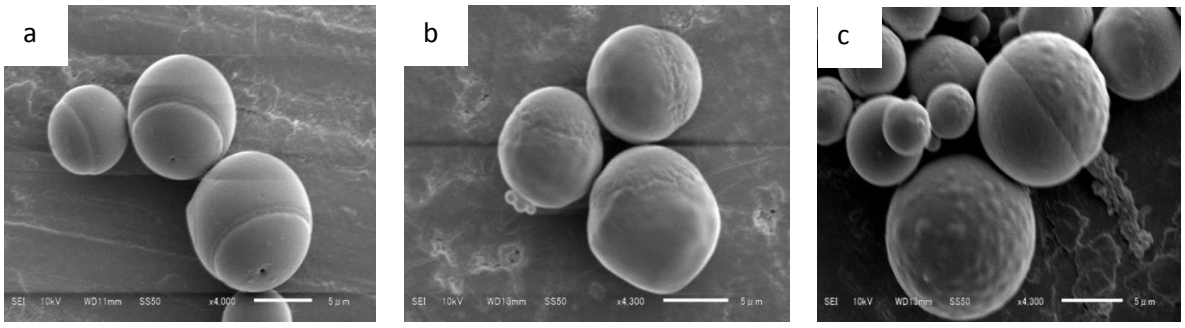


**Figure 2-15**: SEM photographs of polymer particles prepared by seed polymerization of 10 wt % of styrene using ternary (PS/PS-b-PMMA/PMMA) polymer blend seed particles. φPS/φPS-b-PMMA/φ PMMA: (a) 0.45/0.1/0.45; (b) 0.4/0.2/0.4; (c) 0.35/0.3/0.35.

## 2.4) Conclusion

The microspheres with various types of surface and inside morphologies consisting of PS/PMMA polymer blend, PS-*b*-PMMA block copolymer and ternary (PS/PS-*b*-PMMA/PMMA) polymer blend were fabricated by a solvent evaporation method. Ternary blends afforded a unique morphology, intermediate between Janus and core-shell types. Bi-compartment morphology was confirmed by TEM observation. The difference between

interfacial tension of two polymers with aqueous phase decreased by addition of block copolymer. Seed polymerizations of Styrene and MMA were also conducted, and the morphologies change was investigated. The particles with snowman-like morphology were obtained by seed polymerization of styrene using PS/PMMA binary blend micro-spheres as seed particles. Some seed polymerizations also controlled the surface roughness, i.e., polymerization of MMA in the block copolymer seed, and that of Styrene in the ternary blend seed. The microspheres with various surfaces and inside structure have potential applications in photonic and electronic fields.

## Refrences


[1] Pancholi, K., Ahras, N., Stride, E., Edirisinghe, M., *J. Mater. Sci.: Material in Medicine*, **20**, 917-923 (2009).

[2] Xie, J., Huang, J., Li, X., Sun, S., Chen, X., *Current Med. Chem.*, **16**, 1278-1294 (2009).

[3] Perrier-cornet, R., Heroguez, V., Thienpont, A., Babot, O., Toupance, T., *J. Chromatogr. A.* **1179**, 2-8 (2008).

[4] Garnett, M.C., Ferruti, P., Ranucci, E., Suardi, M.A., Heyde, M., Sleat, R., *Biochem. Soc. Trans.*, **37**, 713-716 (2009).

[5] He, Y., Daniel, E.S., Klein, A., El-Aasser, M.S., *J. Appl. Polym. Sci.*, **65**, 511-523 (1997).

[6] Joensson, J.E., Hassander, H., Toernell, B., *Macromolecules*, **27**, 1932-1937 (1994).

[7] Cunningham, M.F., Mahabadi, H.K., Wright, H.M., *J. Polym. Sci. ;Part A: Polym. Chem.*, **38**, 345-351 (2000).

[8] Oi, D.M., Bao, Y.Z., Huang, Z.M., Weng, Z.X., *J. Appl. Polym. Sci.*, **99**, 3425-3432 (2006).

[9] Muroi, S. Hashimoto, H., Hosoi, K., *J. Polym. Sci.; Polym. Chem. Ed.*, **22**, 1365-72 (1984).

[10] Daniel, E.S., Dimonie, V.L., El-Aasser, M.S., Vanderhoff, J.W., *J. Appl. polym. Sci.*, **41**, 2463-2477 (1990).

[11] Zhao, J., Yuan, H., Pan, Z., *J. Appl. Polym. Sci.*, **53**, 1447-52 (1994).

[12] El-Aasser, M.S., Hu, R., Dimonie, V.L., Sperling, L.H., *Colloid. Surf.; A: Phys. Chem. Eng. Asp.*, **153**, 241-253 (1999).

[13] Yabu, H., Tajima, A., Higuchi, T., Shimomura, M., *Hyomen Kagaku*, **28**, 277-282 (2007).

[14] Han, S.H., *J* Ma, G.H., Du, Y.Z., Omi, S., Gu, L.X., *Appl. Poly. Sci.*, **90**, 3811-3821 (2003).

[15] Hu, G., Yu, D., Zhang, J., Liang, H., Cao, Z., *Colloid J.*, **73**, 557-564 (2011).

[16] Zhang, Q., Yang, Z., Zhan, X., Chen, F., *J. Appl. Polym. Sci.*, **113**, 207-215 (2009).

[17] Okubo, M., Fujibayashi, T., Yamada, M., Minami, H., *Colloid. Polym. Sci.*, **283**, 1041-1045 (2005).

[18] Fujibayashi, T., Tanaka, T., Minami, H., Okubo, M., *Colloid Polym. Sci.*, **288**, 879-886 (2010).

[19] Okubo, M., Fujibayashi, T., Terada, A., *Colloid Polym. Sci.*, **283**, 793-798 (2005).

[20] Higuchi, T., Tajima, A., Motoyoshi, K., Yabu, H., Shimomura, M., *Angew. Chem.*, **48**, 5125-5128 (2009).

[21] Higuchi, T., Tajima, A., Yabu, H., Shimomura, M., *Soft Matter*, **4**, 1302-1305 (2008).

[22] Ma, G.H., Nagai, M., Omi, S., *J. Colloid Interf. Sci.*, **214**, 264-282 (1999).

[23] Okubo, M., Saito, N., Fujibayashi, T., *Colloi. Polym. Sci.*, **283**, 691-698 (2005).

[24] Saito, N., Kagari, Y., Okubo, M., *Langmuir*, **22**, 9397-9402 (2006).

[25] Ogino, K., Sato, H., Tsuchiya, K., Suzuki, H., Moriguchi, S., *J. Chromatog.: A*, **699**, 59-69 (1995).

# Chapter 3

# Fabrication of Microspheres Based on Poly (4-butyltriphenylamine) Blends with Poly(methyl methacrylate) and Block Copolymer by Solvent Evaporation Method

## 3.1) Introduction

Triarylamine derivatives have been used as hole-transporting materials in organic photoconductors, electroluminescent devices [1, 2]. Our group originally synthesized polyarylamines (PAAs) where triarylamine units are linked together at *para* positions by chemical oxidative polymerization using ferric chloride as an oxidant Mono-butyl substituted PAA, poly (4-butyltriphenylamine) (PBTPA) showed the excellent photoconductivity compared with a conventional poly (N-vinylcarbazole). Palladium catalyzed C-N coupling reaction is also applied to prepare PAA and block copolymers consisting of PAA block from A-B type monomer [5, 6]. PAAs are also promising materials for photovoltaic [7], and photorefractive [8, 9] applications.

Meanwhile, polymeric microspheres have attracted much interest and have been utilized in a number of fields. As for PAAs, we reported PBTPA microspheres and PBTPA / polystyrene (PS) composite microspheres prepared by chemical oxidative dispersion polymerization and seeded polymerization of BTPA, respectively.

Morphologically controlled microspheres have been widely investigated. For conventional vinyl polymers, seeded emulsion [12-14], dispersion [15-17], and suspension polymerizations have been utilized to obtain particles with the unique morphologies. In order to fabricate nanoparticles with inner micro-phase separated structure, Yabu et al. reported self-organized precipitation method [19, 20] in which a good solvent is evaporated from a block copolymer solution containing poor and good solvents. In order to fabricate the microspheres from polymer solutions, the other type of solvent evaporation method has been used, where a polymer solution is dispersed in an aqueous medium, and then the solvent is evaporated to solidify the polymer

[21-23]. Phase-separation during the solvent evaporation afforded core-shell, inverted core-shell, microdomain, hemisphere morphologies and non-spherical shape of polystyrene /poly (methyl methacrylate) composite [22, 23].

In this chapter, the solvent evaporation method was applied to fabricate the microspheres based on PBTPA/poly (methyl methacrylate) (PMMA) binary blends, and PBTPA/PBTPA-*b*-PMMA/PMMA ternary blends, and the relationship between the fabrication conditions and the morphologies was investigated. It is found that molecular weight of PBTPA in the case of PBTPA homopolymer and PBTPA/PMMA binary polymer blend, molecular weight of PMMA domain in PBTPA-b-PMMA block copolymers and also the concentration of original polymer solutions has a significant effect on the morphologies of the resulting particles.

## 3.2) Experimental

### 3.2.1) Synthesis of 4-(4'-bromophenyl)-4"-n-butyldiphenylamine (BTPA monomer)

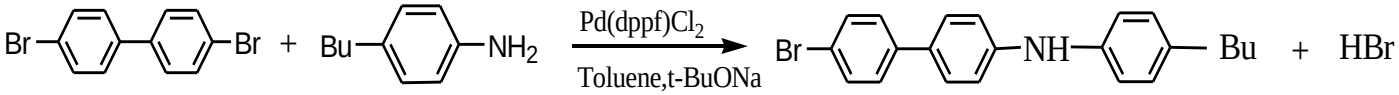


<Materials>

4-n-butylaniline (Aldrich), 4,4'-dibromobiphenyl (Aldrich), Sodium tert-butoxide (t-BuONa) (TCI); Reagent grade>98.0%, [1,1'- bis-(diphenylphosphino)ferrocene] dichloropalladium(II) ($Pd(dppf)Cl_2$) (Wako), Toluene (Wako).

<Operations>

The mixture of 4-n-butylaniline (5.96 ml, 40 mmol), 4,4'-dibromobiphenyl (12.48 g, 40 mmol), t-BuONa (5.38 g, 56 mmol) and $Pd(dppf)Cl_2$ (0.32 g, 0.4 mmol) was dissolved into dry toluene (80 ml) under nitrogen atmosphere and was stirred under reflux for 24 hr in a two-neck 200 ml flask. After that in order to stopping the reaction, a few drops of distillated water added to reaction flask. For more ease to phase separation, the reaction mixture filtrated to remove impurities (cat., salt and etc). Then solution washed at least 3 times by saturated brine, dried with

anhydrous $MgSO_4$, respectively. By filtration, concentrated solution separated and became ready for evaporation. In this step, residue purified by chromatographic column (toluene: hexane = 1:1). Finally, the product was extracted with Re-crystallization through hexane. The yield was 6.24 g (41%). $^1$H NMR [300 MHz,$CDCl_3$, δ (ppm)]: δ7.51 (d, 2H), 7.43 (d, 2H), 7.41 (d, 2H), 7.11 (d, 2H), 7.07 (d, 2H), 7.04 (d, 2H), 5.71 (s, 1H), 2.57 (t, 2H), 1.59 (m, 2H), 1.37 (m,2H), 0.93 (t, 3H).

### 3.2.2) Synthesis of 2-(*p*-bromophenoxy) ethanol

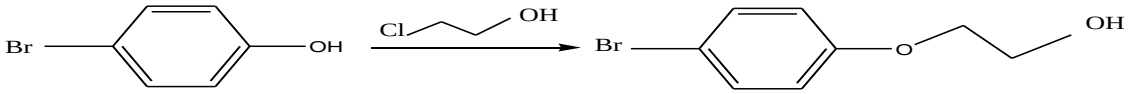


<Materials>

*p*-bromophenol (Wako), 2-chloroethanol (Wako), Sodium Hydroxide (Wako).

<Operation>

The mixture of p-bromophenol (5.2 g, 30 mmol) and 2-chloroethanol (20.2 ml, 300 mmol) in 10% aqueous NaOH solution (120 ml) was stirred under at room temperature. After 24 hr, the mixture was extracted with $CH_2Cl_2$, washed with 10% aqueous NaOH solution and distillated water and dried with anhydrous $MgSO_4$. The residue filtrated, and evaporated by rotary evaporator. Finally, product was Recrystallized by hexane. Yield was 4.54 g (69.7%).$^1$H NMR [300MHz, $CDCl_3$, δ (ppm)]: δ 7.39(d, 2H, aromatic), 6.81(d, 2H, aromatic), 4.02 (d, 2H, $CH_2$), 3.98 (d, 2H, $CH_2$), 2.01(t, 1H, OH).

### 3.2.3) Synthesis of 2-(*p*-bromophenoxy) ethoxy-t-butyldimethylsilane

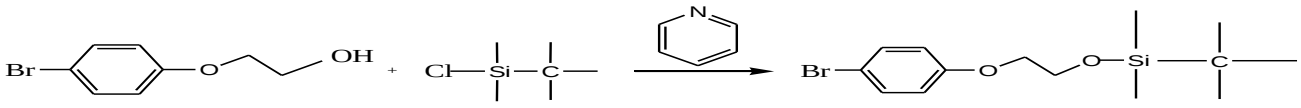


<Materials>

2-(*p*-bromophenoxy) ethanol, t-butyldimethylchlorosilane (TCI), Pyridine (Wako); dehydrated,

4-dimethylaminopyridine (DMAP) (Wako), Dichloromethane ($CH_2Cl_2$) (Wako)

<Operation>

2-(*p*-bromophenoxy) ethanol (1.411 g, 6.5 mmol) and DMAP (0.025 g, 0.02 mmol) located in 50 ml flask, under nitrogen atmosphere and 0° C, $CH_2Cl_2$ (10 ml) as a solvent injected to flask and stirred, then tert-butyldimethylchlorosilane (0.98 g, 6.5 mmol) dissolved into $CH_2Cl_2$ (10 ml) and added to flask. In this stage, pyridine (0.56 ml, 7 mmol) injected to flask. For 30 min reaction stirred at 0° C and then temperature was increased to room temperature. After 24 hr, solution evaporated to remove dichloromethane and extract by DEE. By adding dis.water phase separation carried out and dried by $MgSO_4$. In the next step, by filtration and evaporation concentrated product obtained. Finally, the residue purified by column chromatography ($CHCl_3$). Transparent liquid was obtained. The yield was 1.8 g (83.7%).$^1$H NMR [300MHz, $CDCl_3$, δ (ppm)]: δ 7.39(d, 2H, aromatic), 6.81(d, 2H, aromatic), 4.02 (d, 2H, $CH_2$), 3.98 (d, 2H, $CH_2$), 0.90 (s, 9H, $CH_3$), 0.11 (s, 6H, $CH_3$).

## 3.2.4) Synthesis of polybutyltriphenylamine with t-butyldimethylsilyl-terminated (PBTPA-TBS)

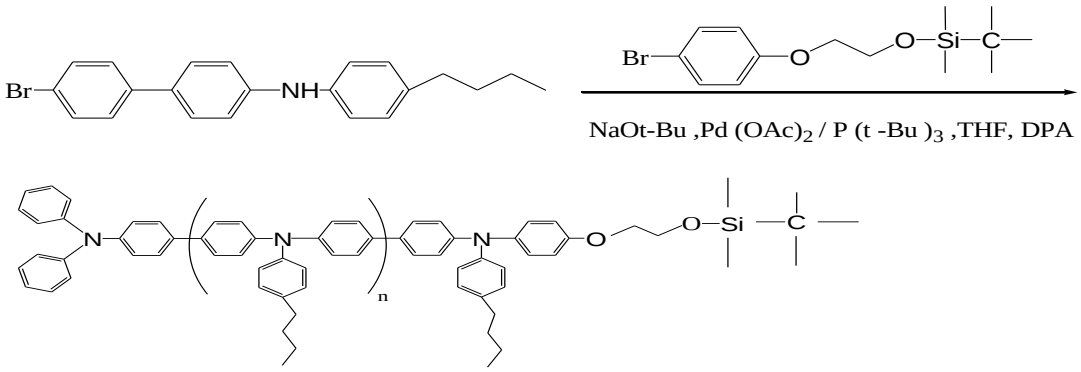


<Materials>

4-(4'-bromophenyl)-4"-n-butyldiphenylamine (BTPA), 2-(*p*-bromophenoxy) ethoxy-t-butyldimethylsilane, Sodium tert-butoxide (TCI); Reagent grade>98.0 %, Palladium acetate (II) ($Pd(OAc)_2$) (Aldrich); Reagent grade, Tri-tert-butylphosphine ($P(t\text{-}Bu)_3$) (Wako), Diphenylamine (DPA) (TCI), Toluene (Wako).

<Operation>

BTPA (0.95 g, 2.5 mmol) and sodium tert-butoxide (0.29 g, 3 mmol) located in two-neck 10 ml flask 1 under nitrogen atmosphere. Under this condition, dry toluene (5 ml) added to flask. In 10 ml flask 2, Pd $(OAc)_2$ (0.0105 g, 0.05 mmol) located under nitrogen atmosphere. 2-(*p*-bromophenoxy) ethoxy-t-butyldimethylsilane (initiator) (0.1655 g, 0.5 mmol) injected to flask and then dry toluene (3 ml) added to mixture, while stirred. In this stage, $(P(t\text{-}Bu)_3)$ (50 µl, 0.2 mmol) injected to solution. The content of flask 2 added to flask 1, while stirred. After the mixture was stirred under reflux (120 ° C) for 24 hr, the solution of DPA (0.845 g, 5 mmol) injected to reaction content for 1 hr. By waiting for 1 hr to decrease the temperature (60 ° C), and adding a few drops of distillated water to flask, reaction was finished. In this stage, with filtration and brine the impurities were separated. Next steps were included drying by $MgSO_4$, filtration, evaporation and dissolving in toluene. Then, concentrated solution precipitated in methanol, washed by (hexane, distillated water and acetone). Finally, light yellow solid dried under vacuum. The yield was 0.8 g (83.6%). $^1$H NMR [300MHz, $CDCl_3$,δ (ppm)]: δ 7.43 (d, 42H), 7.15-7.03 (m, 88H), 6.84(d, 2H), 4.02 (d, 2H), 3.98 (d, 2H), 2.58 (t, 22H), 1.61 (m, 22H), 1.38 (m, 22H), (m, 42H), 0.11 (s, 6H).

## 3.2.5) Synthesis of polybutyltriphenylamine with hydroxyl-terminated (PBTPA-O-H)

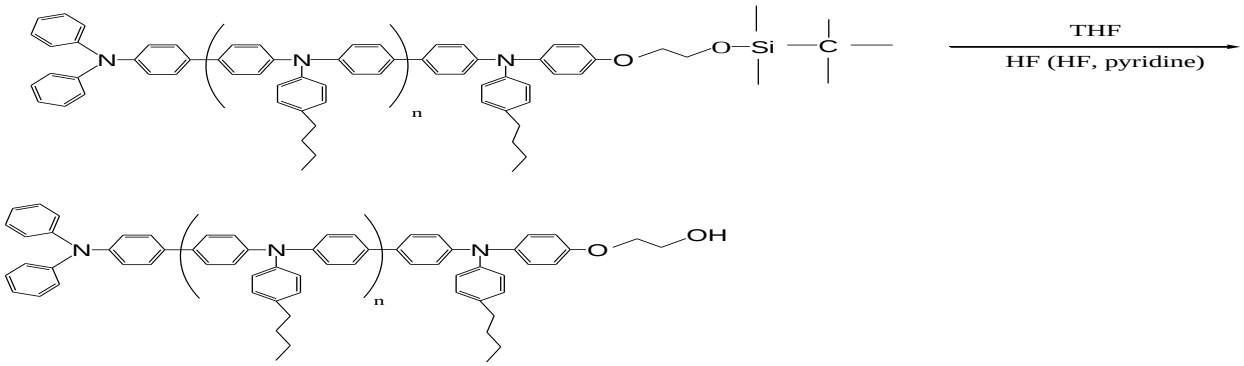


<Materials>

Polybutyltriphenylamine with t-butyldimethylsilyl-terminated (PBTPA-TBS), Hydrogen fluoride pyridine (HF, pyridine) (Aldrich); hydrogen fluoride 70%; pyridine 30%, THF (Wako).

<Operation>

The mixture of PBTPA-TBS (0.59 g, 0.16 mmol), THF (50 ml) and (HF, pyridine) (1.8 ml) was located in 100 ml flask and stirred for 48 hr. after that, a few drops of distillated water added to flask to terminate the reaction. By filtration and evaporation of THF concentrated mixture was obtained. In the next step, the residue was diluted by toluene. Then, by brain and drying with $MgSO_4$ the row product filtrated and evaporated. Viscose mixture dissolved in THF and precipitated into acetone and washed by (Dis. water, acetone). Finally the product dried under vacuum. The yield was 0.43 g (75%).$^1$H NMR [300MHz, $CDCl_3$,δ (ppm)]: δ 7.43 (d, 42H), 7.15-7.03 (m, 88H), 6.84(d, 2H), 4.02 (d, 2H), 3.98 (d, 2H), 2.58 (t, 22H), 1.61 (m, 22H), 1.38 (m, 22H), 0.94 (t, 33H).

### 3.2.6) Synthesis of polybutyltriphenylamine with bromo ester-terminated (PBTPA-O-Br) [PBTPA-MI]

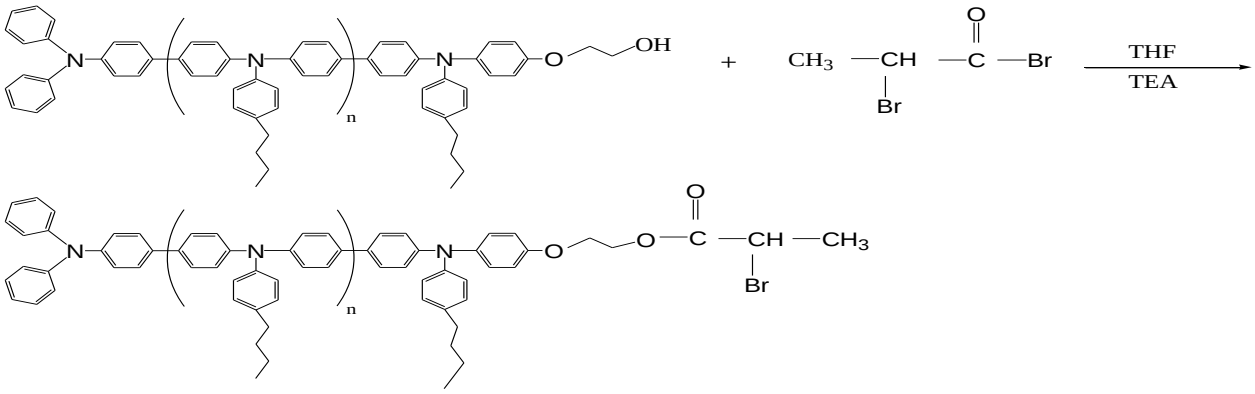


## <Materials>

Polybutyltriphenylamine with hydroxyl-terminated (PBTPA-O-H), 2-bromopropionylbromide (Wako), Triethylamine (TEA) (Wako), THF (Wako).

## <Operation>

PBTPA-OH (0.324 g, 0.09 mmol) was located in 100 ml flask. Under nitrogen atmosphere, THF 50 ml injected to 100 ml flask to dissolve PBTPA-OH and then TEA (2.67 ml, 19.2 mmol) added to mixture while stirred. In this time, temperature decreased from room temperature to 0 °C. By adding 2-bromopropionylbromide (1.83 ml, 17.4 mmol) to flask content the reaction initiated. For 30 min waited at 0 ° C and then remove the ice. The reaction continued after 48 hr at room temperature by adding a few drops of distillated water reaction was terminated. Filtration, remove THF, are the next stages. In this time, concentrated solution precipitated into acetone and

washed with hexane, distillated water and acetone. Finally, the product dried under vacuum. The yield was 0.286 g (85.1%).$^{1}$H NMR [300MHz, $CDCl_3$,δ (ppm)]: δ 7.43 (d, 42H), 7.15-7.03 (m, 88H), 6.84(d, 2H), 4.45 (d, 2H), 4.35 (m, 1H), 4.10 (d, 2H), 2.58 (t, 22H), 1.78 (d, 3H), 1.61 (m, 22H), 1.38 (m, 22H), 0.94 (t, 33H).

## 3.2.7) Synthesis of PBTPA-b-PMMA

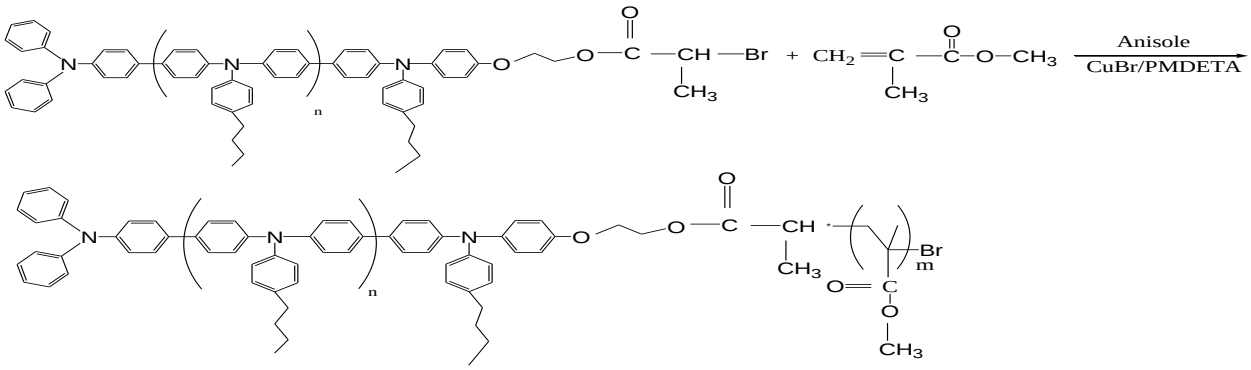


<Materials>

polybutyltriphenylamine with bromo ester-terminated (PBTPA-O-Br) [PBTPA-MI], Copper (I) bromide (CuBr) (Wako), N,N,N',N",N"- pentamethyldiethylenetriamine (PMDETA) (Wako), Methylmethacrylate (MMA) (Wako), Anisole (Wako).

<Operation>

CuBr (0.094 g, 0.66 mmol) located in tube flask under nitrogen atmosphere. Mixture of PBTPA-MI (0.13 g, 0.03 mmol), anisole 1 ml, MMA (0.315 ml, 3 mmol) and PMDETA (165 µl, 0.729 mmol) added to flask. Immediately after injection the ingredients, Freeze-thaw-pump cycle for 5 times carried out. Then wait for 15 min, temperature increased to 100 ° C for 24 hr. In the next stage, the raw product extracted with chloroform and filtrated by alumina column then, evaporated. High concentration of solution precipitated in methanol and washed by hexane. Finally, the product dried under vacuum. The yield was 0.17 g (39.5%).

## 3.2.8) Preparations of Seed Particles by Solvent Evaporation Method

A polymer solution (in chloroform, 2.5 or 5 %) was dispersed in ten times volume of water containing 0.3% of PVA with a homogenizer (X520, CAT Scientific, US) at 11,000 RPM to

obtain 2-10 μm sized droplets (usually 5 min treatment). The weight ratio for the binary blend was fixed to be 1/1 (PBTPA/PMMA). In the case of ternary blends, the content of block copolymer was 10, 30 or 50 wt% keeping the weight ratio of PBTPA component to PMMA component constant (1/1). The homogenized mixture was stirred by a mechanical stirrer at 100 rpm for 24 hr to evaporated $CHCl_3$ slowly. The resulting microspheres were washed with distilled water four times with a centrifugation process. Finally, polymer seeds dried under vacuum.

### 3.2.9) Characterization

Resulting PBTPA and PBTPA-*b*-PMMA were characterized with $^1$H-NMR (ECX 300, JEOL, Japan) and GPC. The surface feature and inside morphologies of microspheres were characterized by scanning electron microscope (SEM) (JSM-6510, JEOL, Japan) and transmission electron microscope (TEM) (JEM-2100, JEOL, Japan), respectively. The specimens for SEM and TEM observations were prepared as described elsewhere. The PBTPA domain was stained by exposing the specimens to the vapor of an aqueous $RuO_4$ solution (0.5%) for 90 min in a sealed bottle at room temperature.

## 3.3) Results and Discussion

### 3.3.1) Synthesis of PBTPA-O-TBS Precursor

The BTPA monomer with bromophenyl and diphenylamine moieties for fabrication of well-defined polymer via C-N coupling reaction has been synthesized so that could be functionalized at both terminals separately by adding terminal modifying derivatives like an aryl bromide or aryl amine derivatives as a terminator. Here, aryl bromide with hydroxyl group and with protected TBS group was prepared as it was discussed. The polymerization was carried out using palladium acetate and tri (t-butyl) phosphine ligand as the catalyst, and sodium t-butoxide as base in THF and toluene for 24 hr, respectively.

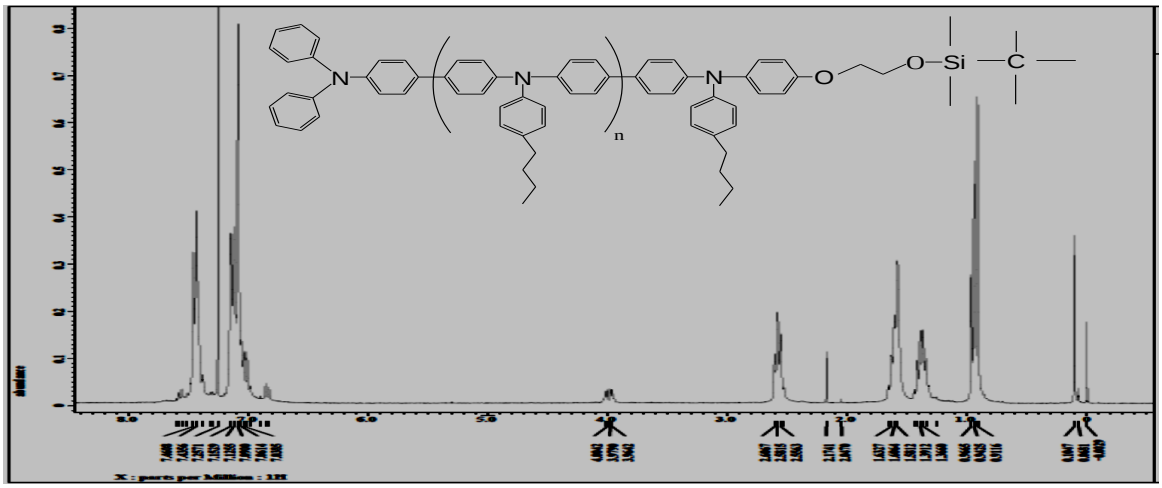

**Figure 3-1**: $^{1}H$ NMR spectra of PBTPA-O-TBS precursor

As seen in NMR spectra, aryl bromide derivative containing TBS termination have signals at 0.11 ppm and 0.9 ppm corresponding to methyl groups of Si and t-butyl, respectively.

**Table 3-1**: characteristics of PBTPA-O-TBS prepared by C-N coupling under various reaction conditions by THF

| | M:I | t(h) | m(g) | Yield | NMR | Mn | PDI |
|---|---|---|---|---|---|---|---|
| E.73 (H1) | 5:1 | 24 | 0.32 | 33.43% | 5802 | 2900 | 2.39 |
| E.75 (H2) | 3:1 | ” | 0.288 | 35.12 | 9988 | 2190 | 2.54 |
| E.81 (H3) | ” | 18 | 0.318 | 24.16 | 4008 | 1750 | 2.63 |
| E.85 (H4) | 1:1 | 24 | 0.183 | 25.48 | 4905 | 2000 | 1.67 |
| E.87 (H5) | ” | 48 | 0.156 | 21.72 | 8493 | 1800 | 1.95 |
| E.91 (H6) | 5:1 | 24 | 0.575 | 60.08 | 7895 | 2860 | 2.91 |
| E. 96 (H7) | ” | 24 | 0.532 | 55.59 | 8792 | 7070 | 2.35 |

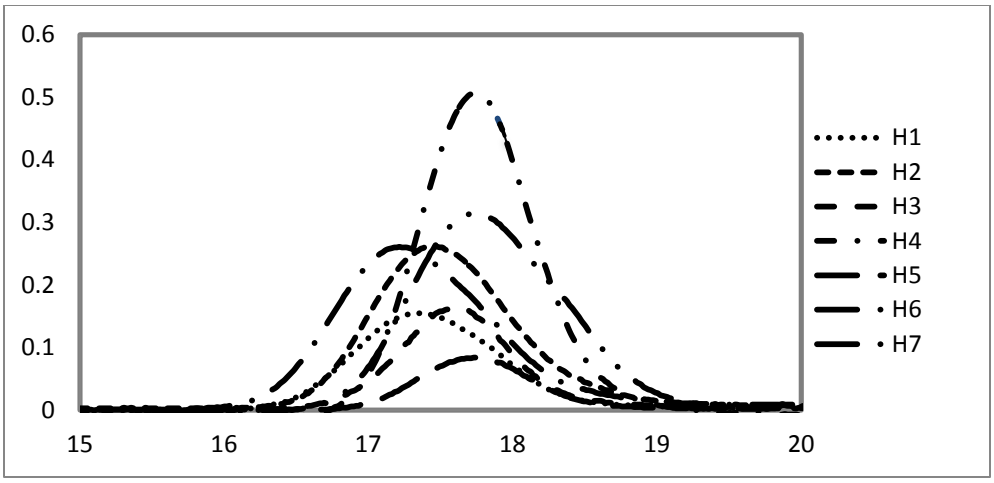


**Figure 3-2**: GPC traces of PBTPA-O-TBS prepared by C-N coupling under various reaction conditions by THF

Table 3-1 shows the characteristics of PBTPA-TBS prepared with various reaction conditions by THF. All the polymers showed low yields and scatter polydispersity indexes less than 2 and more than 2. MW of NMR determined from $^{1}H$ NMR spectra by the comparing the integration of methylene protons from BTPA moiety (2.58 ppm) with that from end group (3.97 ppm). On one hand as data confirmed, we can't conclude truly about the result and judgment is difficult. On the other hand, for sensivity of this reaction to water content of solvent (THF), we replaced THF by toluene. Since toluene is hydrophobic and stronger than THF, the polymerization reaction propagates easily and rapidly in comparing with THF.

**Table 3-2**: characteristics of PBTPA-O-TBS prepared by C-N coupling under various reaction times by toluene

| Column1 | M:I | t(h) | m(g) | yield (%) | NMR | Mn | PDI |
|---|---|---|---|---|---|---|---|
| **E.120 (H8)** | 5:1 | 3 | 0.71 | 74.71 | 4307 | 4060 | 2.52 |
| **E.130 (H9)** | " | 2 | 0.936 | 97.8 | N-H | ? | ? |
| **E.134(H10)** | " | 3 | 0.803 | 83.9 | 3709 | 3490 | 2.47 |
| **E.140(H11)** | " | 6 | 0.713 | 74.5 | 3410 | 3310 | 2.25 |
| **E.170(H12)** | " | 24 | 0.678 | 70.84 | 4606 | 3080 | 1.91 |
| **E.196(H13)** | " | 12 | 0.77 | 80.46 | 3709 | 3280 | 1.85 |
| **E.204(H14) Scale Up** | " | 24 | 1.6 | 83.6 | 4307 | 4060 | 2.09 |

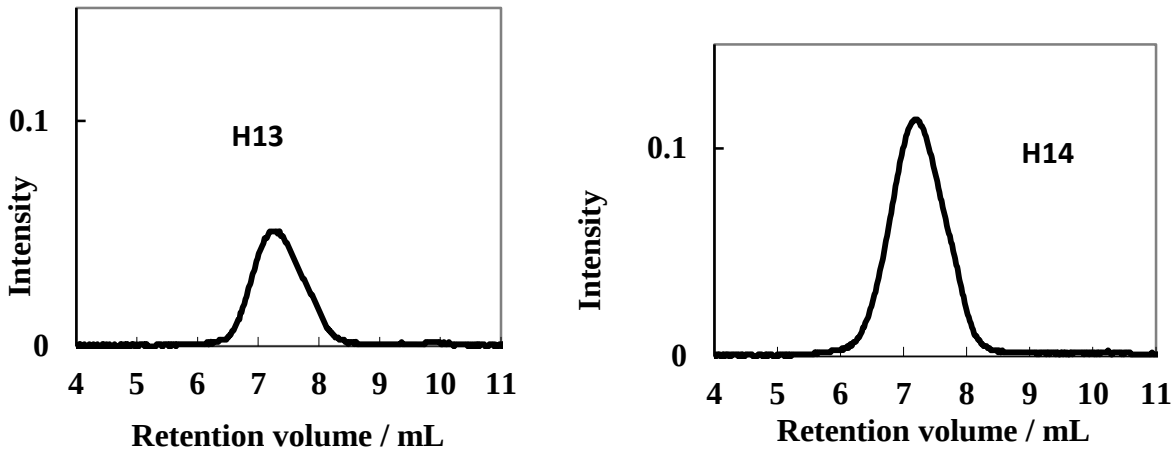


**Figure 3-3**: GPC traces of PBTPA-O-TBS prepared by C-N coupling under various reaction time by toluene

Table 3-2 exhibits the characteristics of PBTPA-TBS prepared with various reaction times by toluene. As it is seen after 2 hr reaction is completed and changing the reaction time doesn't have special effect on product. By comparing the result between the THF and toluene we can claim the data obtained from toluene more reasonable than THF. As we continue the PDI became better more and more. In another consideration, the ratio between M/I changed by 2.5:1 and 7.5:1 as showed at table3 that results are discussed in below.

**Table 3-3**: characteristics of PBTPA-O-TBS prepared by C-N coupling under various ratio of M: I by Toluene

| | M:I | t(h) | m(g) | yield | DOP | NMR | Mn | PDI |
|---|---|---|---|---|---|---|---|---|
| E.170(H12) | 5:1 | 24 | 0.678 | 70.84 | 14 | 4606 | 3080 | 1.91 |
| E.222(H15) | 2.5:1 | " | 0.365 | 62.58 | 10 | 3410 | 2240 | 1.66 |
| E.223(H16) | 7.5:1 | " | 0.92 | 71.23 | 21 | 6699 | 6370 | 1.95 |

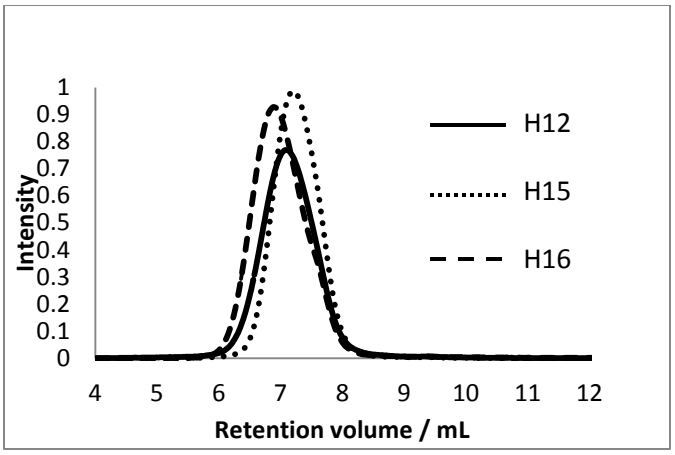


**Figure 3-4**: GPC traces of PBTPA-O-TBS prepared by C-N coupling under various M/I ratio by toluene

Table 3-3 demonstrated outcome of changing the M/I ratio. It should be noted in each three experiments the amount of solvent and temperature selected constant. It could be concluded that at 2.5:1 ratio, high amount of solvent lead to low disperse product but the difference between NMR and GPC data is high. Visa versa, at 7.5:1 ratio, low amount of solvent caused to high disperse but difference between NMR and GPC data is low.

## 3.3.2) Synthesis of PBTPA-O-H

De-protection of TBS group of PBTPA-TBS was conducted using HF/pyridine in the THF solvent. After the reaction time (48 hr), by precipitation the concentrate solution in methanol then re-dissolving in chloroform and re-precipitation in acetone carried out to remove the low molecular weight to waste. The conversion of TBS group to hydroxyl group was confirmed by the complete disappearance of signals of signals for methyl protons at 0.11 ppm in $^{1}$H NMR.

## 3.3.3) Synthesis of PBTPA-O-Br

PBTPA with hydroxyl end group (PBTPA-O-H) was esterified with 2- 2-bromopropionyl bromide. The structure of the PBTPA with bromo ester end group (PBTPA-O-Br) is used as macro initiator for ATRP was confirmed by $^{1}$ H NMR. Besides the signals derived from PBTPA backbone, the characteristic signals assignable for bromo ester end group were observed at 4.35 and 1.78 ppm. The conversion was estimated to be nearly 100% due to the complete position shift of methylene protons belonged to end groups.

## 3.3.4) Synthesis of PBTPA-b-PMMA

Preparation of di-block copolymers containing both PBTPA segment and PMMA segment was carried out by ATRP using CuBr as a catalyst, PMDETA as a ligand and PBTPA-O-Br as a macro-initiator. It is known that the typical ATRP is conducted in bulk. As, macro-initiator insoluble in MMA monomer it's necessary to utilize solvent. For this reason anisole was selected as solvent.

**Table 3-4**: characteristics of PBTPA-b-PMMA prepared via ATRP under various reaction time and M/MI ratios

| Column1 | M/MI | t(hr) | m(gr) | yield(%) | NMR | Mn | PDI |
|---|---|---|---|---|---|---|---|
| E.77 (B1) | 1130:1 | 96 | | | 22600 | 3790 | 2.96 |
| E.80 (B2) | " | 60 | 0.397 | 35.84 | 53400 | 3650 | 2.72 |
| E.118(B3) | " | 24 | 0.476 | 20.93 | 38000 | 7850 | 2.14 |
| E.133(B4) | " | 12 | 0.594 | 26.12 | 33800 | 9600 | 2.42 |
| E.146(B5) | 200:1 | 24 | 0.06 | 12.9 | 14000 | 5560 | 2.49 |
| E.151(B6) | 100:1 | " | 0.04 | 16.55 | 7600 | 4980 | 2.19 |
| E.154(B7) | " | " | 0.022 | 5.5 | 5100 | 3840 | 2.23 |
| E.164(B8) | " | " | 0.036 | 9 | 4400 | 3950 | 1.68 |
| E.179(B9) | " | " | 0.117 | 29 | 7300 | 6600 | 1.88 |
| ".186(B10 | " | " | 0.148 | 33.7 | 9400 | 9020 | 2.1 |
| ".227(B11 | " | " | 0.17 | 39.5 | 8500 | 7050 | 1.9 |

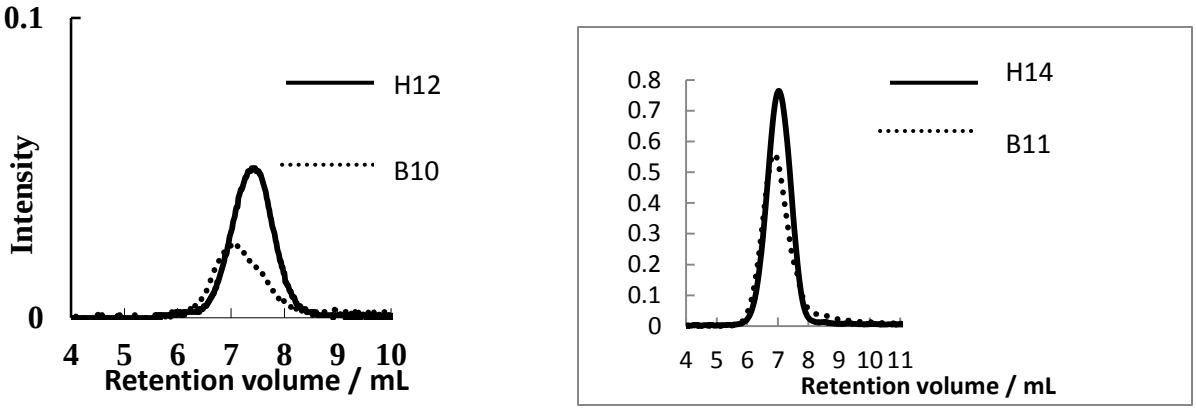


**Figure 3-5**: GPC traces of PBTPA-O-Br (MI) and PBTPA-b-PMMA

## 3.3.5) Preparations of Seed Particles

### 3.3.5.1) Consideration of Singular PBTPA Homopolymer Seed Particles

In order to investigate the effect of MW on particles morphology, two types of PBTPA were utilized, Mn (NMR): 3700, Mn (NMR): 6400. Figure 3-6 shows SEM images of microspheres with PBTPA homopolymer fabricated at the initial polymer concentration of 5 %. As shown in Figure 3-6 (a, b), low molecular weight polymer (PBTPA-L) afforded spherical polymer particles with external smooth surface. In the case of high molecular weight polymer (PBTPA-H), irregular and in some extents, non-spherical particles with rough surfaces were produced even at the same experimental conditions Figure 3-6 (c, d). Since the both polymers exhibit the same solubility (miscible in chloroform), it is considered that slightly increased viscosity of the solution made resulting particle irregular in the case of PBTPA-H.

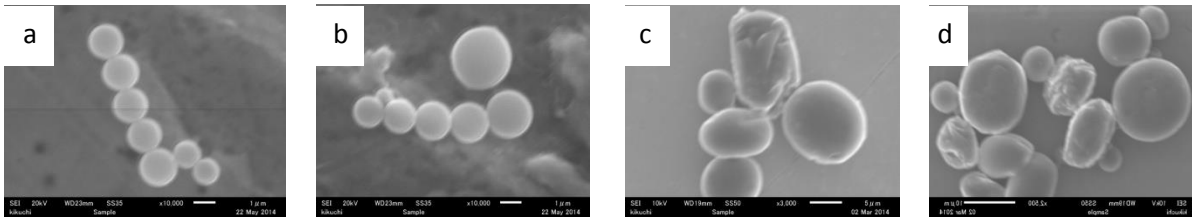


**Figure 3-6**: SEM images of singular PBTPA seed particles: (a), (b): PBTPA-L (3700), (c), (d): PBTPA-H (6400)

### 3.3.5.2) Considerations of Binary (PBTPA/PMMA) Polymer Blend Seed Particles

In this case, microspheres based on the binary blend PBTPA/PMMA (weight ratio 1/1) were fabricated, and the effect of molecular weight of PBTPA was investigated. Figure 3-7 and 3-8 shows the SEM and OM images of these binary polymer blend systems, the former PBTPA-L and latter BPTPA-H. Basically bi-compartmental morphologies were observed for both composites. In the case of PS/PMMA blend (weight ratio 1/1) particles, core-shell morphology is observed when a PVA solution is used as a continuous phase [21-24].

As Ge et al. discussed thermodynamically, the interfacial tension between dichloromethane solution of PS and water at the point of the phase separation should be larger compared with the sum of that between two polymer solutions and that between PMMA solution and water for the core-shell morphology (PMMA; shell, and PS; core). In this study, it is reasonable that the interfacial tension between chloroform solution of PBTPA and water decreased compared with PS due to the presence of nitrogen atoms, and is comparable to that between chloroform solution of PMMA and water. PBTPA-L/PMMA composites afforded a Janus-like morphology, whereas PBTPA-H/PMMA a dumbbell-like morphology. This difference is probably due to the molecular weight dependence of the interfacial tension between both polymer solutions [25, 26]. Meanwhile, optical micrographs for the dispersions just after the dispersing processes indicate that phase separation of both PBTPA and PMMA solutions occurs at an early stage in the solvent evaporation process, and the morphology at phase separation retains in final particles. It is noteworthy that the binary blend based on PBTPA-L homopolymer provided particles with a regular shape and surface smooth morphology compared with PBTPA-H homopolymer.

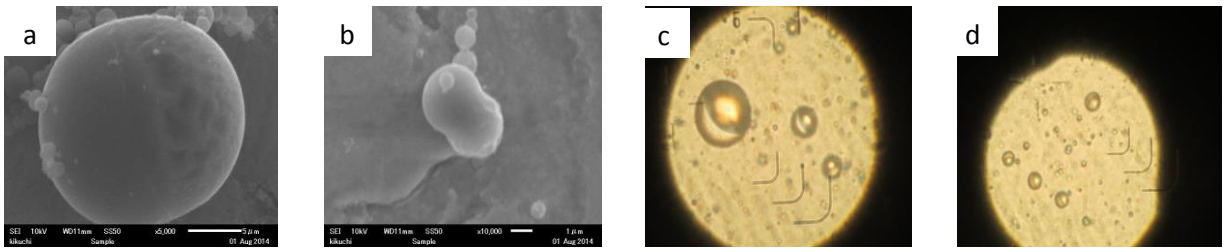


**Figure 3-7**: (a), (b) SEM images of binary PBTPA/PMMA seed particles: PBTPA-L (3700), (c), (d) OM images

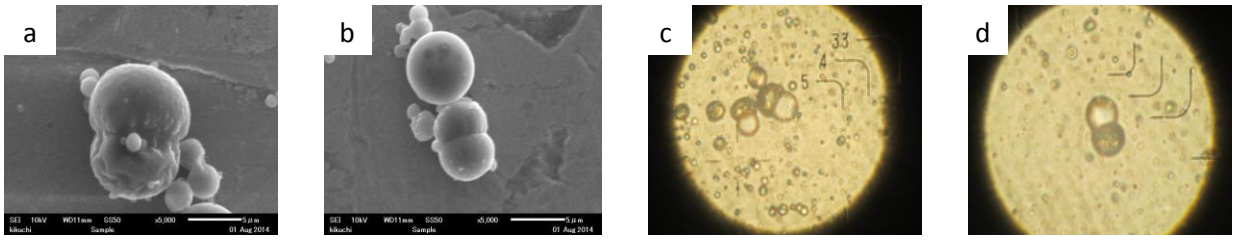


**Figure 3-8**: (e), (f) SEM images of binary PBTPA/PMMA seed particles: PBTPA-H (6400), (g), (h) OM images

### 3.3.5.3) Considerations of (PBTPA-b-PMMA) Block Copolymer Seed Particles

Figure 3-9 Represents SEM images of two kind of asymmetric block copolymer (PBTPA-b-PMMA). The first one prepared with Mn (6100) [PBTPA: 4300, PMMA: 1800] (a, b), whilst the second one prepared with Mn (13100) [PBTPA: 4300, PMMA: 8800] (c, d). They were selected deliberately to evaluate their morphologies. As the it's observed, in the case of low molecular weight of block copolymer spherical seeds prepared while high molecular weight of block copolymer lead to deformed and irregular shapes obtained. Again, it seems the molecular weight has a major effect on final morphology.

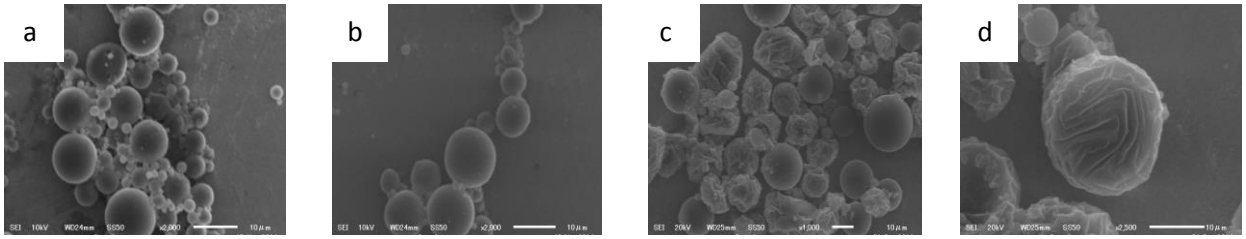


**Figure 3-9**: SEM images of singular PBTPA-b-PMMA particles: (a, b): low MW (6100), (c, d): high MW (13100)

### 3.3.5.4) Considerations of Ternary (PBTPA/PBTPA-PMMA/PMMA) Polymer Blend Seed Particles

In order to investigate the effect of block copolymer on the surface and inside morphologies, various amount of PBTPA-*b*-PMMA was added to the binary blend. All ternary blend particles were fabricated keeping the weight ratio of PBTPA component to PMMA component constant (1/1), and low molecular weight PBTPA-L was utilized. Figure 3-10 shows SEM images for the particles based on ternary blends. The effect of the ratio of the block copolymer [(a), (b); 10%, (c),(d); 30%, (e),(f); 50%], and the initial concentration dependence on the morphology [(a), (c), (e); 5%, and (b), (d), (f); 2.5%] were also investigated. By adding of block copolymer, bi-

compartmental microspheres observed in the binary blends particles were not formed. Ternary blends with 10% of the block copolymers at the initial concentration of 5% afforded particles with some patches on the surface. In the high concentration regions, it is possible that microdomain type, a nonequilibrium morphology is observed, because of high viscosity in the droplets [21]. Particles were fabricated at low initial concentration to assure the equilibrium in the formation of particles. However, as shown in Figure 3-10(b), more irregular shape was observed at 2.5 %. At 5% of total polymer concentration, the increase of the ratio of the block copolymer made the surface smoother as shown in Figure 3(c) and 3(e). At 30%, particles seem to have navel. At 50%, smooth and spherical particles were obtained. At both block copolymer contents, the low initial concentration afforded particles with irregular shapes as shown in Figure 3-10(d, f).

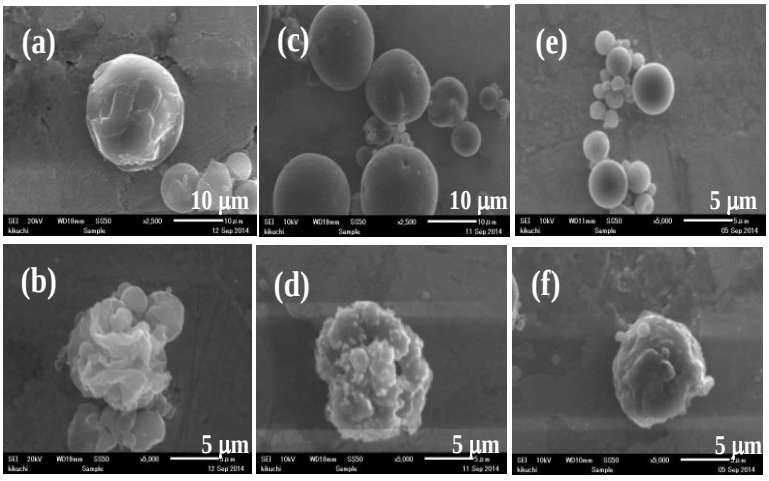


**Figure 3-10**: SEM images of microspheres based on PBTPA/PBTPA-b-PMMA/PMMA ternary blend. The content of PBTPA-b-PMMA is (a, b); 10 wt%, (c, d); 30 wt% and (e, f); 50 wt%. the initial concentration of polymer solution is (a, c, e); 5% and (b, d, f); 2.5%.

In order to investigate morphologies inside microspheres and to explore the origin of unique surface features, TEM measurements were carried out. Figure 3-11 shows TEM images of microspheres based on ternary blends fabricated from 5% of polymer solutions. At 10% of the block copolymer content, the Janus type morphology was no longer observed, and PMMA-rich bright domain was partially engulfed by PBTPA-rich dark domain as shown in Figure 3-11(a). It is considered that protruded PMMA rich domain formed patch like morphologies at the surface. At 30%, PMMA-rich domain was almost completely engulfed as shown in Figure 3-11(b). The formation of navels is attributed to the contact point of two domains near the surface. At 50%, a nearly concentric circle image (Figure 3-11(c)) exhibits the formation of particles with core-shell

morphology. It is generally accepted that the block copolymer plays a role of a compatibilizer and the addition of block copolymer decrease the difference of the interfacial tension between two polymer solutions and solids. Therefore it is expected that size of phase separated domain is decreased. In this experiment, however, the formation of microdomains was not observed, and the type of morphology changed by the addition of block copolymers. In our previous study for the blend of PS and PMMA, the morphologies changes from core-shell to Janus by the addition of the corresponding block copolymers. Until now it is difficult to explain the discrepancy, and the further study is necessary.

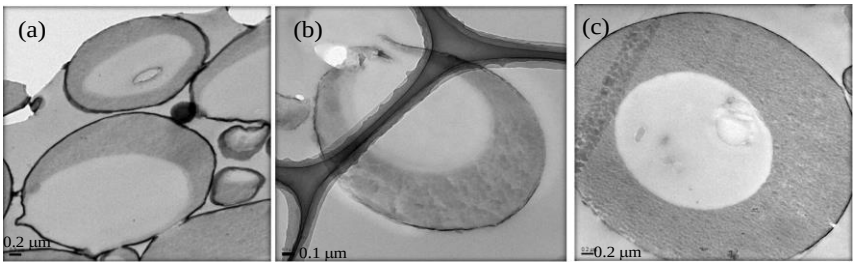


## 3.4) Conclusion

PBTPA homopolymer with low molecular weight (PBTPA-L) afforded spherical particles on the conditions we examined in a solvent evaporation method. On the other hand, the particles based on PBTPA with high molecular weight (PBTPA-H) were non-spherical and irregular. Unique bi-compartmental particles were obtained from binary blends with PMMA. Molecular weight dependence on the final morphologies was also observed, i.e., the particles based on PBTPA-L / PMMA and PBTPA-H / PMMA exhibited Janus and dumbbell type morphologies, respectively. This observation is reasonably explained by molecular weight dependence of the interfacial tension between two kinds of phase separated polymer solutions. Bi-compartmental morphologies was no longer observed for the particles based on ternary blends containing PBTPA-b-PMMA. Instead the particles showed core-shell (PMMA; core, PBTPA; shell) morphologies. As the content of the block copolymer increased, the extent of engulfment of PMMA domain increased. Since physical properties such as dielectric constant and refractive index of PBTPA are considerably different from those of PMMA, the particles with various morphologies have potential applications in photonic and electronic fields.

## References


[1] Adachi, C. and Tsutsui T. (1999) Molecular LED: Design Concept of Molecular Materials for High Performance OLED. In: Miyata, S. and Nalwa H.S., Ed., *Organic Electroluminescence Materials and Device*, Gordon and Breach, Amsterdam, 43-65.

[2] Tang, C.W., Van Slyke, S.A., Nalwa, H.S., *Appl. Phys. Lett.*, **51**, 913-915 (1987).

[3] Ogino, K., Kanegae, A., Yamaguchi, R., Sato, H., Kurjata, J., *Macromol. Rap. Commun.*, **20**, 103-106 (1999).

[4] Takahashi, C., Moriya, S., Fugono, N., Lee, H.C., Sato, H., *Macromol. Rap. Commun.*, **129**, 123-128 (2002).

[5] Tsuchiya, K., Shimomura, T., Ogino, K., *Polymer*, **50**, 95-101(2009).

[6] Tan, Y., Gu, Z., Tsuchiya, K., Ogino, K., *Polymer*, **53**, 1444-1452 (2012).

[7] Tsuchiya, K., Kikuchi, T. Songeun, M., Shimomura, T., Ogino, K., *Polymer*, **3**, 1051-1064 (2001).

[8] Cao, Z., Abe, Y., Nagahama, T., Tsuchiya, K., Ogino, K., *Polymer*, **54**, 269-276 (2013).

[9] Kinashi, K., Shinkai, H., Sakai, W., Tsutsumi, N., *Org. Electron.*, **14**, 2987-2993 (2013).

[10] Fujioka, M., Kurihara, H., Kawamura, R., Sato, H., Tsuchiya, K., Ogino, K., *Colloid Polym. Sci.*, **286**, 313-318 (2008).

[11] Fujioka, M., Sato, H., Ogino, K., *Colloid Polym. Sci.*, **285**, 915-921 (2007).

[12] Zhao, J., Yuan, H., Pan, Z., *J. Appl. Polym. Sci.*, **53**, 1447-1452 (1994).

[13] Han, S.H., Ma, G.H., Du, Y.Z., Omi, S., Gu, L.X., *J. Appl. Polym. Sci.*, **90**, 3811-3821 (2003).

[14] Hu, G., Yu, D., Zhang, J., Liang, H., Cao, Z., *Colloid J.*, **73**, 557-564 (2011).

[15] Okubo, M., Fujibayashi, T., Yamada, M., Minami, H., *Colloid Polym. Sci.*, **283**, 1041-1045 (2005).

[16] Fujibayashi, T., Tanaka, T., Minami, H., Okubo, M., *Colloid Polym. Sci.*, **288**, 879-886 (2010).

[17] Okubo, M., Fujibayashi, T., Terada, A., *Colloid Polym. Sci.*, **283**, 793-798 (2005).

[18] Ogino, K., Sato, H., Tsuchiya, K., Suzuki, H., Moriguchi, S., *J. Chromatog.: A*, **699**, 59-69 (1995).

[19] Higuchi, T., Tajima, A., Motoyoshi, K., Yabu, H., Shimomura, M., *Angew. Chem. Int. Ed.*, **48**, 5125-5128 (2009).

[20] Higuchi, T., Tajima, A., Yabu, H., Shimomura, M., *Soft Matter*, **4**, 1302-1305 (2008).

[21] Ma, G.H., Nagai, M., Omi, S., *J. Colloi. Interf. Sci.*, **214**, 264-282 (1999).

[22] Okubo, M., Saito, N., Fujibayashi, T. *Colloid Polym. Sci.*, **283**, 691-698 (2005).

[23] Saito, N., Kagari, Y., Okubo, M., *Langmuir*, **22**, 9397-9402 (2006).

[24] Taherzadeh, H., Sotowa, S., Ogino, K., *Open Journal of Organic Polymer Materials*, in press.

[25] Ge, X., Wang, M. Ji, X., Ge, X., Liu, H., *Colloid Polym. Sci.*, **287**, 819-827 (2009).

[26] Tanaka, T., Nakatsuru, R., Kagari, Y., Saito, N., Okubo, M., *Langmuir*, **24**, 12267-12271 (2008).

[27] Maric, M., Macosko, C.W., *J. Polym. Sci.: Part B: Polymer Physics*, **40**, 346-357 (2002).

# Chapter 4

# Fabrication of Microporous Film and Microspheres Hybrids

## 4.1) Introduction

Highly ordered microporous polymer films with honeycomb structure have been fabricated by a simple non-template method utilizing various types of block copolymers [1-8]. Although rod-coil type poly(*p*-phenylene)-*b*-poly(styrene) was used in a pioneer study [1], other type of block copolymers have been also utilized including T-shape copolymer[5] and amphiphilic block copolymers [7, 8]. It is recognized that the mechanism for the formation of honeycomb structure can be explained by dissipative processes, where controlled condensation and growth of water droplets on the cold surfaces resulting from solvent evaporation of polymer solutions may be used to create a patterned surface. Although non-block copolymers such as end-functionalized polymer [9], and amphiphilic random copolymers [10, 11], the utilization of block copolymer gives rise to another advantage because of self-assembly nature of block copolymers. Hayakawa et al. reported that using a specially designed block copolymer, resulting porous films have highly ordered hierarchical structures over multiple length scales from angstroms to micrometers [6]. Furthermore the surface aggregation of selective component is expected [5]. Various applications of honey comb films have been considered such as separation membranes [12], super hydrophobic materials [13], photonic or optoelectronic devices [14], cell-culturing substrates [15, 16], and micropatterning templates [10, 17, 18]. In author's laboratory, micropores were utilized as micro reactors. Poly (aniline) dots were successfully fabricated via electro polymerization of aniline using a micro porous film on indium tin oxide electrode as a template [7]. Yabu et al prepared honey comb nanoparticles hybrid in order to obtain multiple-periodic structures [19]. A specially developed sliding apparatus was used for embedding the submicron polystyrene particles.

In this chapter, a microporous film and polymeric microspheres hybrids were fabricated via a simple method without a special apparatus. Poly (acrylic acid)-*block*-polystyrene was used to

fabricate a microporous film. It is found that surface properties of the pore and microsphere play an important role in hybridization processes.

## 4.2) Experimental

### 4.2.1) Synthesis of Poly(acrylic acid)-*block*-Polystyrene

Block copolymers are synthesized via atom-transfer-radical polymerization as a previously reported method [7]. Preparation of macroinitiator was carried out as follows. A 100-mL three necked flask equipped with a stirrer bar, a nitrogen inlet, and a rubber septum was charged with CuBr (0.74 g, 5.2 mmol), $CuBr_2$ (0.058 g, 0.26 mmol) under nitrogen. After the evacuation followed with backfilling of nitrogen, distilled *t*-butyl acrylate (*t*-BA, 40 g, 0.31 mol) was added via gas-tight syringe followed by N,N,N',N",N"- pentamethyldiethylenetriamine (PMDETA, 2.17 mL, 10.4 mmol) and acetone (5 mL). After two freeze-pump-thaw cycles, *t*-butyl 2-bromopropionate (1.72 mL, 10.4 mmol) was added and the mixture was allowed to stir at room temperature for 10 min. The flask was then placed in a 60$^{o}$C oil bath and the polymerization proceeded for 1 h under nitrogen atmosphere. THF solution of the reaction mixture was filtered with an $Al_2O_3/SiO_2$ plug in order to remove the catalysts. After the concentration of solution, the polymer was precipitated into 50 vol% of methanol/$H_2O$ mixture. The degree of polymerization was determined by the end group analysis based on $^{1}$H-NMR spectroscopy. Molecular weight and its distribution were estimated with GPC calibrated with polystyrene standards. Yield; 43%, *DP*=5 (from NMR), *M*n= 2.0x10$^{3}$, *M*w/*M*n=1.3.

A 50-mL three necked flask equipped with a stirrer bar, a nitrogen inlet, and a rubber septum was charged with poly (*t*-BA) (0.801g, 0.380 mmol), CuBr (54 mg, 0.380 mmol) under nitrogen. After degas process as mentioned above, styrene (St) (19.75 g, 0.19 mol) (500 equivalent to the macroinitiator) and PMDETA (0.33g, 0.380 mmol) was added. Polymerization was carried out at 90$^{o}$C for 24 h, Similar procedures were utilized for purification. Yield; 42%, DP=285 (for styrene), *M*n= 3.1x10$^{4}$, *M*w/*M*n=1.7.

A 50-mL three necked flask equipped with a stirrer bar, a nitrogen inlet, and a condenser was charged with 3.0 g of poly(*t*-BA)-*block*-poly(St), *p*-toluene sulfonic acid monohydrate (0.33 g, 1.72 mmol), and 3.0 ml of dioxane under nitrogen atmosphere. The reaction mixture was

refluxed for 10 h to eliminate *t*-butyl group. After cooling the solution was poured into excess amount of water to precipitate the product (2.8 g).

### 4.2.2) Synthesis of Microspheres (PS and PS-DM)

Uniform sized polystyrene microsphere (PS) with a diameter of 1.7 µm was synthesized via dispersion polymerization in aqueous ethanol as previously reported [20]. Seed polymerization of N, N-dimethylaminoethyl methacrylate (DM) was conducted in the presence of ethylene glycol dimethacrylate (EDMA). PS (1.0 g) dispersed into 15 mL of water was placed into 100-mL three necked flask equipped with a mechanical stirrer, and a nitrogen inlet was charged. With gentle stirring, DM (0.970 g, 6.37 mmol), EDMA (30.2 mg 0.152 mmol), 2, 2'- azobis(2-amidinopropane) dihydrochloride)(60.3 mg, 0.222 mmol) were charged. Polymerization was carried out at 60$^{o}$C for 12 h.

### 4.2.3) Fabrication of Microporous Films

Carbon disulfide solution (0.1-0.5 wt%, 50 µl) was drop-cast on a cleaned glass slide over an area of ca. 1.1 cm$^2$ (circle with a diameter of 1.2 cm) in a custom designed flow-hood (640 cm$^3$) [7]. The humidity was kept at 75% at 25 $^{o}$C by Bubbling the air through a reservoir containing saturated NaCl solution. The flow-rates were controlled to be 5-10 L/min using a flow meter.

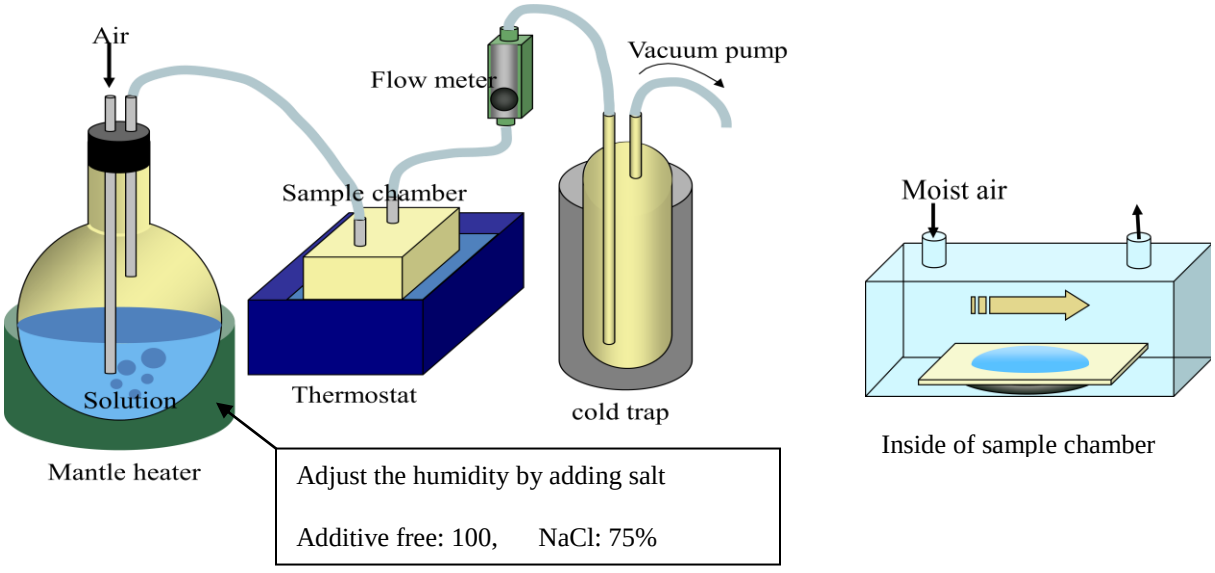


**Figure 4-1**: Schematic fabrication of microporous film

### 4.2.4) Fabrication of Microporous Film and Microsphere Hybrid

Microspheres (PS or PS-DM) (1.0 g) were dispersed in 15 ml of distilled water. Microporous film on a glass slide was immersed in the slurry for 30 min with gentle stirring. After washing with water, the hybrid film was dried in vacuum.

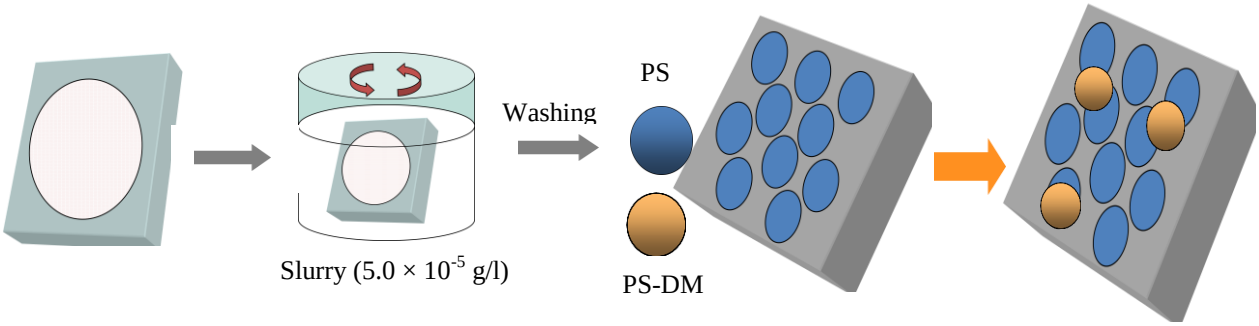


**Figure 4-2**: Schematic fabrication of hybrid films

### 4.2.5) Characterization

Resulting polymers were characterized with $^{1}$H-NMR (ECX 300, JEOL, Japan), IR (FT/IR-4100, JASCO, Japan), and GPC [20]. The surface features of microporous films, microspheres, and hybrid films were characterized by scanning electron microscope (SEM) (JSM-6510, JEOL, Japan).

## 4.3) Results and Discussion

### 4.3.1) Preparation of Microsphere

Successful preparation of PS-DM was confirmed by solubility change and IR spectroscopy. PS-DM showed partial solubility in chloroform due to the presence of PDM (insoluble in chloroform) and crosslinking with EDMA. Figure 4-3 shows IR spectra of PS and PS-DM. PS-DM shows a stronger absorption at 1730 cm$^{-1}$ assigned to C=O stretching. Figure 4-4 shows SEM images of PS (a) and PS-DM (b). Both types of particle were found to be had almost the same size (1.7 µm).

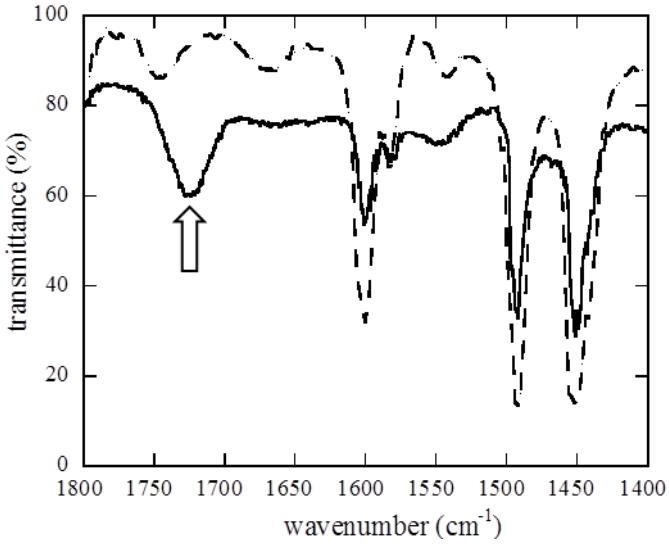


**Figure 4-3**: IR spectra of PS (broken line) and PS-DM (solid line)

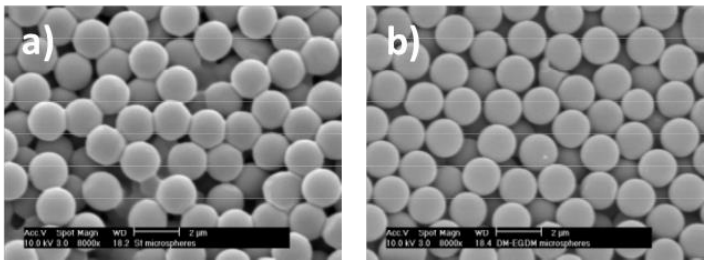


**Figure 4-4**: SEM images of PS (a) and PS-DM (b)

## 4.3.2) Fabrication of Microporous Films

As described in a previous report [7], the resulting pore size was strongly dependent on the characteristics of the polymers and fabrication conditions. In this study, poly (*t*-BA)-*block*-poly (St) with high molecular weight was utilized in order to obtain robust microporous films. In Figure 4-5, the pore size is plotted against the flow rate for the different concentration of block copolymer. With the increase of the flow rate, the resulting pore size increased. Lower initial polymer concentration afforded the larger pore size. In the initial stage of solvent evaporation, it is reported that the number of nuclei formed increases with the increase of polymer concentration and the amount of condensed water is almost the same each other, leading to the smaller pores [7]. Compared with a low molecular polymer (in [7]) ($M$n=1.3x$10^4$ from GPC, DPs of acrylic acid and styrene were 10, and 73, respectively), however, higher molecular weight polymer

exhibited much smaller concentration and flow rate dependencies. This is probably due to the formation of "harder shell" on the surface of the high molecular weight polymer solution in the evaporation of solvent. It is reasonable that the shell retard the solvent evaporation resulting in the impediment of increase the amount of condensed water.

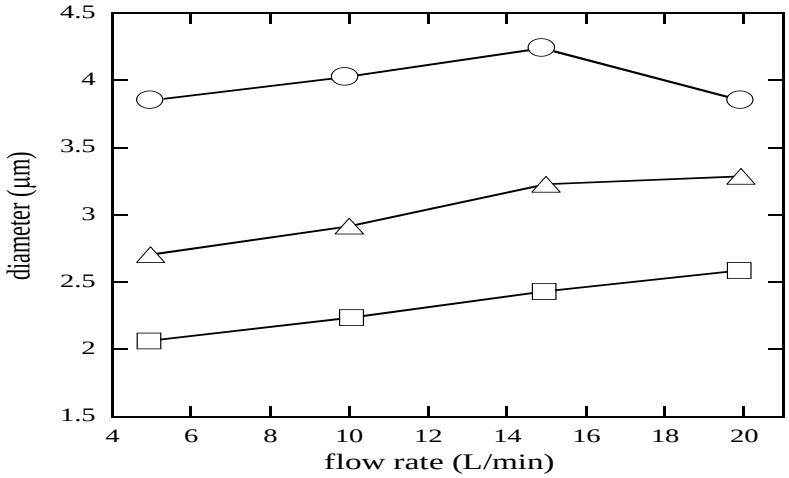


**Figure 4-5**: Flow rate dependence of pore size in the fabrication of microporous films. Initial concentration of polymer was 0.1 wt % (circle), 0.3 wt % (triangle) and 0.5 wt % (square).

## 4.3.3) Fabrication of Hybrid Film

After drying a microporous film in vacuo for 24 h, the film was immersed in slurry of microspheres for 30 min. In this process, however, almost no particles were embedded as shown in Figure 4-6. Although the electrostatic interaction between carboxyl group in the film and dimethylamino group in PS-DM is expected, no significant difference was observed between two types of microspheres.

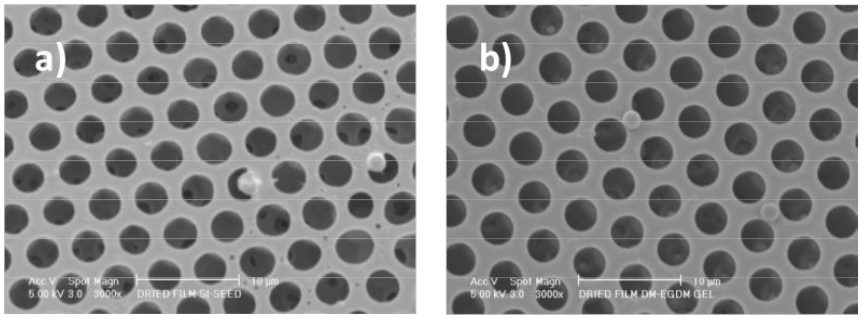


**Figure 4-6**: SEM images of microporous films after immersion in slurry of PS (a) and PS-DM (b) microporous film was dried for 24 h in vacuo before immersion

During the formation of pores, it is considered that water droplets were stabilized by the carboxyl groups. Collapse and coalescence of droplets were prevented by this stabilization. On other words, it is speculated that pore walls are covered with carboxyl groups just after the evaporation of water. However, it is considered that carboxyl groups go inside the film when it is exposed to air in order to lower the surface tension. As Kajiyama reported, the mobility of film surface is much higher than that of bulk [21], which makes it possible to alter the surface properties.

In order to put back the carboxyl groups to the surface, microporous films were soaked in methanol. Once the surface is rich in hydrophilic carboxyl groups, it is expected that wettability is improved, and electrostatic interaction is enhanced. Figure 4-7 shows SEM images of hybrids. It is revealed that microspheres were embedded in pores after immersion in methanol. In the case of PS-DM, much more microspheres were fixed compared with PS. These observations were attributed to improved wettability of film, and enhanced electrostatic interactions. As shown in this Figure, more than 2 microspheres are sometimes embedded in a single pore. In Figure 4-8, relationships between the ratio of pores with microsphere(s) and soaking time in methanol. After 10 min soaking, the number of embedded PS-DM microsphere increased remarkably. As for PS, the increase of fixed microsphere was not observed even after 60 min soaking.

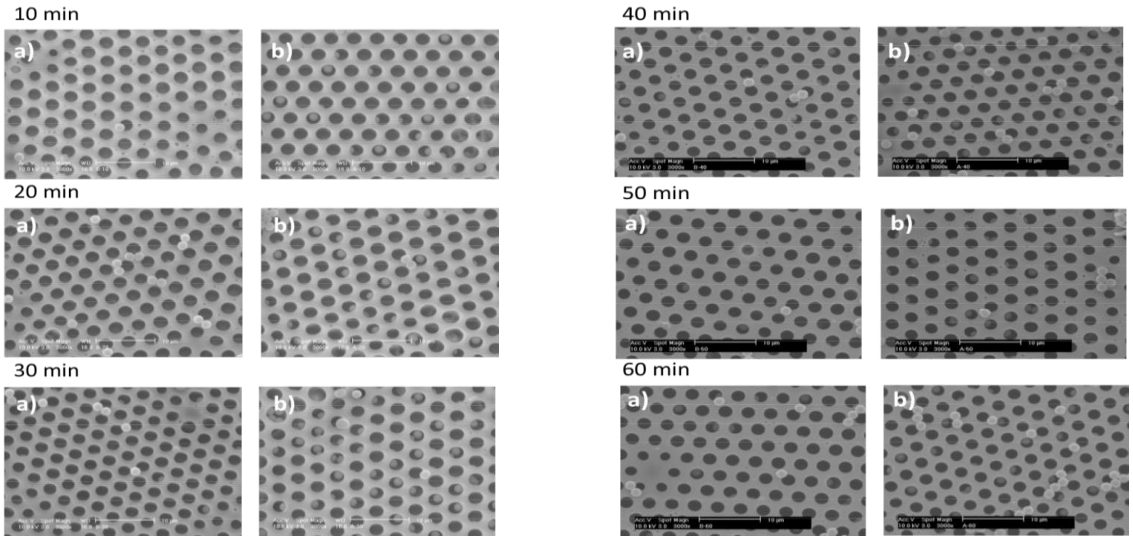


**Figure 4-7**: SEM images of microporous films after immersion in slurry of PS (a) and PS-DM (b)

Microporous film was soaked in methanol for 10-30 min before immersion.

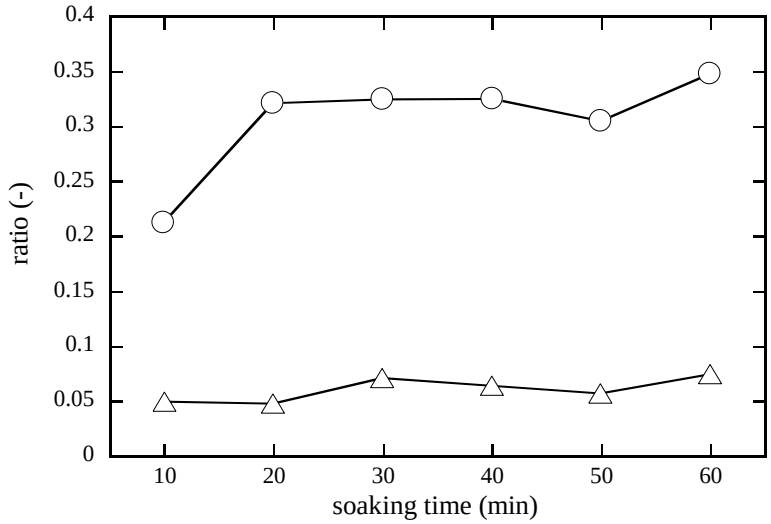


**Figure 4-8**: Relationship between the ratio of pores with microsphere(s) and soaking time in methanol (circle); PS-DM, (triangle); PS

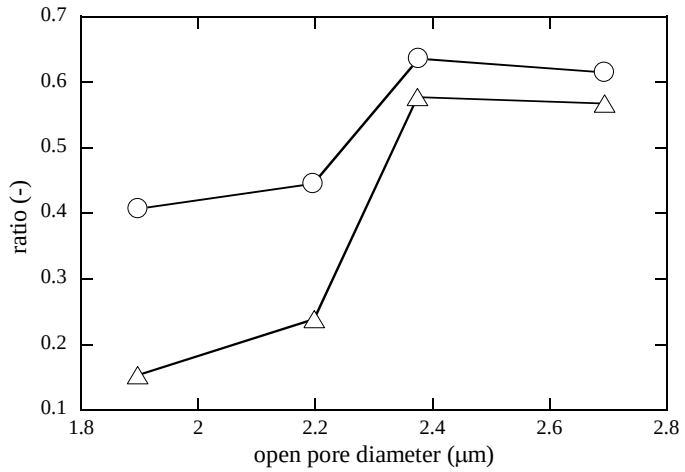


**Figure 4-9**: Relationship between the ratio of pores containing microspheres and pore size (circle); the ratio of pore with microspheres, (triangle); the ratio of pore with more than one microspheres. Film was soaked in methanol for 20 min.

As mentioned in 4.3.2, the open pore size of microporous film can be controlled. Finally we investigated the relationship between the ratio of pores containing microsphere(s) and pore size. As the pore size increases, the ratio of pore containing microsphere increased as shown in Figure 4-9. Below 2.4 μm of the pore diameter, the ratio of the pores with a single microsphere is higher

compared with the multi-number of microspheres. When the diameter was 2.4 or 2.7 μm, almost all pores where the microspheres were embedded contained multi-numbers of microspheres.

## 4.4) Conclusion

Honeycomb films were successfully fabricated from the amphiphilic block copolymer, poly(acrylic acid)-*block*-polystyrene) prepared via atom transfer radical polymerization followed by the acid catalyzed elimination reaction. After drying, the surface of the film was hydrophobic since carboxyl groups go inside the film in order to minimize the surface energy, and hybridization did not occur by immersing the film into slurry of polymer particles. By soaking the film in methanol, the wettability increased, and hybrid films were successfully obtained, where microspheres were embedded in the pore. The embedding efficiency of microspheres modified with amino groups was much higher than that of conventional polystyrene microspheres. Electrostatic interaction plays an important role for the hybridization. With the increase of open pore size, multi-numbers of microspheres were embedded in a single pore. It is noteworthy that our process utilized no special apparatus for the fabrication of hybrids. It is expected that periodic arrangements of aggregates of microspheres can be fabricated using various combinations of pore size of microporous films and diameter of microspheres.

## References


[1] Widawski, G., Rawiso, M., François, B., *Nature*, **369**, 387 (1994).

[2] François, B., Pitois, O., François, J., *Adv. Mater.*, **7**, 1041 (1995).

[3] Jenekhe, S.A., Chen, X.L., *Science*, **283**, 372 (1999).

[4] De Boer, B., Stalmach, U., Nijland, H., Hadziioannou, G., *Adv. Mater.*, **12**, 581 (2000).

[5] Maeda, Y., Koshiyama, Y., Shimoi, Y., Ogino, K., *Sen'i Gakkaishi*, **60**, 268 (2004).

[6] Hayakawa, T., Horiuchi, S., *Angew. Chem. Int. Ed.*, **42**, 2285 (2003).

[7] Maeda, Y., Σημοι, Y., Ogino, K., *Polym. Bulle.*, **53**, 315 (2005).

[8] Li, X.Y., Zhao, Q.L., Xu, T.T., Huang, J., Wei, L.H., Ma, Z., *Eur. Polym. J.*, **50**, 135 (2013).

[9] Srinivasarao, M., Collings, D., Philips, A., Petel, S., *Science*, **292**, 79 (2001).

[10] Karthaus, O., Maruyama, N., Cieren, X., Shimomura, M., Hasegawa, H., Hashimoto, T., *Langmuir*, **16**, 6071 (2000).

[11] Nishikawa. T., Ookura, R., Nishida, J., Arai, K., Hayashi, J., Kurono, N., Sawadaishi, T., Hara, M., Shimomura, M., *Langmuir*, **18**, 5734 (2002).

[12] Tanaka, M., Takebayashi, M., Miyama, M., Nishida, J., Shimomura, M., *Bio-med. Mater. Eng.*, **14**, 439 (2004).

[13] Yabu, H., Takebayashi, M., Tanaka, M., Shimomura, M., *Langmuir*, **21**, 3235 (2005).

[14] Saunders, A.E., Shah, P.S., Sigman, M.B., Hanrath, T., Hwang, H.S., Lim, K.T., Johnston, K.P., Korgel, B.A., *Nano Lett.*, **4**, 1943 (2004).

[15] Nishikawa, T., Nishida, J., Oookura, R., Nishimura, S., Wada, S., Karino, T., Shimomura, M. *Mater., Sci. Eng. C.*, **8–9**, 495 (1999).

[16] Hernandez-Guerrero, M., Min, E., Barner-Kowollik, C., Müller, A.H.E., Stenzel, M.H., *J. Mater. Chem.*, **18**, 4718 (2008).

[17] Yabu, H., Shimomura, M., *Langmuir*, **21**, 1709 (2005).

[18] Li, L., Zhong, Y., Ma, C., Li, J., Chen, C., Zhang, A., Tang, D., Xie, S., Ma, Z., *Chem. Mater.*, **21**, 4977 (2009).

[19] Yabu, H., Inoue, K., Shimomura, M., *Colloid. Surf. A. Physicochem. Eng. Asp.*, **284**, 301 (2006).

[20] Ogino, K., Sato, H., Tsuchiya, K., Suzuki, H., Moriguchi, S., *J. Chromatogr. A.*, **699**, 59 (1995).

[21] Kajiyama, C., Tanaka, K., Takahara, A., *Polymer*, **39**, 4665- 4673 (1998).

# Chapter 5

# Summary

In this thesis, we investigated fabrication of polymer particles and their morphology in various states.

In chapter 2, we prepared PS, PMMA and PS-b-PMMA by living anion polymerization and utilized them for preparation of seed particles by the solvent evaporation method. Four kinds of seed particles including: PS and PMMA homopolymer, binary PS/PMMA polymer blend, PS-b-PMMA block copolymer and finally ternary PS/ PS-b-PMMA/PMMA polymer blend was made in which the first three were spherical with smooth surface but the last one had a spherical shape with bi-compartment morphology. We carried out seed polymerization of styrene or MMA utilizing the resulting microspheres as seed particles in order to control the shape, and the surface morphology of particles. The particles with snowman-like morphology were obtained by seed polymerization of styrene using PS/PMMA binary blend microspheres as seed particles. Surface roughness was controlled by the polymerization of MMA in the block copolymer seed, and that of styrene in the ternary blend seed**.**

In chapter 3, we synthesized PBTPA and PBTPA-b-PMMA by C-N cross coupling and atom transfer radical polymerization (ATRP), respectively. Again we carried out solvent evaporation method for preparation of seed particles. PBTPA, PBTPA/PMMA, PBTPA-b-PMMA and PBTPA/PBTPA-b-PMMA/ PMMA seed particle were obtained in which the surface of the first three was spherical and smooth at lower molecular weight (LMW), but irregular and non spherical at higher molecular weight (HMW). Meanwhile in the case of binary PBTPA/PMMA polymer blend at LMW, the morphology resulted was Janus type while HMW was dumbbell type. Also, we investigated the effect of concentration on morphology. In this item we realized that the concentration of polymer solution has a major effect on seed particles so that at low concentration of polymer solution (2.5 %), the prepared particles were non spherical and irregular in comparing with high concentration of polymer solution (5 %) that were nearly spherical and more regular. Eventually, we investigated the effect of block content on final morphology of ternary polymer blend. The particles based on the ternary blends containing

PBTPA-*b*-PMMA showed core-shell type morphologies (PMMA; core, PBTPA; shell). Degree of engulfment of PMMA-rich domain increased with the content of the block copolymer. The decrease of domain size was not observed although the block copolymer had suitable structure as a compatibilizer for the blend.

In chapter 4, we fabricated microporous film and microsphres hybrid. Highly ordered microporous polymer films with honeycomb structure were fabricated by a dissipative process utilizing amphiphilic poly(acrylic acid)-*block*-polystyrene, which was synthesized by atom transfer radical polymerization followed by an acid-catalyzed ester cleavage reaction. In order to embed the microsphere efficiently, the dried microporous films should be soaked in methanol to alter the surface functionality and to improve the wettability of the film surface. The introduction of amino functionality to polystyrene microspheres by seeded polymerization of N,N-dimethylaminoethyl methacrylate drastically improved the embedding efficiency. Meanwhile with the increase of open pore size, multi-number of microspheres was embedded in a single pore.

# Appendix 1

# Block Copolymer

## A-1) Block Copolymers

Block copolymers are composed of two or more chemically distinct polymer chains linked together at one or more junction points through covalent or non-covalent bonds (Figure A-1-1(A)) [1]. As a consequence of the inherent immiscibility of different polymer segments, block copolymers undergo micro-phase separation in the ***bulk phase*** and in ***thin films***. This lead to different morphologies with domain sizes of about 10–100 nm (Figure A-1-1(B), A-1-1(C))[2, 3]. In solution, block copolymers will form ***micelles*** when the solvent is selective for one of the blocks. A wide variety of micelle morphologies is known, and these depend on the composition of the polymer and the processing conditions (Figure A-1-1(D)) [4]. Most of the desirable properties of block copolymers originate from their ability to form well-defined nanostructures with different morphologies of tunable periodicity or size, and this provides the primary driving force for the intensive interest in this field. The scope of possible applications for block copolymers is rapidly expanding, with multidisciplinary contributions involving the fields of chemistry, physics, materials science, as well as the biological and medical sciences.

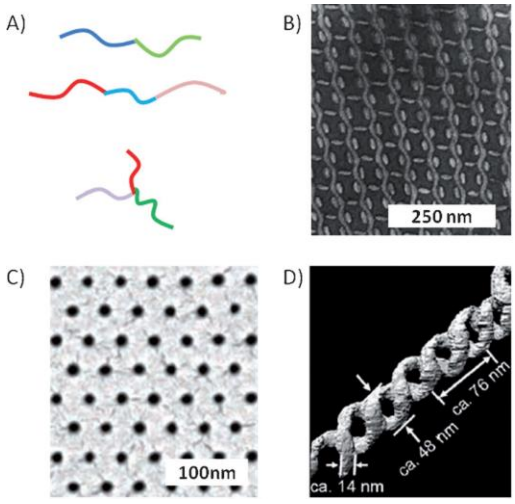


**Figure A-1-1**: **A)** Schematic representation of an AB diblock copolymer, ABC triblock terpolymer, and m-ABC-miktoarm star block terpolymer [1]. **B)** TEM micrograph of a "knitting pattern" formed by the self-assembly of an ABC triblock terpolymer in the bulk state [2]. **C)** TEM micrograph of a high-density hexagonal patterned thin film formed by the templated self-assembly of a diblock copolymer [3]. **D)** TEM tomography image of a double helix formed from the self-assembly of an ABC triblock terpolymer in solution [4].

## A-1.1) Di-Block Copolymers

Di-block copolymers are one special type of copolymers, in which the polymer chains are composed of two blocks of different monomers [5, 6]. Physicists and chemists are fascinated about Di-block copolymers because, despite their simple chemical structure, they can self-assemble into a variety of ordered structures with the domain size in the order of nanometers. Different morphologies can be formed as a result of a competition between the interaction energy and the chain stretching. First of all, different blocks do not like mixing and tend to separate out into distinct parts. On the other hand, the chemical bonds linking different blocks prevent the separation at a macroscopic length. Therefore, Di-block copolymers have to make some comprise between the separating and mixing, resulting in the formation of various ordered structures. For Di-block copolymers, the simplest and most common morphologies are the so called classical structures: lamellae consisting of alternating layers (LAM), cylinders packed on a hexagonal lattice (HEX), and spheres arranged in a body-centered cubic lattice (BCC). There are also some complex structures: gyroid (G) which is a bicontinuous [7, 8], perforated-lamellar phase (PL) [9], and a very recently discovered FDDD phase which is non-cubic network morphology [10-12]. Schematic of these morphologies are shown in Figure A-1-2 [13].

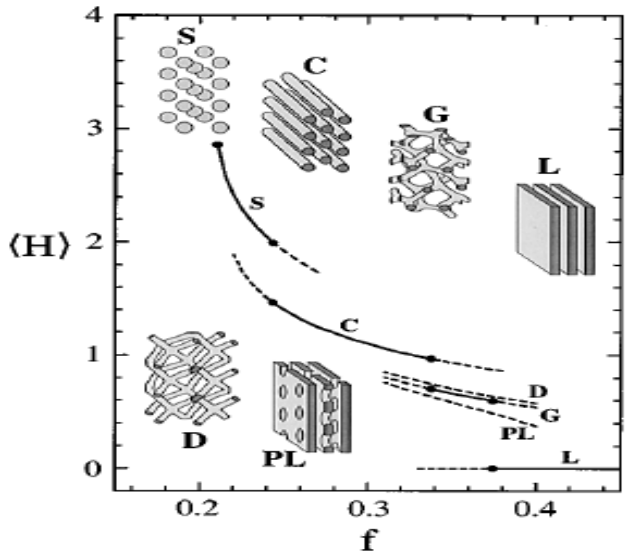


**Figure A-1-2**: Area-averaged mean curvature (H) as a function of the A-block volume fraction *f* for each of the structures shown schematically calculated using self consistent mean field theory. The stable and metastable states are shown with solid and dashed lines, respectively, and transitions are denoted by dots. As the molecules become asymmetric, structures with more curvature are preferred [13].

As already mentioned, One of interesting and useful aspect of the behavior of block copolymers (also Di-block copolymer) is that they are able to self assemble on the nanometer scale into ordered structures through the process of phase separation. The driving force for this is the enthalpy of the de-mixing of the locks which leads to a tendency for blocks to phase separate in a similar way to polymer blends. In block copolymers, there is the extra constraint in that constituent blocks are connected through covalent bonds that prevent the macroscopic phase separation found in polymer blends. This also means that the dimensions of the ordered structures are relatively small compared with blends. The overall phase separation process in block copolymers is, therefore, controlled by two factors: the system is trying to minimize the area of the interface between the two micro-phases whilst trying to maximize the entropy of the polymer chains. It is found that the phase structure of block copolymers is controlled by only three parameters: the composition of the copolymer characterized by $f_A$ (the overall volume fraction of component A), the overall degree of polymerization ***N*** and the Flory-Huggins A-B segment interaction parameter ***X***.

The transformation of a homogenous molten Di-block copolymer into heterogeneous micro-phase is known as an ***order-disorder transition*** that is shown schematically in Figure A-1-3.

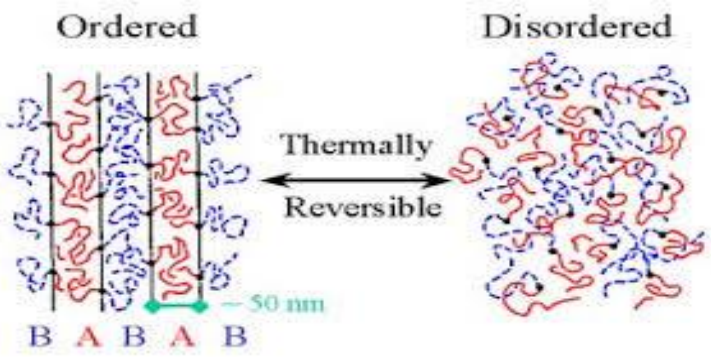


**Figure A-1-3**: Schematic illustration of the order-disorder transformation in a Di-block copolymer

The difference between the symmetric Di-block copolymer and the symmetric polymer blend is that, in addition to the loss of mixing entropy with a one-component system, due to the connectivity in the Di- block copolymer there is also a loss in entropy due to chain stretching in the two separated phases, not encountered in a phase-separated blend. This entropy penalty is proportional to the overall degree of polymerization ***N***. for most Di-block copolymers, the interaction parameter has a temperature dependence given by: $\boldsymbol{X}$=a+b/T, where a, b (>0) are

constants. Increasing the interaction parameter $\boldsymbol{X}$ of a disordered block copolymer melt by reducing the temperature will drive the system toward local ordering as shown in Figure 1-6. On the other hand, if $\boldsymbol{X}$ (or $\boldsymbol{N}$) is decreased sufficiently for an ordered Di-block copolymer, it will transform to a disordered phase. It is possible to extend consideration of the thermodynamics of block copolymers using the mean-field approach to predict the dependence of the order-disorder transition and other upon $\boldsymbol{XN}$ and $f_A$.

Various theoretical approaches have been developed to study the phase behavior of Di-block copolymers. Among them, the ***self-consistent field theory*** (SCFT) proves to be one of the most successful [14-25]. It is possible to extend consideration of the thermodynamics of block copolymers using this method to predict the dependence of the order-disorder transition and other upon $\boldsymbol{XN}$ and $f_A$. Figure A-1-4 exhibits the phase diagrams of Di-block copolymers calculated from self-consistent field theory. It can be concluded that self-consistent field theory provides a powerful theoretical framework to study block copolymers [26].

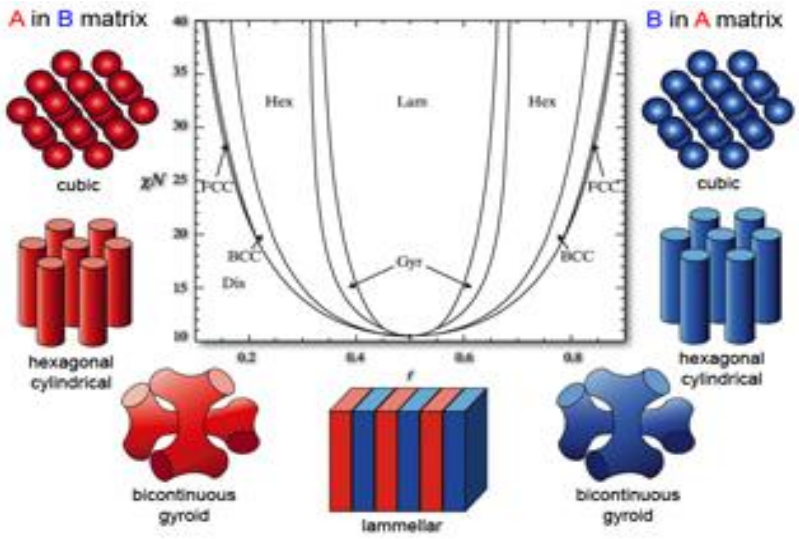


**Figure A-1-4**: Theoretical phase diagram calculated using the self-consistent field theory [26].

As it can be seen from this diagram when the product $\boldsymbol{\chi N}$ exceeds 10.5, the molecular segments in ***symmetric*** Di-block copolymers ($f_A = f_B = 0.5$) self assemble to form a lamellar micro-phase structure (LAM) which consists of alternating parallel layers. In the case of ***asymmetric*** Di-block copolymers ($f_A \neq f_B$), it is more energetically favorable for the phases to

have curved interfaces and the molecular segments self assemble into different structures. The formation of the different phase structures also is constrained by the entropy penalty of ensuring that the polymer chains are not stretched too much. Hence, the microstructures obtained involve keeping a balance between interface curvature and chain stretching. When there is strong segregation, then as the copolymer composition moves away from $f_A = 1/2$ increasing interfacial curvature leads to firstly a bicontinuous gyroid phase (GYR), then a phase of hexagonal close-packed cylinders (HEX) and finally a body-centerd cubic phase (BCC) as shown in Figure 1-7. If the length of the segment A and B is the same in the copolymer, this behavior is symmetrical either side of ($f_A = f_B = 0.5$). A phase rich in component B becomes the countinuous phase in the micro structure as $f_A$ decreases, and similarly a phase rich in component A becomes the continuous phase in the microstructures as $f_A$ increases.

## A-1.2) Phase Behavior of Di-Block Copolymers

### A-1.2.1) In Bulk

Di-Block copolymers of exhibit phase separation in bulk state on microscopic scale [27]. This microscopic separation is possible through the simultaneous existence of two opposite forces in the system: long range repulsive and short-range attractive forces [28]. Incompatibility of the two blocks causes long-range repulsive interactions whereas the covalent bond, which links the blocks together, is responsible for the short-range attractive force (Figure A-1-5.a). Micro-phase separated copolymers can form various periodically ordered structures of the length-scale between 1-100 nm. The type of morphology produced depends on the first approximation of the copolymer composition, represented as the volume ratio *(*f = *VA/VB)* of the individual blocks, determining the curvature radius *R* of the interface as shown in (Figure A-1-5.b) [29].


**Figure A-1-5.a)**: Schematic representation of two simultaneously present interactions leading to the self-organisation of block copolymers. **b)**: Local geometry and the curvature of domains and interfaces; *A, B* – domains; *R* – curvature radius of the interface (for a planar interface $R = \infty$) [29].

There are three regimes, categorized by the magnitude of the $\boldsymbol{X}\,N$ value:

- $\boldsymbol{X}N \sim 10$ – *Weak Segregation Limit (WSL),* where the polymer blocks are highly miscible;
- $\boldsymbol{X}N \sim 10\text{-}100$ – *Strong Segregation Limit (SSL),* where the regime of stable morphologies occurs;
- $\boldsymbol{X}N >> 100$ – *Super Strong Segregation Limit (SSSL),* postulated by Khokhlov [30] for systems in which the phase interface consists only of covalent bonds connecting the A and B blocks (the domains contain essentially pure components).

### A-1.2.2) In Solution

Block copolymers undergo specific separation not only in bulk but also in solution. By bringing an AB block copolymer into the solvent, which acts as a good solvent for block B but not for block A, can induce the spontaneous self-organization process, called *micellisation* [31]. Produced aggregates, which in the easiest case, are spherical micelles, consist of a core, containing the insoluble block A surrounded by a corona of the soluble block B, for low molecular surfactants, in dilute solutions of block copolymers, spherical or cylindrical micelles [32, 33], as well as more complex vesicular aggregates [34, 35] can be formed. However, the dynamic of the aggregate formation and equilibration is for block copolymers in solution much slower, comparing to low molecular weight surfactants, due to much lower diffusion coefficients.

## References


[1] Abetz, V., Simon, P.F.W., *Springer*, **189**, 125-212 (2005).

[2] Breiner, U. Krappe, U., Stadler, R., *Macromol. Rapid Commun.*, **17**, 567-575 (1996).

[3] Ruiz, R., et al., *Science*, **321**, 936-939 (2008).

[4] Dupont, J., et al., *Angew. Chem.*, **121**, 6260- 6263 (2009).

[5] Hamley, I., The Physics of Block Copolymers, Oxford University Press, Oxford (1998).

[6] Bates, F.K., Fredrickson, G.H., *Physics of today*, **52**, 33 (1999).

[7] Hajduk, D.A., et al., *Macromolecules*, **27**, 4063 (1994).

[8] Schulz, M.F., Bates, F.S., Almdal, K., Mortensen, K., *Phys. Rev. Lett.*, **73**, 86 (1994).

[9] Hamley,I.W., et al., *Macromolecules*, **26**, 5959 (1993).

[10] Tyler, C.A., Morse, D.C., *Phys. Rev. Lett.*, **94**, 208302 (2005).

[11] Takenaka, M., et al., *Macromolecules*, **40**, 4399 (2007).

[12] Kim, M.I., et al., *Macromolecules*, **41**, 7667 (2008).

[13] Matsen, M.W., Bates, F.S., *Macromolecules*, **29**, 7641-7644 (1996).

[14] Edwards, S., *Proc. Phys. Soc.*, **85**, 613 (1965).

[15] Helfand, E., *J. Chem. Phys.*, **62**, 999 (1975).

[16] Helfand, E., *Macromolecules*, **8**, 552 (1975).

[17] Hong, K.M., Noolandi, J., *Macromolecules*, **14**, 727 (1981).

[18] Shull, K., *Macromolecules*, **25**, 2122 (1992).

[19] Vavasour, J.D., Whitmore, M.D., *Macromolecules*, **25**, 5477 (1992).

[20] Banaszak, M., Whitmore, M.D., *Macromolecules*, **25**, 3406 (1992).

[21] Leibler, L., *Macromolecules*, **13**, 1602 (1980).

[22] Semenov, A.N., *Sov. Phys.*, **61**, 733 (1985).

[23] Matsen, M., Schick, M., *Phys. Rev. Lett.*, **72**, 2660 (1994).

[24] Drolet, F., Fredrickson, G., *Phys. Rev. Lett.*, **83**, 4317 (1999).

[25] Tzeremes, G., et al., *Phys. Rev. E.*, **65**, 041806 (2002).

[26] Matsen, M.W., Bates, F.S., *Macromolecules*, **29**, 1091-1098 (1996).

[27] Bates, F.S., Fredrickson, G.H., *Annu. Rev. Phys. Chem.*, **41**, 525-557 (1990).

[28] Förster, S., Plantenberg, T., *Angew. Chem. Int. Ed.*, **41**, 688-714 (2002).

[29]Hamley, I.W., *The Physics of Block Copolymers*, Oxford University Press: New York (1998).

[30] Nyrkova, I.A., Khokhlov, A.R., Doi, M., *Macromolecules*, **26**, 3601-3610 (1993).

[31] Riess, G., *Prog. Polym. Sci.*, **28**, 1107-1170 (2003).

[32] Schillen, K., Brown, W., Johnsen, R.M., *Macromolecules*, **27**, 4825-4832 (1994).

[33] Antonietti, M., Heinz, S., Schmidt, S.M., Rosenauer, C., *Macromolecules*, **27** (1994).

[34] Discher, D.E., Eisenberg, A., *Science*, **297**, 967-973 (2002).

[35] Soo, P.L., Eisenberg, A., *J. Polym. Sci., Part B: Polym. Physics*, **42**, 923-938 (2004).

# Appendix 2

## NMR Spectra of Various Components in Chapter 2 and 3

## A-2-1) Chapter 2

### A-2-1.1) PS-b-PMMA

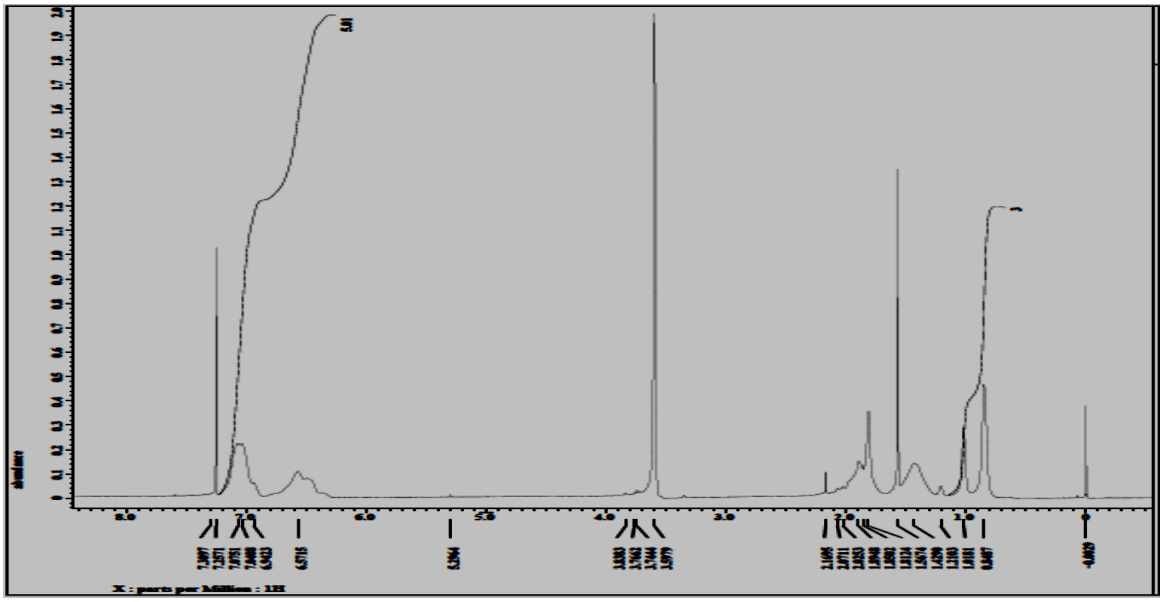

## A-2-2) Chapter 3

### A-2-2.1) Butyltriphenylamine (BTPA) Monomer

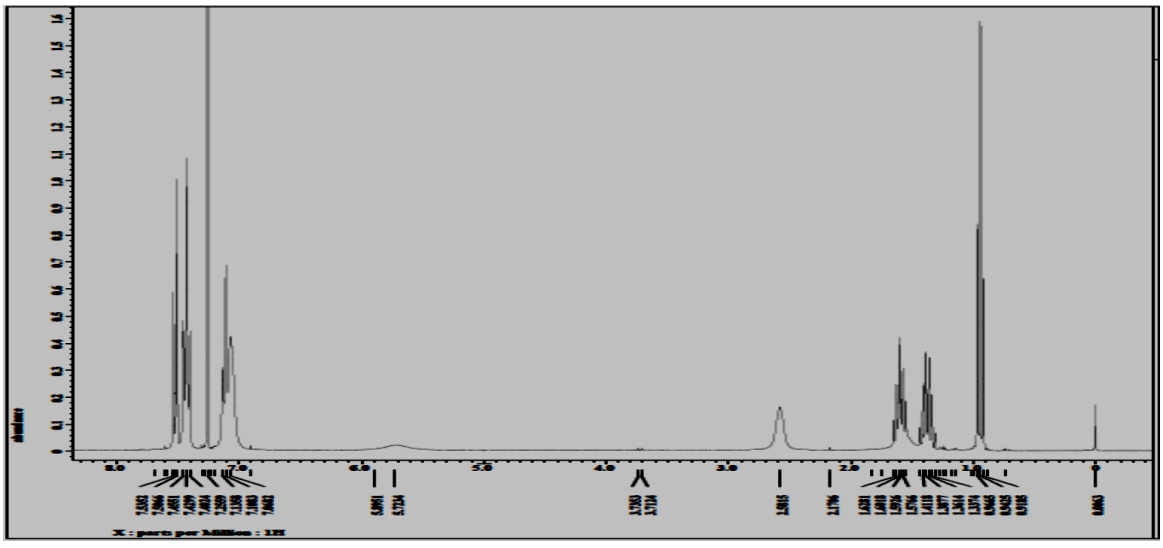

## A-2-2.2) 2-(*p*-bromophenoxy) ethanol

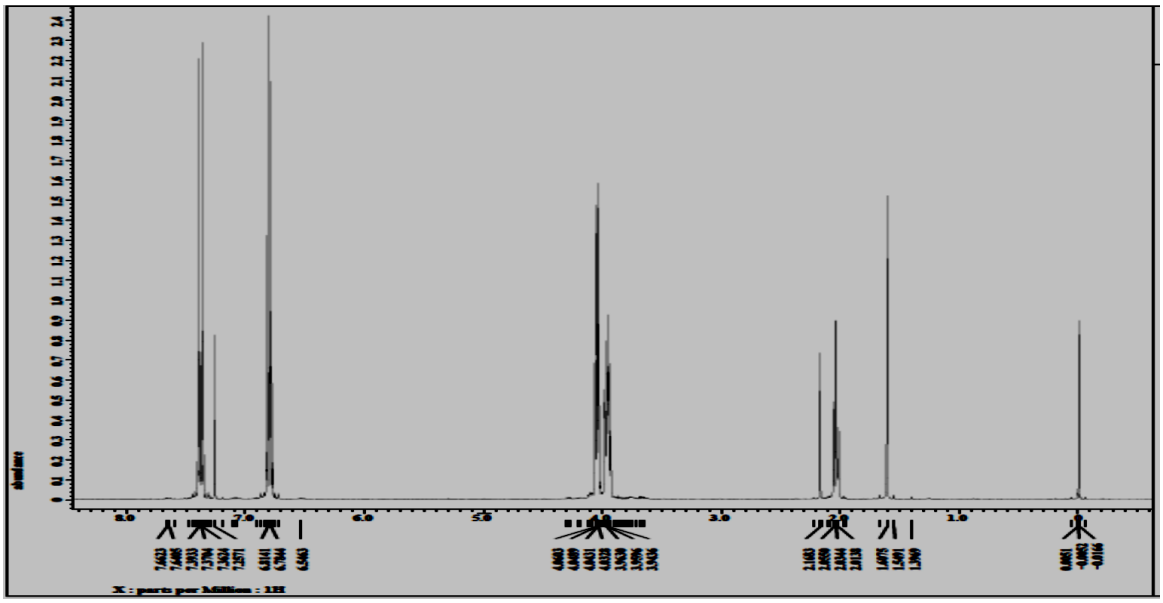

## A-2-2.3) 2-(*p*-bromophenoxy) ethoxy-t-butyldimethylsilane

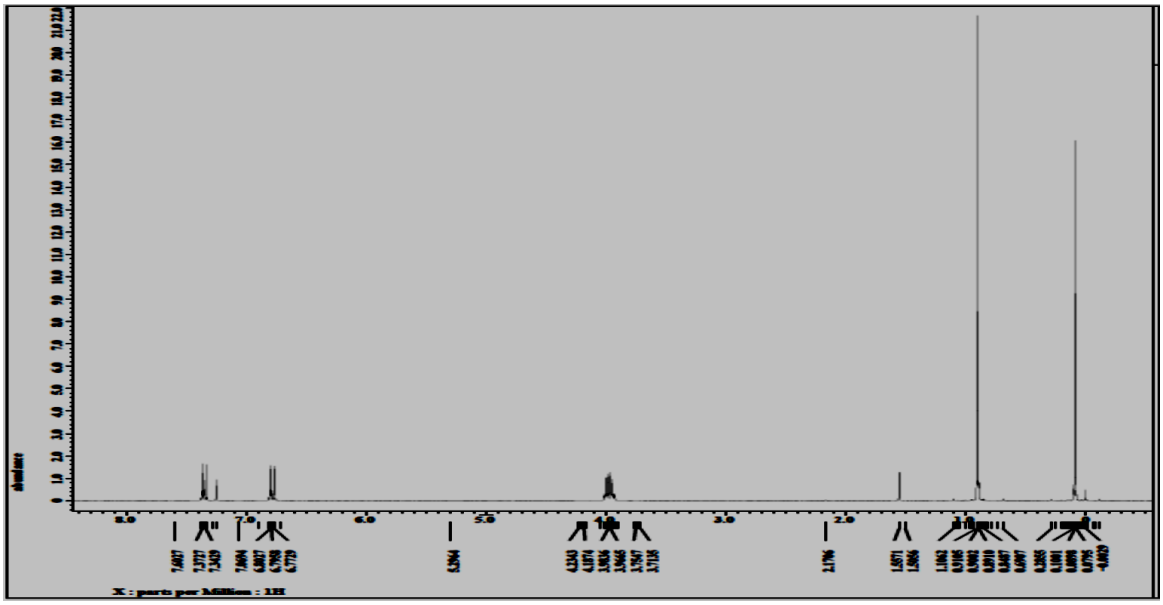

## A-2-2.4) (PBTPA-TBS)

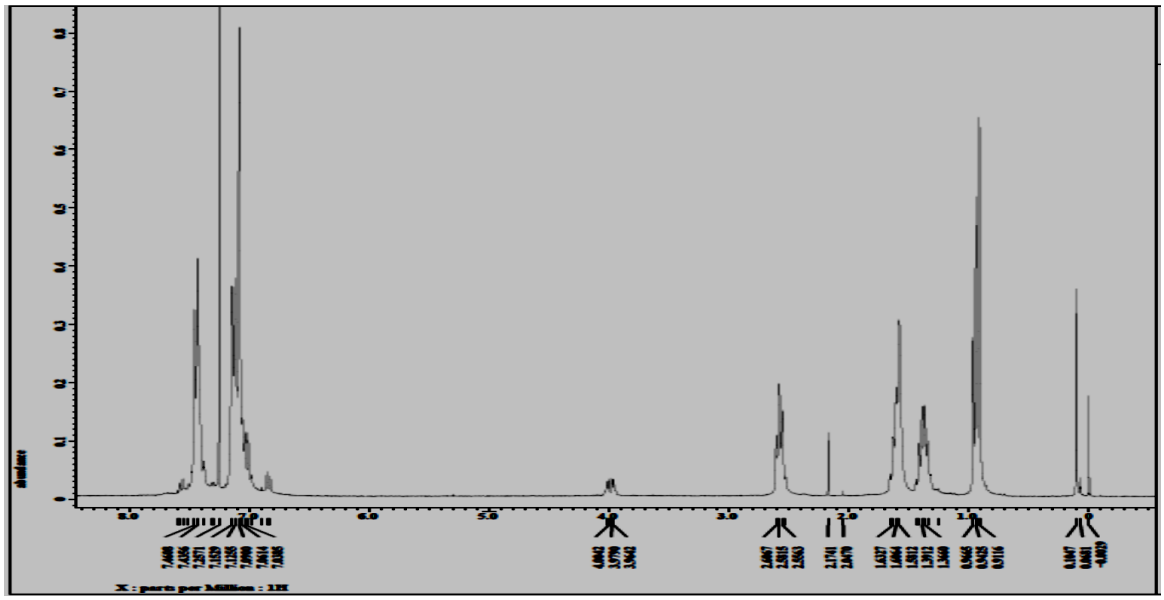

## A-2-2.5) (PBTPA-O-H)

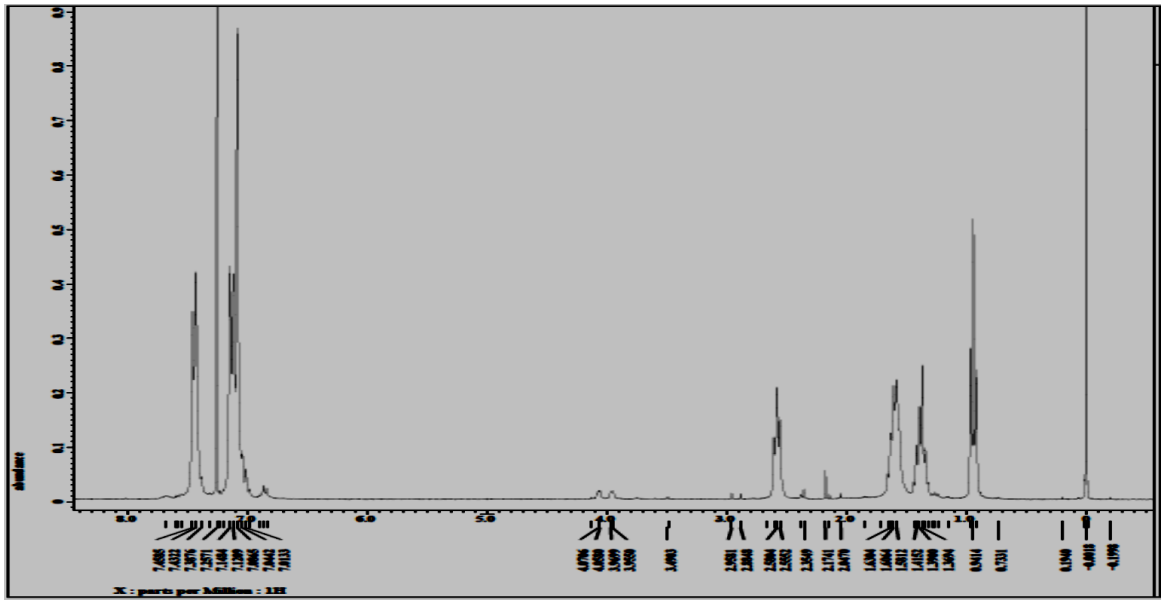

## A-2-2.6) (PBTPA-O-Br) [PBTPA-MI]

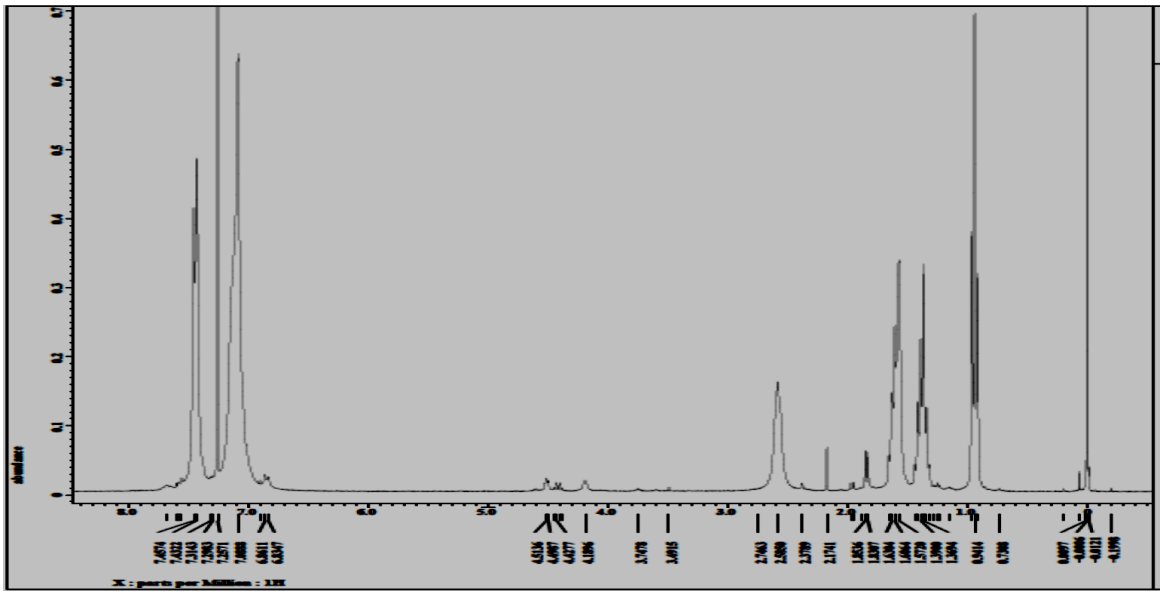

## A-2-2.7) (PBTPA-b-PMMA)